CR 73/18

(Report No. P67-153, Ref. A8076)

STUDY OF APPLICATIONS OF RETRODIRECTIVE AND SELF-ADAPTIVE ELECTROMAGNETIC WAVE PHASE CONTROLS TO A MARS PROBE

By A. T. Villeneuve
J. E. Howard
G. O. Young
A. A. Ksienski

Final Report — Part I

CONTENTS

ILLUSTRATIONS

STUDY OF APPLICATIONS OF RETRODIRECTIVE AND SELF-ADAPTIVE ELECTROMAGNETIC WAVE PHASE CONTROLS TO A MARS PROBE

By A. T. Villeneuve, J. E. Howard,
G. O. Young, and A. A. Ksienski
Hughes Aircraft Company

SUMMARY

The report presents the results of the first phase of a study of the applicability of self-steering and adaptive arrays to planetary probe missions. Analyses were performed of arrays that obtain self-steering by the use of either phase-locked loops or phase inver. ion by mixing. The effectiveness of these two types of arrays in receiving signals modulated by various systems was analyzed, and the probability of error of each type in detecting signals of each modulation in the presence of random gaussian phase errors was determined. Modulation systems were m-ary coherent and differentially coherent phase shift key, coherent and incoherent frequency shift key, and coherent and incoherent amplitude shift key.

Examinations of the signal-to-noise ratios of each type of array indicated that the two systems have comparable performance when the pilot channel bandwidth is sufficiently narrow. When the pilot bandwidth is of the same order of magnitude as the information bandwidth, the performance of the phase-locked loop system is superior to that of the phase-inversion system.

System calculations were performed for a phase-inversion system operating over 4000-mile and 12,000-mile links. Signal-to-noise values were obtained from which probabilities of error can be determined.

INTRODUCTION

This report is Part 1 of the Final Report on Contract NAS 2-3297 and covers work performed from 8 November 1965 to 8 October 1966 (refs. 1-4). The problem under consideration is the applicability of retrodirective and self-adaptive electromagnetic wave phase controls (self-steering arrays) to a Mars probe. While a number of theoretical and experimental studies dealing with the general properties of self-steering antenna arrays have been reported in the literature (refs. 5-15), none of this work has been concerned with the specific problem under consideration in the present study.

The subject of prime interest in the phase of the study reported here has been the performance characteristics of two general types of self-steering arrays when applied to planetary probes as communication antennas. The types of arrays investigated utilize either phase-locked loops or phase inversion by mixing to obtain self-steering. Their operating principles are described in general terms early in the report.

The performance of each type of self-steering array was investigated analytically when the array was operating with a number of different, digitally modulated signals. The modulations treated were m-ary coherent phase shift key (PSK), differentially coherent PSK (DPSK), coherent frequency shift key (FSK), incoherent FSK, coherent amplitude shift key (ASK), and incoherent ASK. The quantity desired in the analysis was the probability of error in the detection of the variously modulated signals as a function of the signal-to-noise ratio in the receiver of each self-steering array. This quantity is a key parameter in determining the reliability with which commands can be transmitted to and data received from a probe.

In the first part of the study, the probabilities of error of symbols and words were computed for ideal conditions; effects such as multipath propagation were neglected. This phenomenon and related conditions will be considered during the remainder of the contract period.

The study resulted in the derivation of analytical expressions necessary for the evaluation of the error performance of self-steering arrays when they are used with digital modulations. It has also resulted in numerous curves of probability of error as a function of signal-to-noise ratio for self-steering arrays. The conclusions drawn from the research results are presented at the end of the technical discussion along with recommendations for further work. The details of the several analyses are given in the appendix.

The authors wish to thank Marjorie Delzell for her very diligent editorial assistance in the preparation of this report.

DISCUSSION

Performance Characteristics of Self-Phased and Adaptive Arrays

The vast distances that must be traversed by radio signals transmitted to and from planetary probes puts some rather severe restrictions on the rate at which information can be transmitted with a given percentage of error. The restrictions are a consequence of the relatively low signal powers that are available at receivers compared with the noise at those receivers. This inverse comparison is especially true when the probe is transmitting, since the stringent size and weight limitations that presently restrict the amount of equipment the probe can carry, translate directly into transmitter power limitations and only rather low powers are available to transmit information from the probe to the earth.

The situation could be alleviated to some extent by the use of sufficiently high gain antennas at each end of the transmission link. However, certain limitations and difficulties exist with this approach when conventional antenna techniques are utilized. First, there is a size limitation that will depend, to some extent, on the type of antenna structure considered. Erectable antennas may present an aperture that is considerably larger than the probe launch vehicle cross-section, but tolerances on phasing may be a problem when large diameter-to-wavelength apertures are used and when conventional feeding and phasing techniques are employed.

The use of high gain antennas also introduces a problem of beam-pointing control. In conventional antenna systems, pointing may be done either mechanically or electronically but a priori pointing information may be required or some electronic tracking technique (eg. , monopulse) would be necessary to maintain the correct beam-pointing direction. The conventional electronic beam-steering techniques require electronically controlled variable phase shifters with their associated control electronics that may become quite complex.

Alternative approaches to the realization of steerable high gain antennas and concomitant increased data transmission rates are desirable. One such approach involves the application of the recently developed self-phasing and adaptive arrays to the planetary probe missions to see in what manner they may allow increased data rates with acceptable accuracy of transmission.

Self-phased and adaptive arrays constitute antenna systems that use the incident r-f energy to phase the elements so that a beam is formed in the direction from which the energy is received. These arrays are also called self-focusing antennas. They may be contrasted with the usual electronically steerable arrays that require external sensors and information to do the steering. Here, no external commands are necessary to

adjust the illumination across the aperture since, in principle, the self-steering array automatically steers the beam in the desired direction. The problems associated with pointing a narrow beam in a specified direction appear to be circumvented. In addition, self-phased arrays can compensate for the effects of atmospheric scintillation which may cause a loss of array gain by decorrelating the signals at the various elements. An important limitation is set on the minimum size of each element in an adaptive array of elements; each element must be large enough so that in conjunction with its receiver, it will be able to detect and phase lock to the incoming signal. Once this is achieved, the several elements in the array may be locked together to realize the gain of the entire array.

Self-phased arrays may take on a variety of forms, depending on the type of circuitry used to implement them and or the sophistication of their operation. In the simplest form, these arrays redirect incident energy back in the direction from which it came. These are termed retrodirective arrays. In the process, the signal is amplified, and information stored at the array is impressed on the signal before retransmission. A number of such systems are described by Kummer and Villeneuve (ref. 14).

Some general types of self-phasing arrays have been proposed by a number of workers. A number of physical embodiments may be realized; the techniques of Rutz-Phillipp (ref. 10), Sichelstiel et al. (ref. 11), Cutler et al. (ref. 6), and Pon (ref. 9) are sketched in figure 1. The principle of operation of all the systems shown in the figure is essentially the same. The phase of the signal incident at each element is reversed by the electronic circuitry. This is just the condition required to steer a beam in the direction of the incident radiation. The signals at various points in the systems are shown on the diagrams of figure 1.

In addition to the arrays discussed above which send energy back in the direction of an incident pilot signal, there are systems which automatically receive information from the direction of an incident signal with full array gain. They may also radiate different information back in the same direction, or in more advanced systems, in some other direction dictated by a pilot signal. Figure 2 presents techniques that use only mixing to form a receiving beam as well as a retransmitting beam. Figure 2a shows a retrodirective system and figure 2b a redirective system.

Since the systems shown in figure 2 are more complex than those in figure 1, an explanation of their method of operation is included. For the system in figure 2a, an information signal at carrier frequency f_1 and with phase ϕ_1 is incident on an element of the array. At the same time a pilot signal at frequency f_p and with phase ϕ_p is incident from the same direction. These signals are first reduced to intermediate frequencies $(f_{LO1} - f_1)$ and $(f_{LO1} - f_p)$ respectively with phases $-\phi_1$ and $-\phi_p$ (the common phase of LO1 is neglected here). The two frequencies are separated in a diplexer, and the pilot signal is amplified in a narrow-band amplifier to provide a clean reference for the second mixer. In this second mixer, the pilot signal is mixed with the information signal to provide a new intermediate

$\cos[(2\omega_{LO}-\omega_0)t - \phi_{0i}]$

$\cos(\omega_0 t + \phi_{0i})$

$\cos(\omega_{LO} t)$

TUNNEL DIODE FREQUENCY
CONVERTER (WITH GAIN)

$\cos(\omega_0 t + \phi_{0i})$

LO

$\omega_{LO} \approx \omega_0$
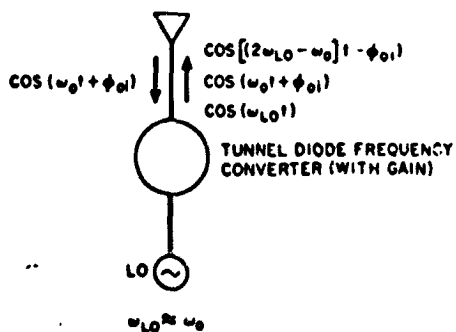
(a) SYSTEM OF RUTZ-PHILIPP (ref., 10)

CIRCULATOR
(OR FILTER)

$\cos(\omega_0 t + \phi_{0i})$

MODULATOR

MIXER   MIXER

$\cos(\omega_T t - \phi_{0i})$

LIMITER

$\cos(\omega_T t - \phi_{0i})$

TO OTHER
ELEMENTS

$\cos([\omega_0 + \omega_T]t)$ $\cos([\omega_T - \omega_0]t)$

LO_1   LO_2

$\omega_T \approx \omega_0$
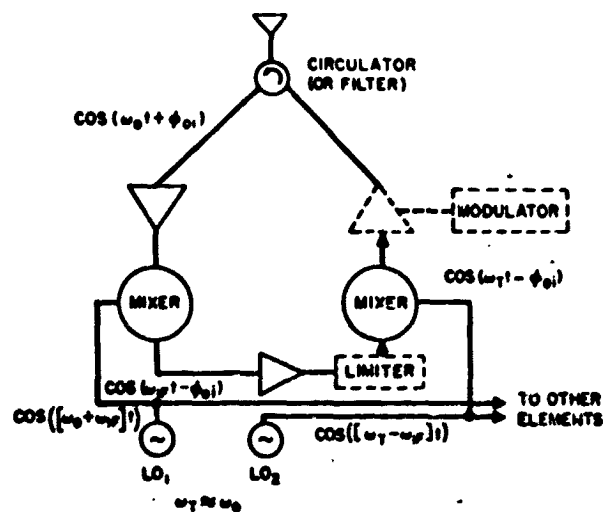
(b) SYSTEM OF SICHELSTIEL ET AL. (ref. 11)

FILTER

$\cos(\omega_0 t + \phi_{0i})$

$\cos([\omega_0 - \omega_0]t - \phi_{0i})$

M

LO   TO OTHER ELEMENTS

$\omega_0 \approx 2\omega_0$
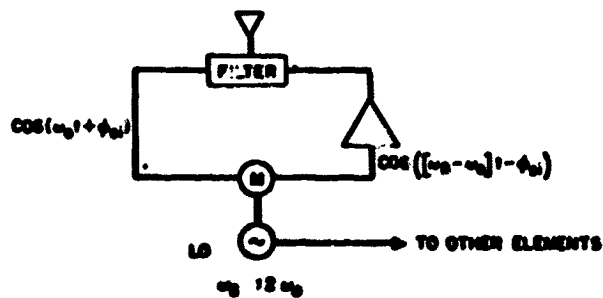
(c) SYSTEM OF CUTLER ET AL. (ref. 6) AND C. Y. PON (ref. 9)

Figure 1. Retrodirective array techniques.
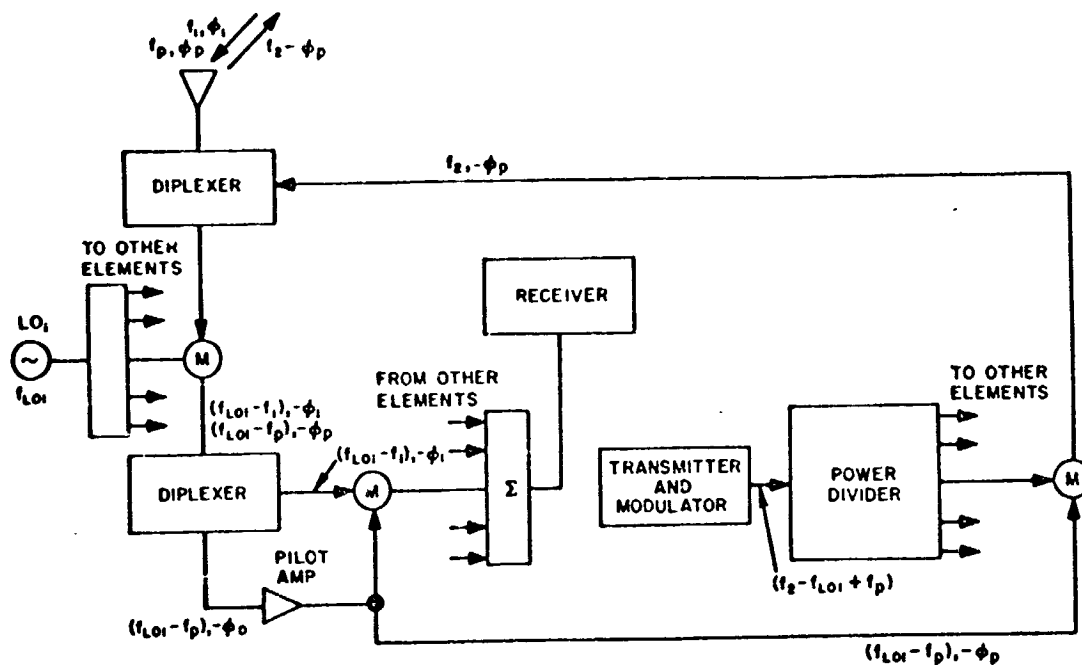
a) RETRODIRECTIVE ARRAY WITH FULL ARRAY GAIN ON RECEIVE
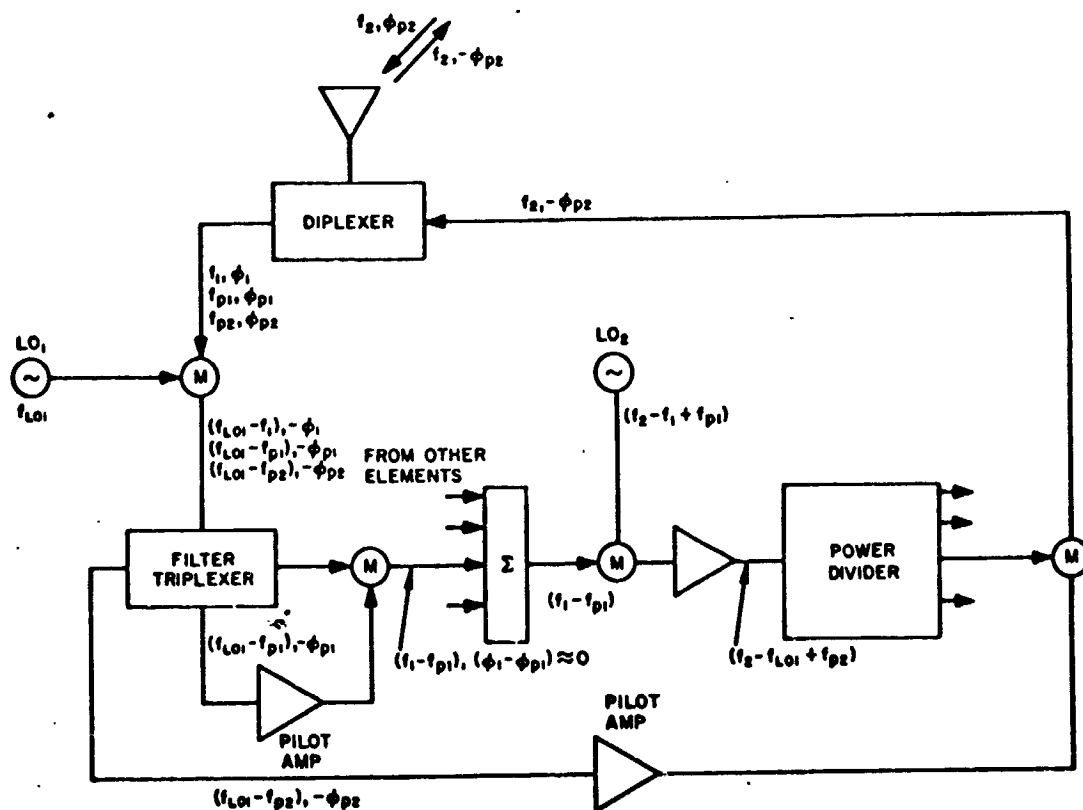
b) REDIRECTIVE ARRAY

Figure 2. Electronic beam-forming techniques.

frequency $f_1 - f_{p1}$ with phase $\phi_1 - \phi_p$. This latter phase angle has most of the interelement phase shift removed because f_1 and f_p are very close together on a percentage basis (even though $f_1 - f_p$ may be of the order of megacycles) so that $\phi_1 \simeq \phi_p$. With the interelement phase shifts removed, the signals from the various elements can be summed coherently, and the array gain is obtained when receiving. For retransmission of a signal back in the direction of the incident wave, the amplified, received pilot signal is mixed with the information signal to be transmitted. The sum frequency thereby obtained has a phase containing the negative of ϕ_p which is the phase required to retransmit in the direction of the incoming pilot.

The system of figure 2b works in the same manner for reception. However, a second pilot at f_{p2} is used to obtain retransmission back toward the source of f_{p2} rather than toward the source of f_1 and f_{p1}.

Several properties of these systems are apparent. First, since the pilot frequency is separated somewhat from the information signal frequency, perfect removal of interelement phase shifts for all angles of arrival is not possible. Consequently, there is some effective gain degradation for most angles of signal arrival. This degradation depends on the relative frequency separations used and on the array configuration. Another property is that the phase reference (i. e. , pilot) is noisy so that the signal-to-noise ratio of the sum signal is not so high as it would be if a noiseless reference were available.

Frequency shifts of both the incoming signal and pilot are essentially removed when the two are mixed so that the second i-f bandwidth need not be capable of handling expected incoming doppler shifts or any frequency shifts due to signal or local oscillator instabilities.

It is also evident that the systems shown very nearly remove the two-way doppler shift from the retransmitted signals because of the phase reversal inherent in the mixing techniques used to obtain self-steering. Additional means must be employed to reinsert this doppler if it is to be used for tracking vehicle velocity during flight. The reinsertion of the doppler can be accomplished by causing LO1 and the transmitting frequency to track the incoming doppler. The tracking can be achieved by adding a single phase-locked loop circuit to the system.

Phase-locked loops have been finding increasing application in recent years as phase synchronizing devices, and their characteristics are well documented (refs. 16, 17). An array of elements employing this type of phase control is called an electronically adaptive antenna system. A receiving antenna system of this type, unlike passive arrays, contains active elements that automatically adjust the electrical phases of the signals received by the array elements to obtain antenna directivity. These arrays can be made retrodirective. A configuration of this type is illustrated in figure 3.

ANTENNA ELEMENT

DIPLEXER

$\omega_4 = (\omega_3 + \omega_1 + \omega_0 - \omega_i)$ $\phi_4 = (\phi_3 + \phi_1 + \phi_0 - \phi_i)$

AMPLIFIER

POWER DIVIDER

LOCAL OSCILLATOR

TO OTHER ELEMENTS

ω_i, ϕ_i

UP-CONVERTER

ω_3, ϕ_3

POWER DIVIDER

INFORMATION SIGNAL

MIXER

ω_0, ϕ_0

$(\omega_i - \omega_0), (\phi_i - \phi_0)$

MIXER

$(\omega_1 + \omega_0 - \omega_i), (\phi_1 + \phi_0 - \phi_i)$

VOLTAGE-CONTROLLED OSCILLATOR

ω_2, ϕ_2

REFERENCE OSCILLATOR

PHASE DETECTOR

LOW-PASS FILTER

$\omega_1, (\phi_1 + \frac{\pi}{2})$

PHASE-LOCKED LOOP

POWER DIVIDER

FROM OTHER ELEMENTS

ADDER

RECEIVED SUM SIGNAL
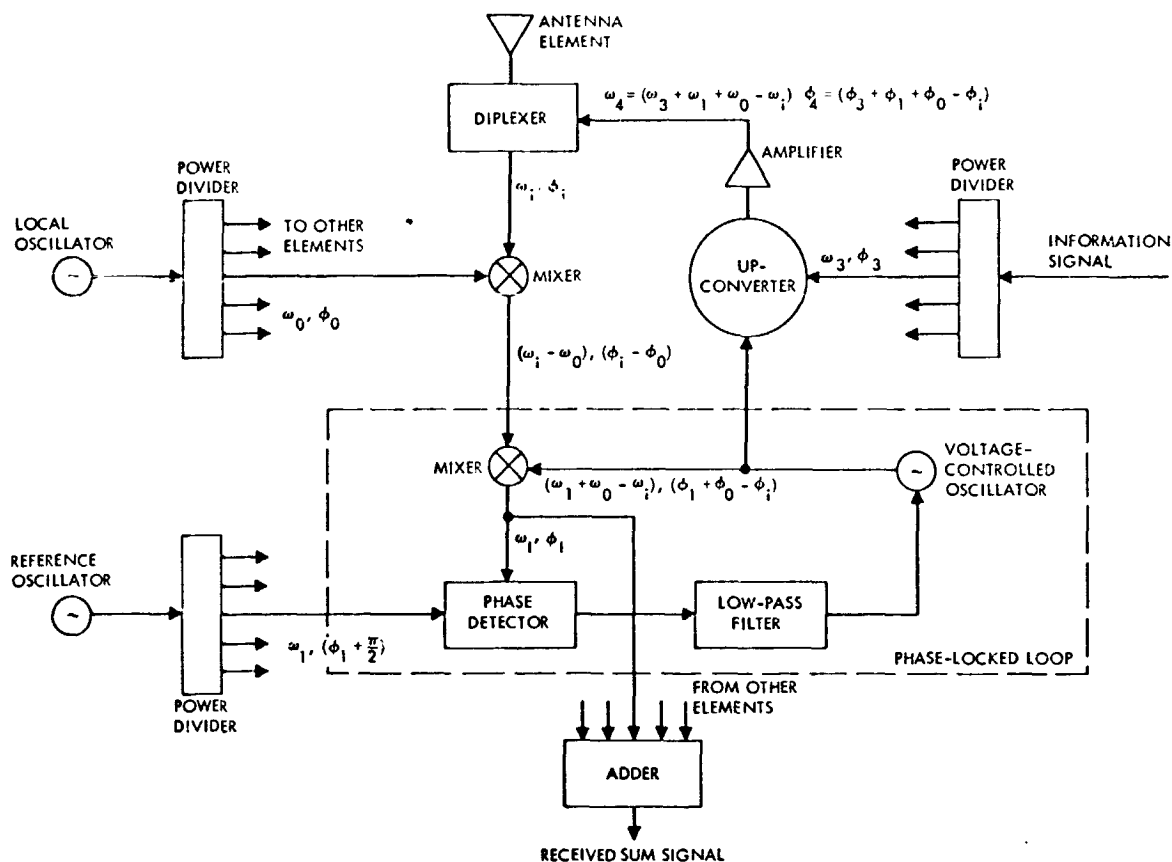
Figure 3. Retrodirective antenna using phase-locked loop.

The element shown in figure 3 is receiving at a frequency ω_i. The total phase of the incoming signal is $\omega_i t + \phi_i$ where ϕ_i may be arbitrary. For purposes of convenience in implementing the phase-locked loop, the signal is converted in the first mixer to an intermediate frequency $(\omega_i - \omega_0)$ with a phase angle $\phi_i - \phi_0$. The signal from the voltage-controlled oscillator is mixed with the intermediate frequency signal, and the sum frequency out of the mixer is compared in the phase detector with the signal from the reference oscillator which is operating at ω_1 with phase ϕ_1. The frequency of the voltage-controlled oscillator is automatically adjusted to minimize the output of the phase detector. This output is minimized when the voltage-controlled oscillator operates at frequency $\omega_2 = \omega_1 + \omega_0 - \omega_i$ and has a phase given by $\phi_2 = \phi_1 + \phi_0 - \phi_i$. Consequently, the phase of the signal from the second mixer is locked to that of the reference oscillator. Since the signals from all elements are locked to the same reference signal, they are in phase with each other and may be added directly. The gain of the array is thereby achieved for reception.

For the transmitting function, the signal for the voltage-controlled oscillator is up-converted, modulated by the desired transmitter intelligence, and fed to the radiating element. The phase is $\phi_4 = \phi_3 + \phi_1 + \phi_0 - \phi_i$. The term $\phi_3 + \phi_1 + \phi_0$ is common to all elements and so may be neglected. The remaining term, $-\phi_i$, is the negative of the phase of the incident wave, and the transmitted signal will be directed back toward the source of the incident wave. As in the phase-inversion type of systems, the doppler shifts may be preserved by the addition of a single phase-locked loop that causes the local oscillator, reference oscillator, and transmitter frequencies to track the incoming doppler shifts.

In the phase-inversion system, there is receiver noise superimposed on the received pilot signal for retransmission. The bandwidth of the filters used in the retransmission process will determine the relative magnitudes of the retransmitted pilot signal and this receiver noise. Unless filters that can have very narrow noise bandwidths are used, the noise relative to the retransmitted pilot signal can be appreciable when the incident pilot signal level is small. For the system that uses phase-locked loops, there is essentially no additive noise on the retransmitted signal, but there is phase noise that is introduced by the jitter in the voltage-controlled oscillators of the phase-locked loops. When the loops are operating properly, however, the phase noise can be expected to be small. Experience with probes such as Mariner IV indicates that the phase noise on a single channel is acceptable, at least for the bit rates used (about 8-1/3 bits per second at Earth-Mars distances).

The construction of phase-locked loops is more complex than that of the mixers and filters required for the phase-inversion systems, but the performance of systems using them may be greatly superior to the performance of the simpler phase-inversion systems. This comparison is especially true when the individual modules are operating at low signal-to-noise ratios. Because of this prospect of better performance, the system using phase-locked loops appears the more desirable for reception. However, from an economic point of view it might be more advantageous to put additional power into the incident signal and to use the simpler phase-inversion scheme than to use the more complicated phase-locked receiving system on the spacecraft.

Characteristics of Transmission Links

Though the details of a Mars or other planetary probe mission are still somewhat undefined, some of the general characteristics of such a mission are available as a guideline to the type of communication links that will be required. It has been assumed during this investigation that the mission will be carried out using a parent vehicle or bus that will orbit the planet and a capsule that will land on the planet. As the bus approaches the planet before going into orbit, the capsule will be ejected and will land on

the planet surface and transmit information back to earth either directly or by relaying the information through the bus. The use of high-gain electronically steerable arrays on the lander capsule and the orbiting bus would permit the transmission of information at high data rates. These reduce the time required for transmission of a given amount of data, or even more advantageous, they permit a reduction in the error probability for a given data rate. It was assumed that the orbiting bus will be a three-axis stabilized vehicle. The capsule/lander may be spin-stabilized during separation and entry. After it lands, its position with respect to the planet surface is, of course, fixed.

The exact nature of the arrays that could be used depends on the configurations of the vehicles. Some array forms can be postulated for somewhat general vehicle shapes. For example, two mechanically fixed, opposite-facing arrays might be used on the orbiting vehicle, each to be used during the time when it generally faces the planet. A single electronics package containing the retrodirective controls could be switched between the two arrays so that the required electronics are kept to a minimum.

As a possible capsule shape, the lenticular arrangement illustrated in figure 4 might be considered. Array elements are distributed over the upper and lower surfaces. The elements are shown as spirals but any other appropriate element could be used. During separation from the bus and entry, the elements on one surface of the capsule would be connected to the retrodirective circuitry. After the landing on the Mars surface, the elements on the upward facing surface would be connected; selection would be
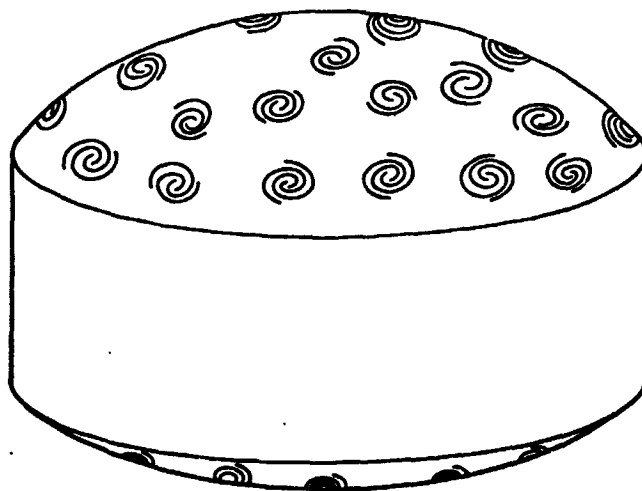
Figure 4. Lenticular capsule with spiral elements distributed over its surface.

obtained by some means such as a gravity sensing device. The retro-directive characteristics of the antennas would then allow the narrow, high-gain beams of the orbiting bus and the capsule/lander to track each other over angular regions determined primarily by the coverage pattern of the individual array elements. Actual allowable communication times achievable will depend on the orbital characteristics of the bus and on the lander position. Since the transmission distances in the relay link are relatively short, retrodirective systems using phase inversion by mixing may be applicable. Such a system is analyzed in a later section of the report.

Communication from the bus to the earth might also employ another retrodirective array on the bus. Since the transmission distance to the earth is very great, it will probably be necessary to use phase-locked loop techniques in this system in order to achieve sufficiently narrow bandwidths in the tracking loops.

Analysis of Systems that Use Phase-Locked Loops

A general study of the performance of self-steering arrays that use phase-locked loops was carried out for six digital modulation schemes: coherent phase shift key (PSK), differentially coherent PSK (DPSK), coherent and incoherent frequency shift key (FSK), and coherent and incoherent amplitude shift key (ASK). The approach used was as follows. Each modulation system was first analyzed for the single-element case. Then the results were extended to include multiple-element adaptive arrays, and curves of error probabilities versus signal-to-noise ratios were plotted with rms phase error as a parameter.

The formulation of a specific system was deliberately avoided in the analysis in order that an optimum system could be analyzed. This approach allowed the comparison of modulation schemes to be made on a fair basis. Nevertheless, it is convenient to have a generalized block diagram of a receiver for purposes of discussion. Such a diagram is shown in figure 5.
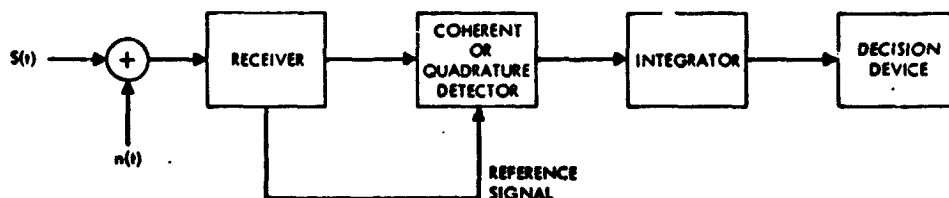
Figure 5. Generalized receiving system.

In this generalized system, the desired signal plus additive noise is fed to an ideal receiver and then to a coherent or quadrature detector, depending on whether a coherent or incoherent modulation system is being employed. The detected signal is integrated over the duration of a symbol and then fed to a decision device that selects from all possible symbols the one that was most likely transmitted. The reference signal for the coherent or quadrature detector is assumed to be derived in some manner from the received signal. Consequently, the reference signal will have some phase uncertainty which will affect detection of coherent systems. This phase uncertainty is a function of received signal-to-noise ratio but for purpose of analysis it has been assumed to be an independent quantity. This method of analysis was convenient because it did not require a model for relating the two quantities. The relationship between signal-to-noise and rms phase uncertainty is considered in a later section (page 37) for a special case.

Coherent phase shift key modulation. — In a coherent m-ary phase shift key (PSK) system, the alphabet of possible symbols consists of waves whose phases take on the values $\frac{2\pi i}{m}$ where i ranges from 0 to (m - 1). The decision rule used in selecting which symbol was transmitted based on the received signal is to select that symbol whose location in signal space is closest to the received signal. Signal space concepts are discussed in Appendix A. The analysis of an m-ary coherent PSK system in the presence of additive noise and with a noisy phase reference is presented in Appendix B. (The effect of finite bandwidth is considered in Appendix C.) The analysis of Appendix B results in the following integral for the probability of error per symbol.

$$
P_e = \frac{2}{(2\pi)^{3/2} \sigma_\theta} \int_0^\infty \exp\left[-\frac{\theta^2}{2\sigma_\theta^2}\right] d\theta \left[\int_{\frac{\pi}{m}}^{\pi+\theta} \exp\left[-\frac{E}{2N_0} \frac{\sin^2\left(\theta - \frac{\pi}{m}\right)}{\sin^2\left(\beta - \frac{\pi}{m}\right)}\right] d\theta \right.
$$

$$
\left. + \int_{\pi+\theta}^{2\pi-\frac{\pi}{m}} \exp\left[-\frac{E}{2N_0} \frac{\sin^2\left(\theta + \frac{\pi}{m}\right)}{\sin^2\left(\beta + \frac{\pi}{m}\right)}\right] d\theta \right] \tag{1}
$$

where θ is the phase error in the reference signal, σ_θ^2 is the variance of θ (assumed gaussian), E is the energy in the received symbol, and N_0 is the two-sided noise spectral density (assumed flat over the region of interest).

12

For the binary case (m = 2) this equation reduces to the relatively simple expression:

$$P_e = 1 - \frac{1}{2\pi\sigma_\theta} \int_{-\infty}^{\infty} \left[\exp\left(-\frac{\theta^2}{2\sigma_\theta^2}\right) \int_{-\infty}^{\sqrt{\frac{E}{N_0}}\cos\theta} \exp\left(-\frac{x^2}{2}\right) dx \right] d\theta \qquad (2)$$

The expression for probability of error for the m-ary case can be put into more easily evaluated forms for the limiting cases of low signal-to-noise ratio and high signal-to-noise ratio (SNR = $E/(2N_0)$). For the case of low SNR ($E/2N_0) \to 0$) the limiting form is

$$P_e \sim 1 - \frac{1}{m} - \sqrt{\frac{E}{2N_0}} \frac{\sin\left(\frac{\pi}{m}\right)}{\sqrt{\pi}} \exp\left(-\frac{\sigma_\theta^2}{2}\right) - \frac{E}{2N_0} \frac{\sin\left(\frac{2\pi}{m}\right)}{2\pi} \exp\left(-2\sigma_\theta^2\right) \qquad (3)$$

As the signal-to-noise ratio becomes very large, a different expansion is used. It is given by

$$P_e \sim 1 - \sum_{n=-\infty}^{\infty} \left[\Phi\left(\frac{\frac{\pi}{m} + 2n\pi}{\sigma_\theta}\right) - \Phi\left(\frac{-\frac{\pi}{m} + 2n\pi}{\sigma_\theta}\right) \right] \qquad (4)$$

where

$$\Phi(x) \equiv \frac{1}{\sqrt{2\pi}} \int_{-\infty}^{x} \exp\left(-\frac{u^2}{2}\right) du \qquad (5)$$

When $\sigma_\theta \ll \pi$, only the n = 0 term is significant and equation (4) reduces to

$$P_e \sim 2\Phi\left(-\frac{\pi}{m\sigma_\theta}\right) \qquad \text{for } \sigma_\theta \ll \pi \qquad (6)$$

$$\text{as } \frac{E}{2N_0} \to \infty$$

This expression shows that for high signal-to-noise ratios the probability of error per symbol increases as m increases.

Differentially coherent phase shift key modulation. — In a system that u̇es differentially coherent PSK (DPSK), the coherent reference is obtained by delaying the received signal by the duration of one character and by noting the change in phase between the delayed signal and the incoming signal. The ith character of an m-ary alphabet is transmitted by phase shifting the signal by an amount $i\,2\pi/m$ over that of the previous signal. The detection consists of computing the angular difference between adjacent received signals. The angular separation between these signals as represented on a polar plot may be designated as ψ. A decision is made by selecting the multiple of $2\pi/m$ that lies nearest to ψ. This decision criterion is in fact the optimum one to use. The analysis of the system is given in Appendix D.

The mean probability of error per symbol is

$$P_e = \frac{1}{\pi} \int_{\eta=\pi/m}^{\pi} \int_{\psi=0}^{\pi/2} \sin\psi \left[1 + \frac{E}{2N_0} (1 + \cos\eta\,\sin\psi) \right] \exp\left[-\frac{E}{2N_0} (1 - \cos\eta\,\sin\psi) \right] d\psi\,d\eta \tag{7}$$

For low signal-to-noise ratios, equation (7) may be expanded directly in powers of $E/2N_0$ to give the following expression to first order,

$$P_e = \left(1 - \frac{1}{m} \right) - \frac{E}{4N_0} \sin\frac{\pi}{m} \tag{8}$$

For high signal-to-noise ratios, Arthurs and Dym (ref. 18) derived an approximate expression for P_e for m >4. It is given by

$$P_e \sim 2\Phi\left(-\sqrt{\frac{E}{N_0}} \sin\frac{\pi}{m\sqrt{2}} \right) \qquad \frac{E}{2N_0} \gg 1 \tag{9}$$

For the binary case, equation (7) may be evaluated in closed form to give

$$P_e = \frac{1}{2} \exp\left[-\frac{E}{2N_0} \right] \tag{10}$$

A separate derivation of equation (10) is given in Appendix D.

Coherent frequency shift key modulation. — In the frequency shift key (FSK) scheme, the ith character of the signal alphabet corresponds to a signal at a corresponding angular frequency ω_i. The signal processing consists of mixing the received signal with a set of coherent local oscillators, one at each frequency ω_i, and integrating the resulting signals over a symbol period. The decision consists of deciding that the received signal is that corresponding to the largest integrator output. The processing is illustrated in figure 6. The reference oscillators contain independent, gaussian, random phase errors denoted by θ_k. The system is analyzed in Appendix E.

The probability of error per symbol is given by

$$P_e = 1 - \frac{1}{\left(2\pi N_0\right)^{m/2}} \int_{-\infty}^{\infty} \frac{\exp\left[-\frac{\theta^2}{2\sigma_\theta^2}\right]}{\sqrt{2\pi}\,\sigma_\theta^2} \int_{-\infty}^{\infty} \exp\left[\frac{-(z - \sqrt{E}\cos\theta)^2}{2N_0}\right]\left[\int_{-\infty}^{z} \exp\left[\frac{-u^2}{2N_0}\right]du\right]^{m-1} dz\, d\theta \quad (11)$$

The binary case may be obtained from this expression directly and may be put into the following form.

$$P_e = \frac{1}{\sqrt{2\pi}\,\sigma_\theta} \int_{-\infty}^{\infty} \exp\left[-\frac{\theta^2}{2\sigma_\theta^2}\right] \phi\left(-\sqrt{\frac{E}{2N_0}}\cos\theta\right) d\theta \quad (m=2) \qquad (12)$$

The asymptotic value of P_e for high signal-to-noise ratios may be derived from equation (11) by letting z be replaced by $(t + \sqrt{E}\cos\theta)$. The last integral then approaches unity for $\cos\theta > 0$ and zero for $\cos\theta < 0$. The resulting expression may then be evaluated asymptotically when $\cos\theta > 0$ to yield

$$\lim_{\frac{E}{2N_0} \to \infty} P_e = 2 \sum_{n=0}^{\infty} (-1)^n \phi\left(-\frac{2n+1}{2\sigma_\theta}\pi\right) \qquad (13)$$

When $\sigma_\theta \ll \pi$, only the $n = 0$ term is significant and equation (13) reduces to

$$\lim_{\frac{E}{2N_0} \to \infty} P_e = 2\phi\left(-\frac{\pi}{2\sigma_\theta}\right) \quad \text{for } \sigma_\theta \ll \pi \qquad (14)$$
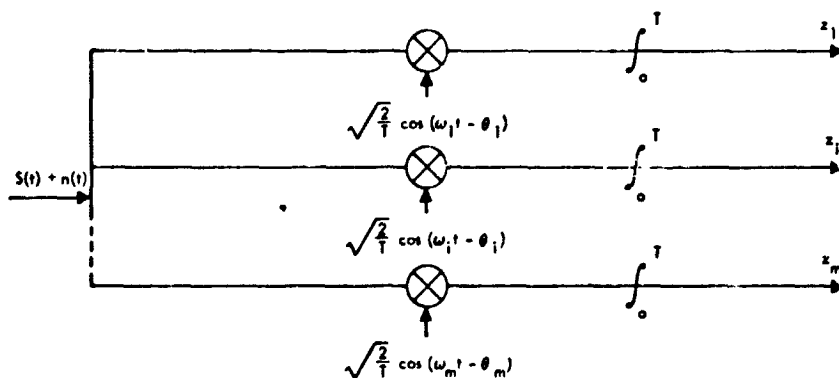
Figure 6. Coherent FSK detection system.

Thus, as the signal-to-noise ratio increases without limit, the probability of error approaches a value that is independent of m.

As the signal-to-noise ratio becomes small, there is no simple method of obtaining an expression that shows how the probability of error approaches its limiting value, except when m = 2. The limiting value itself may be obtained by letting $E/2N_0$ equal zero in equation (6) of Appendix E. It is given by

$$\lim_{\frac{E}{2N_0} \to 0} P_e = 1 - \frac{1}{m} \tag{15}$$

as would be expected since each symbol is equally likely and only one can be correctly interpreted. For the binary case a simple asymptotic expression is available by recognizing that equation (12) is just equation (2) with E replaced by E/2. Therefore, the same expansion used in the derivation of equation (3) may be used for m equal to 2, with the result that for low signal-to-noise ratios,

$$P_e \sim 1 - \frac{1}{m} - \sqrt{\frac{E}{4N_0\pi}} \exp\left[-\frac{\sigma_\theta^2}{2}\right] \tag{16}$$

Incoherent frequency shift key modulation. — Under conditions in which the phase of the incoming FSK signal is not known a priori, squared envelope correlation detection minimizes the probability of error. A system for such detection is shown in figure 7. If z_i^2 is the greatest signal, then it is assumed that the symbol of frequency ω_i was transmitted. This is the optimum decision criterion. The analysis of the system is in Appendix F. The resulting probability of error per symbol is

$$P_e = \frac{1}{m} \exp \left[- \frac{E}{4N_0} \right] \sum_{k=2}^{m-1} \binom{m}{k} (-1)^k \exp \left[\frac{E(2-k)}{4N_0 k} \right] \qquad (17)$$

For the special case of $m = 2$, this expression simplifies to

$$F_e = \frac{1}{2} \exp \left[- \frac{E}{4N_0} \right] \qquad (18)$$
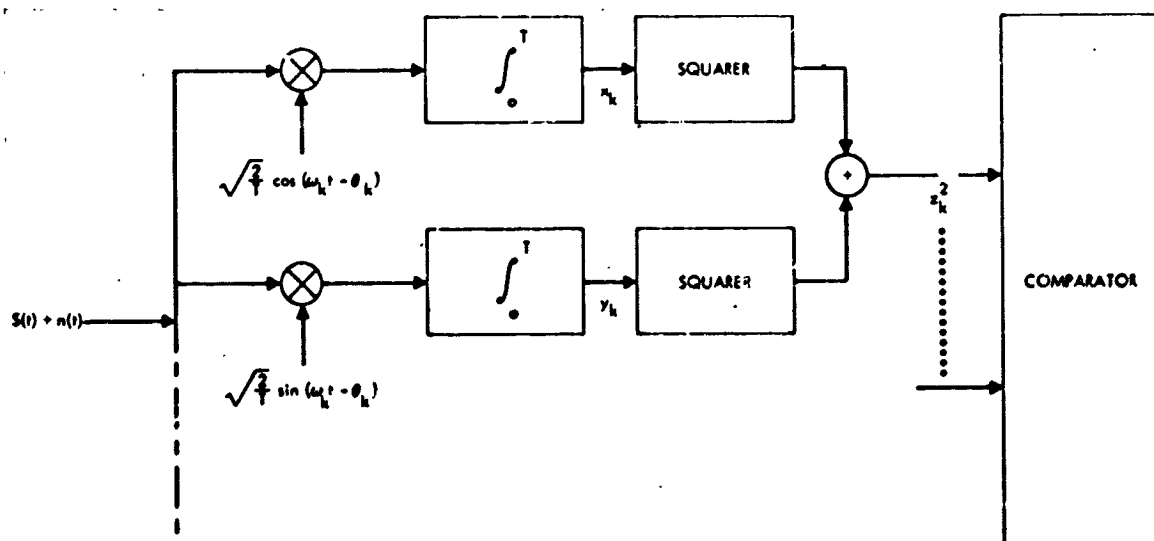
Figure 7. Incoherent FSK detection system.

Coherent amplitude shift key modulation. — In the m-ary amplitude shift key (ASK) scheme, information is transmitted by assigning each of m different equally spaced signal amplitudes to a particular symbol. The signal alphabet is composed of m sinusoidally varying signals of different amplitudes. It is assumed that E_1 is the lowest level and E_m is the highest level. As in the other coherent systems, the incoming signal is mixed with a local oscillator signal and integrated over a symbol period as illustrated in figure 8. The decision device selects the symbol corresponding to the level nearest the received level. Appendix G contains the analysis of coherent ASK modulation systems.
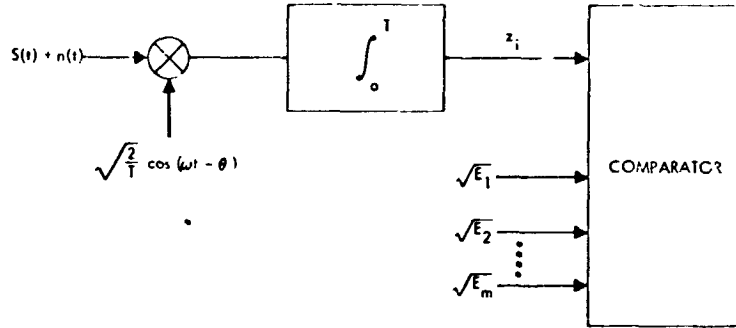
Figure 8. Coherent ASK detection system.

The local oscillator is assumed to have a phase uncertainty, θ. The mean probability of error per symbol is given by

$$P_e = \frac{1}{m} \hat{\Phi} \left(-\frac{\Delta}{2\sqrt{N_0}}\right) + \frac{m-2}{m}$$

$$- \frac{1}{m\sqrt{2\pi}\,\sigma_\theta} \int_{-\infty}^{\infty} \sum_{k=1}^{m-2} \hat{\Phi}\left(\frac{k\Delta}{\sqrt{N_0}}\left[1 + \frac{1}{2k} - \cos\theta\right]\right) \exp\left(\frac{-\theta^2}{2\sigma_\theta^2}\right) d\theta$$

$$+ \frac{1}{m\sqrt{2\pi}\,\sigma_\theta} \int_{-\infty}^{\infty} \sum_{k=1}^{m-1} \hat{\Phi}\left(\frac{k\Delta}{\sqrt{N_0}}\left[1 - \frac{1}{2k} - \cos\theta\right]\right) \exp\left(\frac{-\theta^2}{2\sigma_\theta^2}\right) d\theta$$

(19)

where

$$\Delta = \sqrt{\frac{6E}{(m-1)(2m-1)}}$$

(20)

and E is the average energy per symbol. The limiting value for P_e as the signal-to-noise ratio increases without limit may readily be obtained from equation (19) with the result that as $E/N_0 \to \infty$, the probability of error becomes

$$\lim_{E/N_0 \to \infty} P_e = \frac{1}{m\sqrt{2\pi}\,\sigma_\theta} \sum_{k=1}^{m-1} \int_{\theta:\cos\theta < 1 - \frac{1}{2k}} \exp\left(\frac{-\theta^2}{2\sigma_\theta^2}\right) d\theta$$

(21)

18

When $\sigma_\theta \ll \pi$, only the integration over the ranges of θ nearest the origin gives a significant contribution to the probability of error. Under this assumption the expressions for the probability of error for several specific values of m can be tabulated:

m = 2

$$P_e \to \Phi\left(-\frac{1.048}{\sigma_\theta}\right) \tag{22a}$$

m = 4

$$P_e \to \frac{1}{2}\left[\Phi\left(-\frac{0.585}{\sigma_\theta}\right) + \Phi\left(-\frac{0.723}{\sigma_\theta}\right) + \Phi\left(-\frac{1.048}{\sigma_\theta}\right)\right] \tag{22b}$$

m = 8

$$P_e \to \frac{1}{4}\left[\Phi\left(-\frac{0.379}{\sigma_\theta}\right) + \Phi\left(-\frac{0.412}{\sigma_\theta}\right) + \Phi\left(-\frac{0.451}{\sigma_\theta}\right) + \Phi\left(-\frac{0.506}{\sigma_\theta}\right)\right.$$

$$\left. + \Phi\left(-\frac{0.585}{\sigma_\theta}\right) + \Phi\left(-\frac{0.723}{\sigma_\theta}\right) + \Phi\left(-\frac{1.048}{\sigma_\theta}\right)\right] \tag{22c}$$

m = 16

$$P_e \to \frac{1}{8}\left[\Phi\left(\frac{-0.258}{\sigma_\theta}\right) + \Phi\left(\frac{-0.265}{\sigma_\theta}\right) + \Phi\left(\frac{-0.276}{\sigma_\theta}\right) + \Phi\left(\frac{-0.291}{\sigma_\theta}\right) + \Phi\left(\frac{-0.301}{\sigma_\theta}\right)\right.$$

$$+ \Phi\left(\frac{-0.318}{\sigma_\theta}\right) + \Phi\left(\frac{-0.335}{\sigma_\theta}\right) + \Phi\left(\frac{-0.356}{\sigma_\theta}\right) + \Phi\left(\frac{-0.379}{\sigma_\theta}\right) + \Phi\left(\frac{-0.412}{\sigma_\theta}\right)$$

$$\left. + \Phi\left(\frac{-0.451}{\sigma_\theta}\right) + \Phi\left(\frac{-0.506}{\sigma_\theta}\right) + \Phi\left(\frac{-0.585}{\sigma_\theta}\right) + \Phi\left(\frac{-0.723}{\sigma_\theta}\right) + \Phi\left(\frac{-1.048}{\sigma_\theta}\right)\right] \tag{22d}$$

For low signal-to-noise ratios equation (19) becomes

$$P_e \approx \left(\frac{m-1}{m}\right)\left[1 - \sqrt{\frac{3E}{\pi(m-1)(2m-1)N_0}}\, \exp\left(-\frac{\sigma_\theta^2}{2}\right)\right] \tag{23}$$

Incoherent amplitude shift key modulation. — When the phase of the incoming signal is not known a priori, an incoherent system must be used for detection of ASK modulation. The detection system is a squared envelope detector as shown in figure 9. Following Arthurs and Dym (ref. 18), the decision rule adopted is to assume that the signal transmitted is that of the amplitude level closest to the value of z . This decision criterion approaches optimum as the signal-to-noise ratio increases (ref. 18). Incoherent ASK modulation is analyzed in Appendix I:.

The mean probability of error is

$$P_e = 1 - \frac{1}{m}\sum_{i=1}^{m} P(z \in R_i \mid S_i) \tag{24}$$

where

$$P(z \in R_i \mid S_i) = \int_{\left(i-\frac{3}{2}\right)\frac{\Delta}{\sqrt{N_0}}}^{\left(i-\frac{1}{2}\right)\frac{\Delta}{\sqrt{N_0}}} \nu\, I_0\left(\nu\,\frac{(i-1)\Delta}{\sqrt{N_0}}\right)\exp\left[-\frac{1}{2}\left(\nu^2 + \frac{E_i}{N_0}\right)\right]d\nu \quad i=2,\dots,(m-1)$$

$$\tag{25a}$$

$$P(z \in R_1 \mid S_1) = \int_{0}^{\frac{\Delta}{2\sqrt{N_0}}} \nu\, \exp\left(-\frac{\nu^2}{2}\right)d\nu = 1 - \exp\left(-\frac{\Delta^2}{8N_0}\right) \tag{25b}$$

$$P(z \in R_m \mid S_m) = \int_{\left(m-\frac{3}{2}\right)\frac{\Delta}{\sqrt{N_0}}}^{\infty} \nu\, I_0\left(\nu\,\frac{(m-1)\Delta}{\sqrt{N_0}}\right)\exp\left[-\frac{1}{2}\left(\nu^2 + \frac{(m-1)^2\Delta^2}{N_0}\right)\right]d\nu$$

$$\tag{25c}$$

$$E_i = (i - 1)^2 \Delta^2 \tag{26}$$

and Δ is related to E, the average energy per symbol by equation (20).

For the binary case, equation (24) reduces to

$$P_e = \frac{1}{2} \exp\left(-\frac{E}{4 N_0}\right) + \frac{1}{2}\left[1 - \exp\left(-\frac{E}{N_0}\right)\int_{\sqrt{\frac{E}{2 N_0}}}^{\infty} \nu I_0\left(\nu \sqrt{\frac{2E}{N_0}}\right)\exp\left(-\frac{\nu^2}{2}\right)d\nu\right]$$

$$\tag{27}$$

There appears to be no straightforward method of obtaining asymptotic expansions for equations (24) or (27) for high signal-to-noise ratios. However, Arthurs and Dym (ref. 18) have derived a lower bound on the error probability that is approached at high signal-to-noise ratios. It is given by

$$P_e \geq \frac{1}{m} \exp\left(-\frac{\Delta^2}{8 N_0}\right) \qquad \frac{\Delta}{N_0} \to \infty \tag{28}$$

For low signal-to-noise ratios the integrals may be expanded in powers of Δ/N_0 yielding the following limiting form for P_e

$$P_e \approx \left(1 - \frac{1}{m}\right) 9 \frac{(2 m^4 - 8 m^3 + 11 m^2 + 44 m - 99)}{(m - 1)^2 (2 m - 1)^2 m}\left(\frac{E}{2 N_0}\right)^2 \qquad \left(\frac{E}{2 N_0}\right) \to 0$$

$$\tag{29}$$
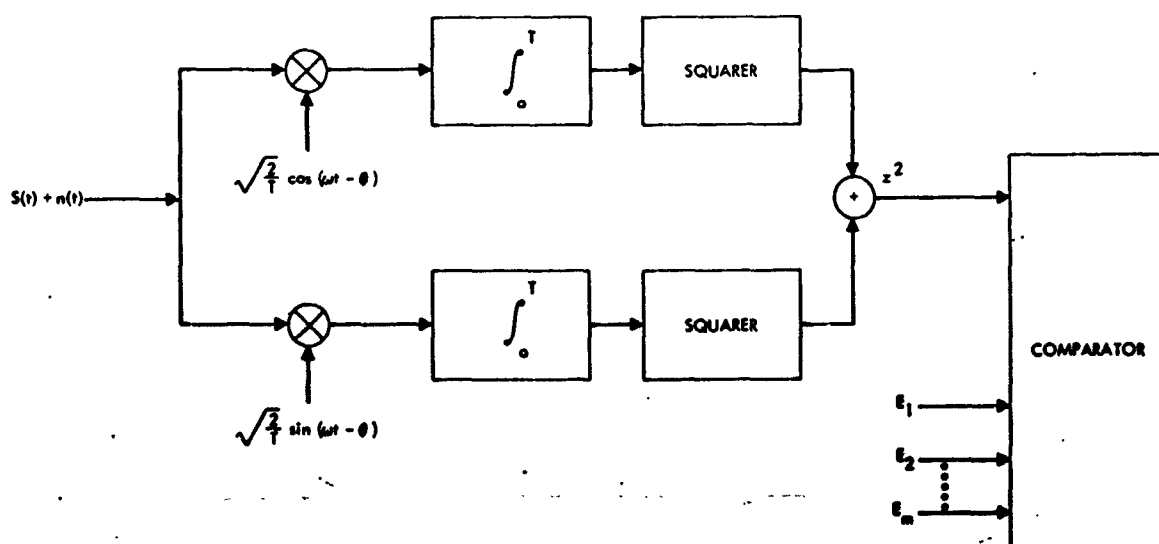
Figure 9. Incoherent ASK detection system.

Model of Array

The results of the single element case were modified to take account of arrays of elements whose outputs are combined through adaptive receivers before detection and decision. A number of approximations are made in the analysis that lead to some particularly simple results.

The analysis was performed under the assumption that the array and system are composed of identical antenna elements whose outputs are connected together at a summing point after being brought into phase by adaptive receivers. A typical channel is shown in figure 10. It was assumed that n_k, the noise in each channel, is independent, additive, gaussian noise with zero mean and a flat spectral density, N_0. The phase error common to all elements is denoted by θ, a gaussian random variable with zero mean and variance σ_θ^2. The independent phase errors in each channel are denoted by β_k and are also gaussian random variables with zero mean and variance σ_β^2. The phase errors, β_k, were specifically treated as arising in the adaptive receiver and θ in the coherent detector (for incoherent systems θ has no effect on probability of error). However, the phase errors may also be considered to be contained in the incident signal as well, so that a medium whose phase shift is random was implicitly included in the analysis.

An exact analysis of the probabilities of error could have been carried out for all systems, but the results would be in the form of multiple integrals and not very useful for purposes of computation. In any practical operating situation, it is expected that the adaptive receivers would maintain the β_k at small values so that an approximate theory of the effects of the arraying was worked out.
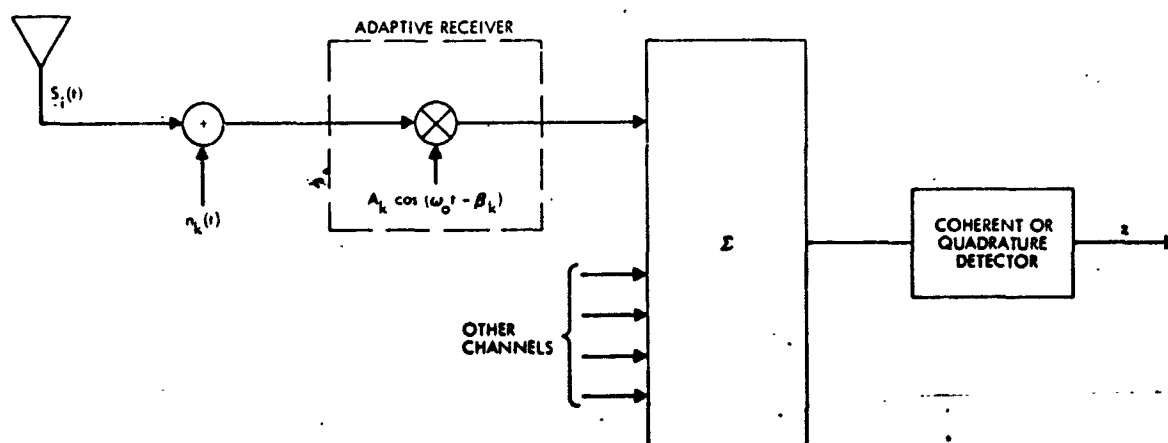
Figure 10. Adaptive array model.

From the analysis in Appendix I, it was found that the results of the single element case may be carried over to arrays of identical elements of moderate and large size merely by replacing (E/N_0), the signal-to-noise ratio for each element, with (E'/N_0') where

$$\frac{E}{N_0}\left(\frac{\exp(-\sigma_\beta^2)}{\sum\limits_{i=1}^{M} A_i^2} + \left[1 - \exp(-\sigma_\beta^2)\right]\right) \equiv \frac{E'}{N_0'} \qquad (30)$$

and by replacing σ_θ with σ_γ where

$$\sigma_\gamma^2 = \sigma_\theta^2 + \sigma_\beta^2 \sum\limits_{i=1}^{M} A_i^2 \qquad (31)$$

M is the number of elements and the A_i are the amplitude weighting coefficients of the element excitations normalized so that

$$\sum\limits_{i=1}^{M} A_i = 1 \qquad (32)$$

The results for the single channel cases can, therefore, be carried over directly to arrays when M is large and/or σ_β is sufficiently small.

Numerical Results for Probabilities of Error

Probabilities of error for all modulations discussed, except incoherent ASK, were computed and are presented in graphic form. The abscissas of the graphs are labeled in terms of effective signal-to-noise ratio as given by equation (30).

23

Coherent phase shift key modulation. — The error probabilities per symbol are presented in detail for coherent binary PSK. Rms phase errors of 0.0, 0.20, 0.40, 0.60, 0.80, and 1.60 radians are included. They are shown in figure 11. Error probabilities per symbol for coherent m-ary PSK are shown for m = 2, 4, 8, and 16 and for two values of rms phase error, 0.20 and 0.40 radian, in figure 12. It can be seen that the probability of error per symbol increases rapidly as m increases. It can also be seen that a given phase error degrades performance more as m increases. This result is as would be expected, since as m increases, the signal points are moved closer together in signal space.
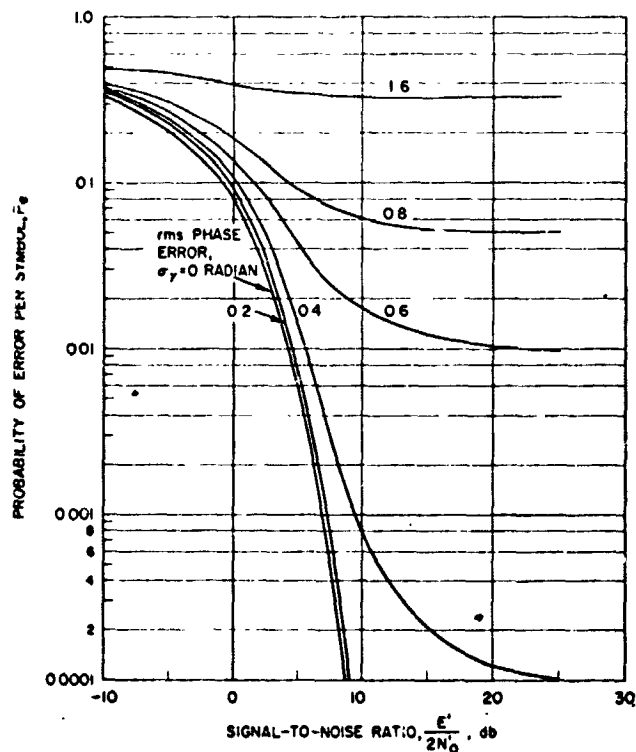
Figure 11. Average error probabilities for coherent binary PSK modulation for various rms phase errors.
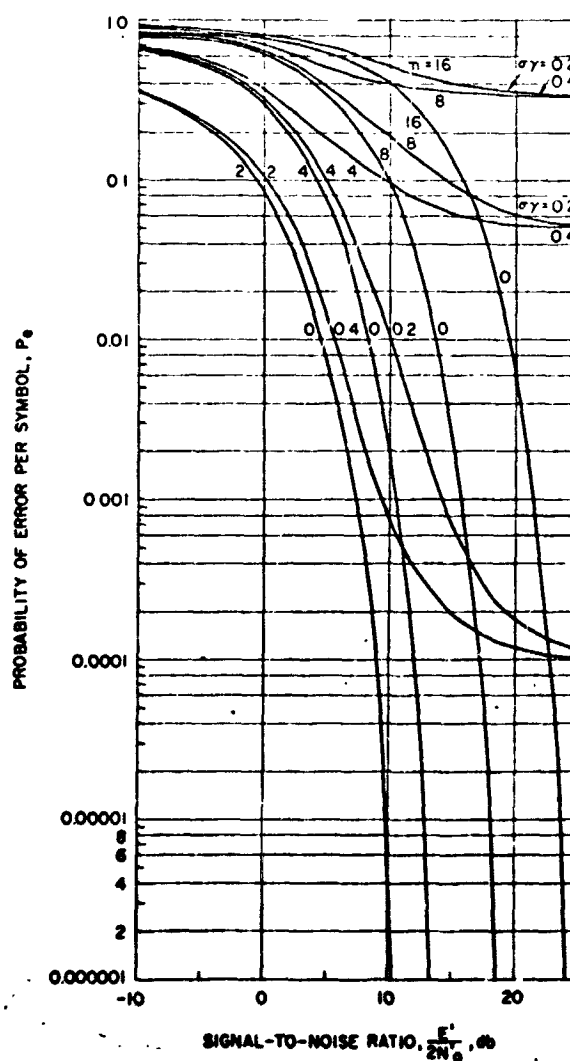
Figure 12. Average error probabilities for coherent m-ary PSK modulation for various rms phase errors.

Coherent frequency shift key modulation. — Figure 13 shows curves of the probability of error per symbol for m-ary coherent FSK modulation with an rms phase error of $\pi/8$ radians. The curves are shown for m = 2, 4, 8, and 16. The m = 2 case was evaluated from the binary coherent PSK case. The remaining curves are approximate. Their limiting values for high and for low signal-to-noise ratios were computed, and values for intermediate signal-to-noise ratios were estimated from the shape of the binary curve. On a probability of error-per-symbol basis, binary modulation is superior.

Coherent amplitude shift key modulation. — Curves of probability of error per symbol for binary coherent ASK modulation are shown for rms phase errors of 0.00, 0.20, 0.40, 0.60, 0.80, and 1.60 radians in figure 14. Curves for m-ary ASK with m = 2, 4, 8, and 16 and with rms phase errors of 0.0, 0.2 and 0.4 radian are shown in figure 15. From these curves it may be seen that coherent ASK degrades more rapidly with increasing phase errors than does coherent PSK.
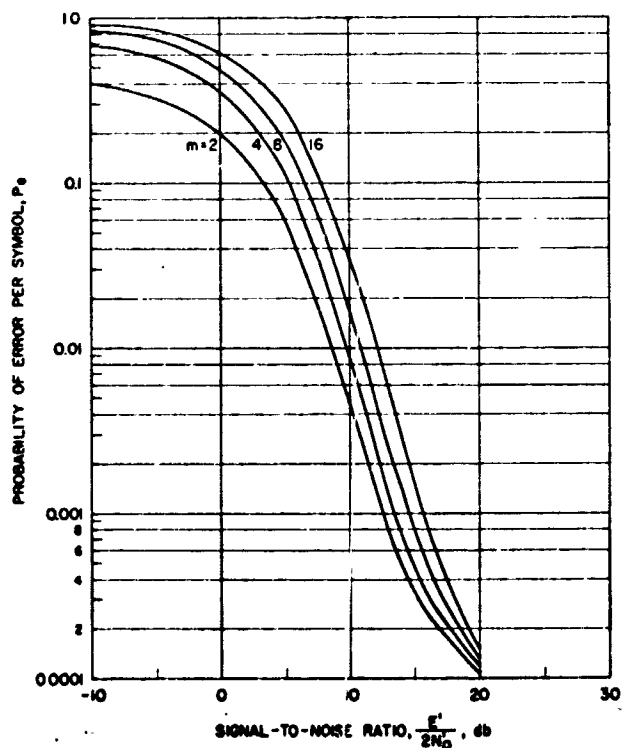
Figure 13. Average error probabilities for coherent m-ary FSK modulation for rms phase error of $\pi/8$ radians.
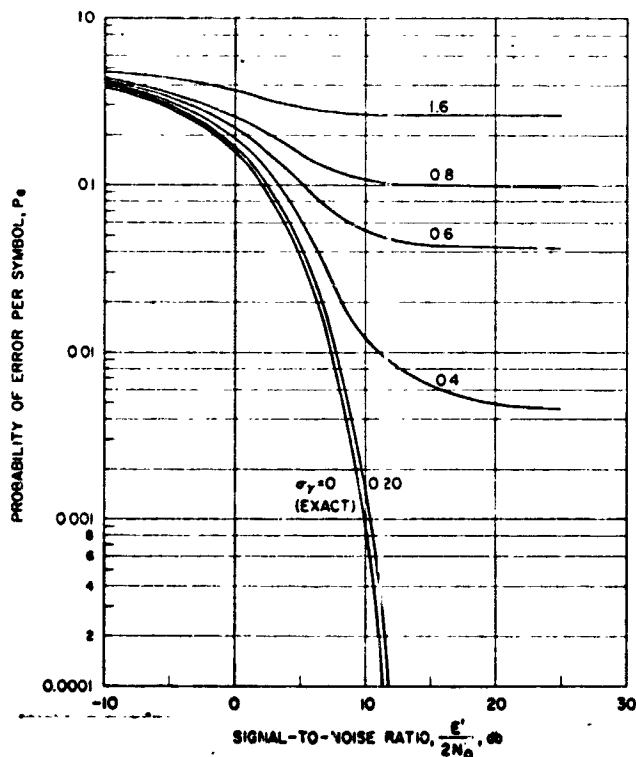
Figure 14. Average error probabilities for coherent binary ASK modulation for various rms phase errors.

25

(a) rms PHASE ERROR = 0.0 RADIAN

(b) rms PHASE ERROR = 0.2 RADIAN

(c) rms PHASE ERROR = 0.4 RADIAN
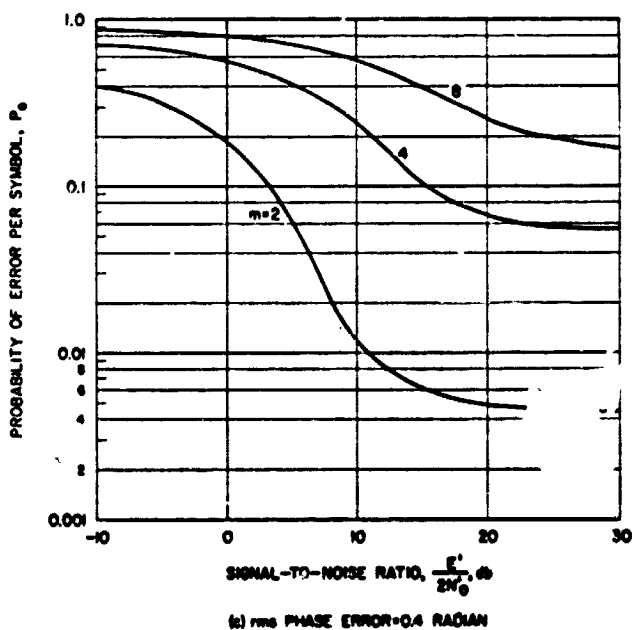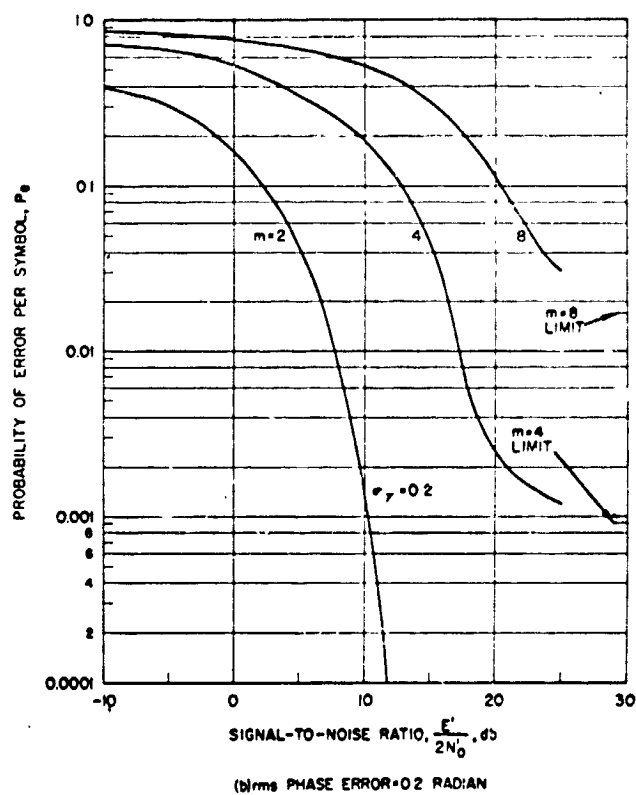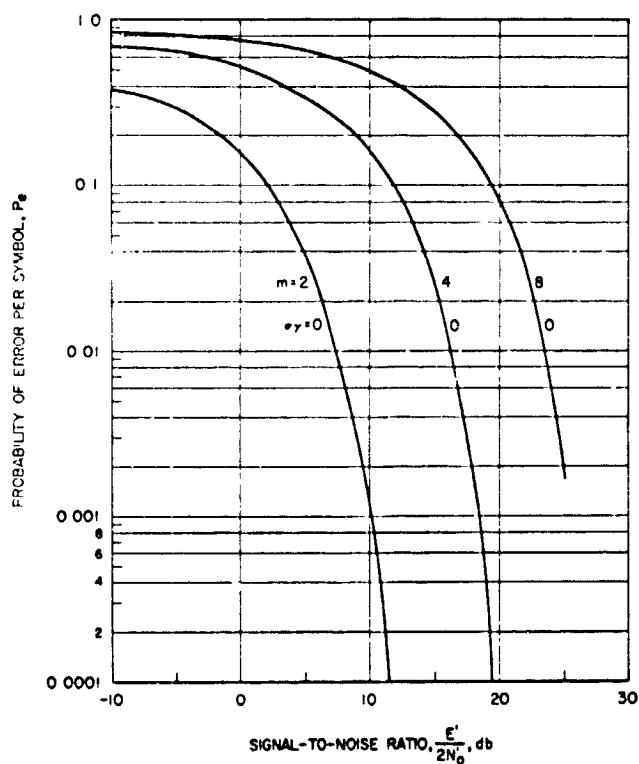
Figure 15.   Average error probabilities for coherent m-ary
ASK modulation for various rms phase errors.

Differentially coherent phase shift key modulation. – Error probabilities per symbol are shown in figure 16 for DPSK modulation. Since DPSK is not affected by phase errors, the curves are valid for any phase error and do not exhibit a limiting value at high signal-to-noise ratios. As with the previously discussed systems, binary systems minimize the probability of error per symbol.

Incoherent frequency shift key modulation. – Probabilities of error per symbol are shown for m-ary incoherent FSK modulation for m = 2, 4, 8, and 16 in figure 17.

Incoherent amplitude shift key modulation. – The probabilities of error for incoherent ASK have not been computed. Computational difficulties have precluded accurate calculations for this modulation.

Word Error Probabilities and Bandwidth Efficiencies of Various Modulating Methods

The results presented in the preceding section show the probability of error per symbol of various modulation schemes. A comparison is made of error probabilities of m level codes for various values of m. These data are necessary for determining the preferred modulation scheme for given
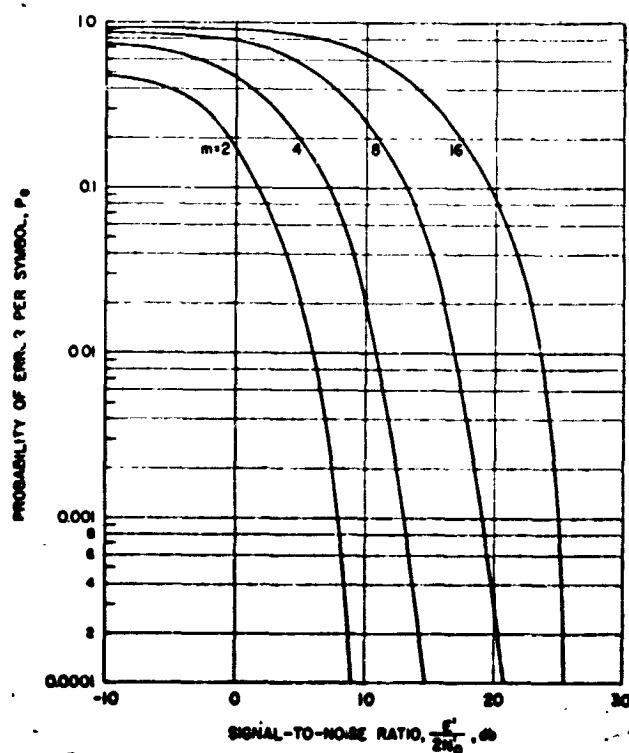
Figure 16. Average error probabilities for differentially coherent PSK modulation.
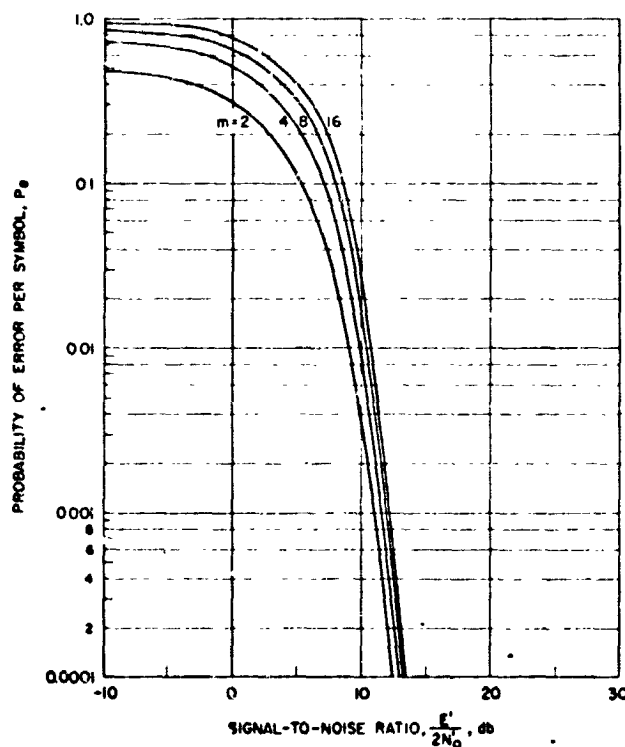
Figure 17. Average error probabilities for incoherent m-ary FSK modulation.

operating conditions. However, these error probabilities are computed with the side constraint that the transmission of each symbol, or character, involves the same amount of energy.

In the comparison of information channels, it is desirable to compute the probability of error per bit or per word. With a constant data rate constraint (i.e., for a given data rate) and with fixed available average power, an m level symbol will be permitted ($\lg_2 m$) times more energy than a binary signal since it carries that much more information (or bits). The earlier curves would have to be translated along the abscissa by ($\lg_2 m$) towards the origin to obtain modified curves that represent the constant data rate constraint.

The expected word length is another factor that should be taken into consideration, however, before a reasonable comparison can be made between the various modulations. Since most transmissions will involve words longer than a single bit, it is of interest to compare word error

probabilities for various modulations. The error probability for a word of n bits transmitted by means of m-ary symbols can be obtained from the m-ary symbol error probability as follows;

$$P_e(n \text{ bit word}) = 1 - \left[1 - P_e(m\text{-ary symbol}) \right]^{n/lg_2 m} \qquad (33)$$

where the transmission utilizes the $(n/lg_2 m)$ extension of the m-ary alphabet.

Figures 18 and 19 present plots of word error probabilities using the above criteria as modified from previously calculated symbol error probabilities. The abscissa is $E_b/2N_0$ where E_b is the energy per bit. Computed results are given for PSK coherent, DPSK, FSK coherent and incoherent, and ASK coherent modulations. The set of five graphs in figure 18 assumes a 4-bit word size, which is common for telemetry transmission. The graphs in figure 19 assume a 10-bit word size, which is common for command transmission.
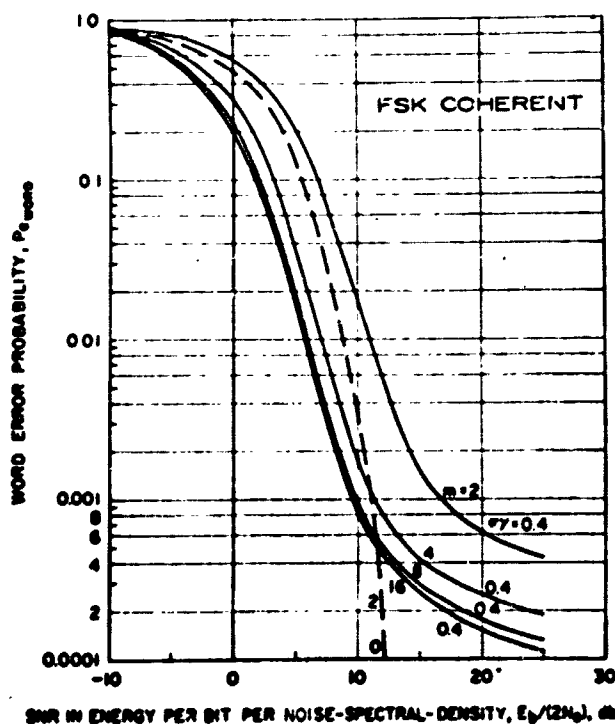
Figure 18. Word error probabilities for a constant word rate for 4-bit words for various modulation systems.
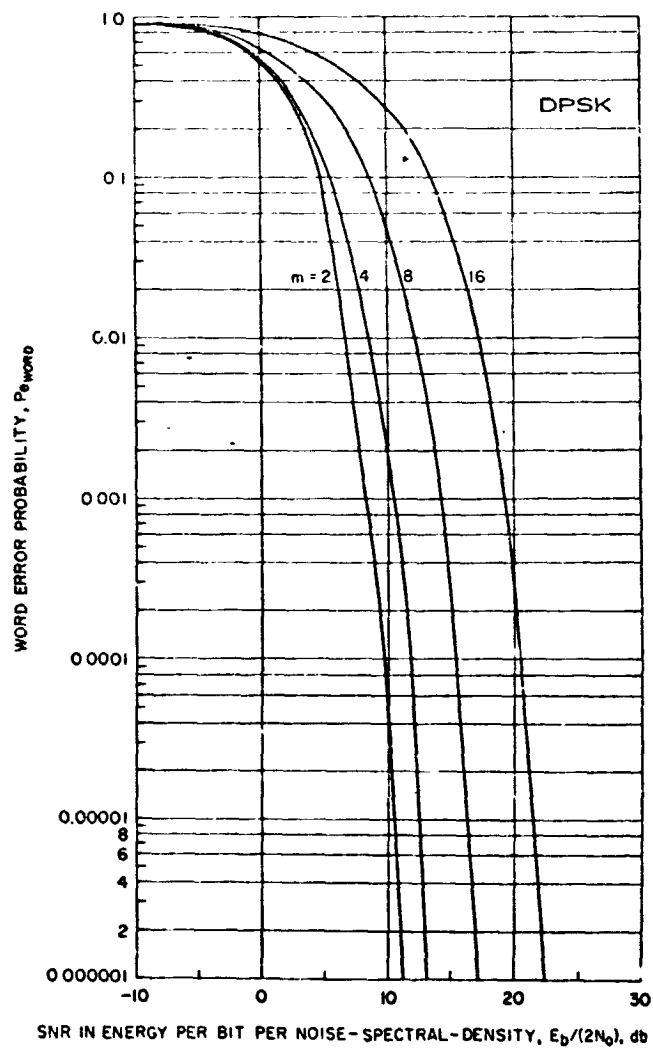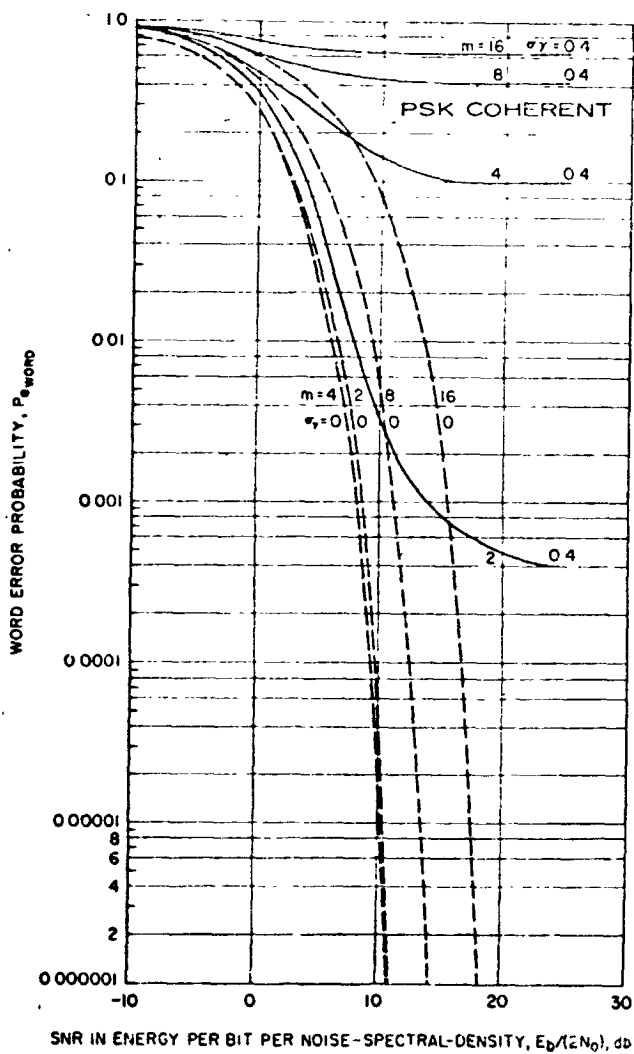
Figure 18. — Continued.
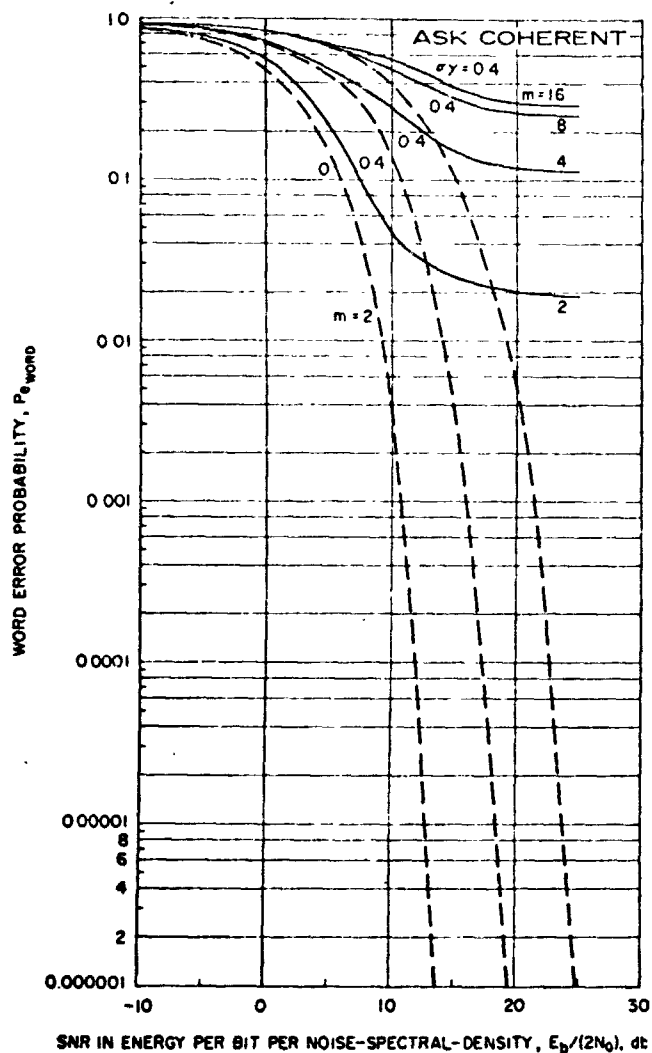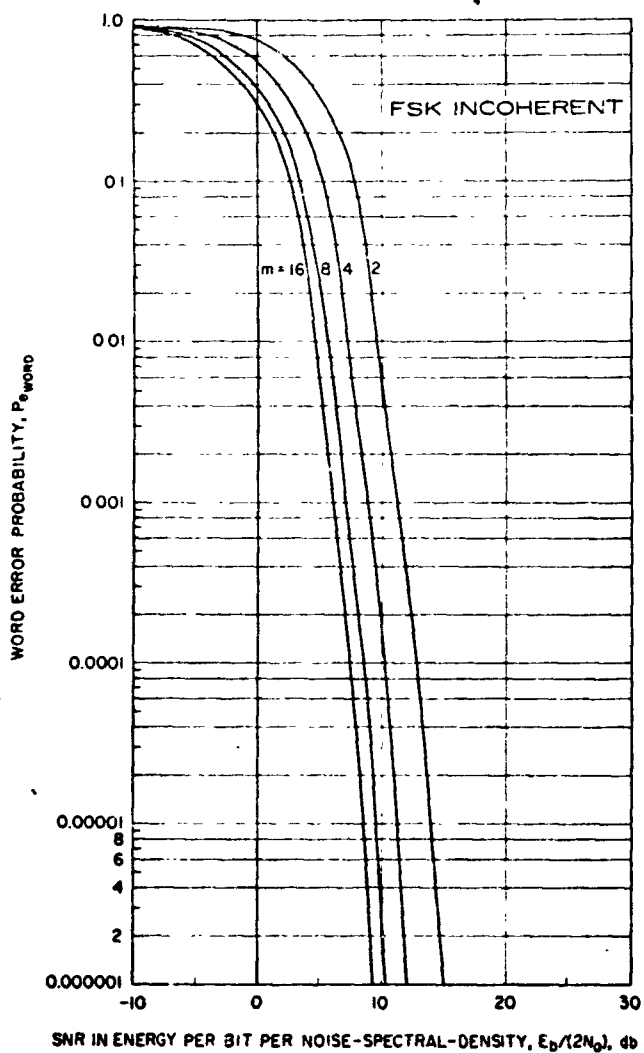
Figure 18. — Concluded.

A further consideration of importance in the comparison of information channels is that of bandwidth. Usually the attempt is to minimize the bandwidth occupancy of a channel (ref. 19) or maximize its bandwidth efficiency (ref. 18). The definition of bandwidth occupancy is given as the ratio of the bandwidth required to transmit the chosen modulation in a given time and the data rate in bits per second. Channel efficiency is the inverse quantity:

$$r = \frac{R}{2B} \tag{34}$$

where $R = \lg_2 m / T$ bits per second and $2B$ is the Nyquist transmission rate which relates to the time duration of the signal. If it is assumed that a passband $B = (1 + \alpha)/T$ $(\alpha > 0)$ is adequate to transmit a pulse of duration T (ref. 3, p. 60), then

$$r = \frac{\lg_2 m}{2(1 + a)} \tag{35}$$
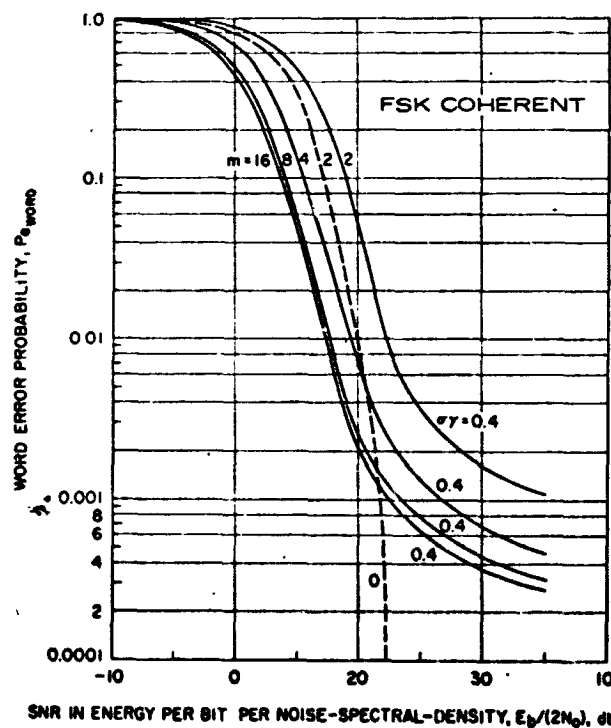
Figure 19.   Word error probabilities for a constant word rate for
10-bit words for various modulation systems.

Figure 19. — Continued.

FSK INCOHERENT

WORD ERROR PROBABILITY, $P_{e \, WORD}$

SNR IN ENERGY PER BIT PER NOISE-SPECTRAL-DENSITY, $E_b/(2N_0)$, db

ASK COHERENT

WORD ERROR PROBABILITY, $P_{e \, WORD}$

SNR IN ENERGY PER BIT PER NOISE-SPECTRAL-DENSITY, $E_b/(2N_0)$, db
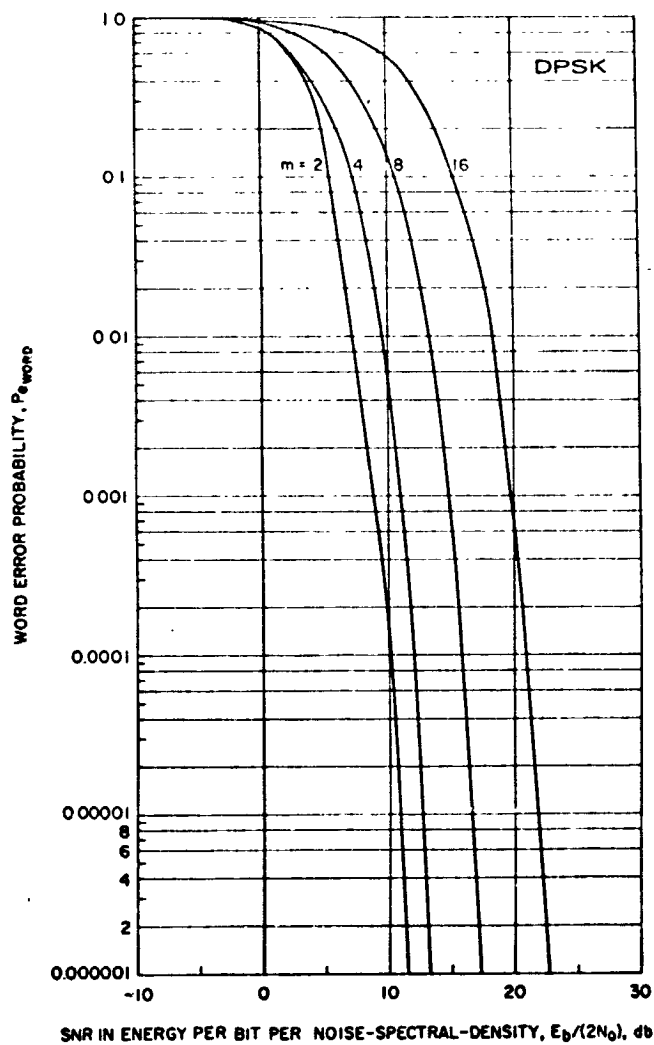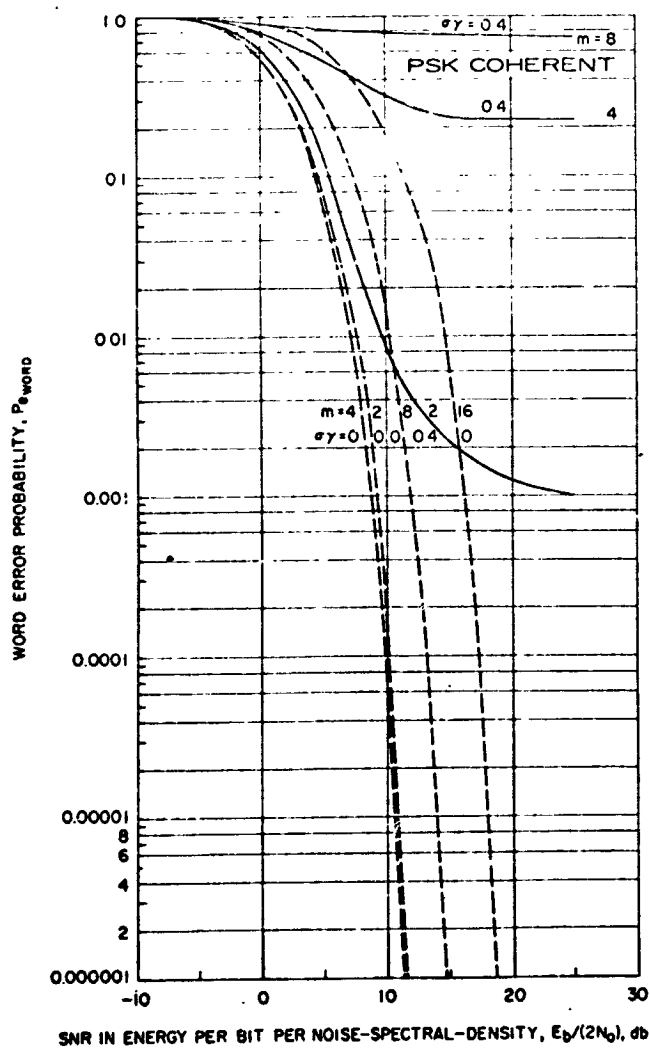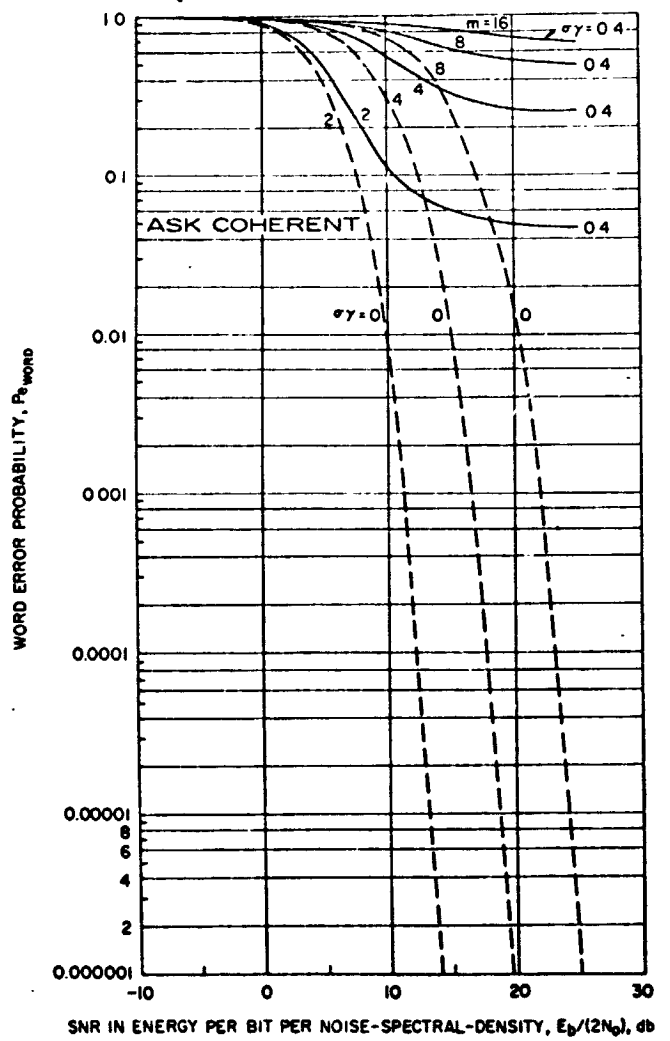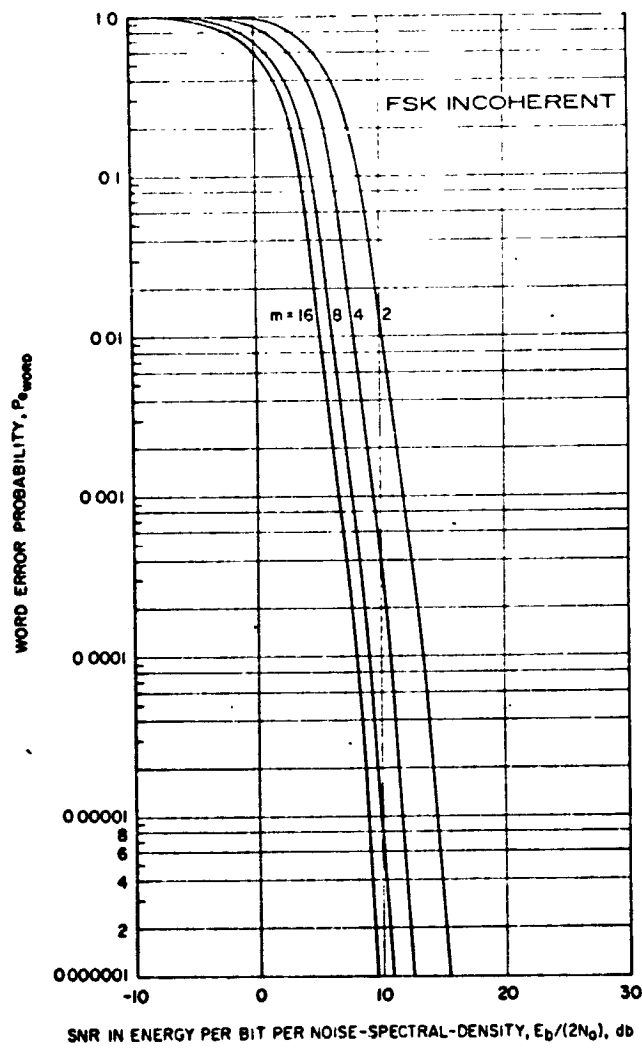
Figure 19. — Concluded.

This bandwidth efficiency applies to PSK and ASK modulation schemes in which the number of levels does not affect the number of pulses per symbol. Equation (35) would not be correct, for example, for a binary coded m level alphabet.

In FSK modulation, the required bandwidth increases linearly with m. The minimum frequency separation to maintain orthogonality of symbols is 1/T for incoherent FSK. The total bandwidth required is thus

$$B = \frac{m + \alpha}{T} \tag{36}$$

and

$$r = \frac{\lg_2 m}{2(m + \alpha)} \tag{37}$$

For coherent FSK, the frequency separation required to maintain orthogonality is 1/2T. Thus, the bandwidth is given by

$$B = \frac{m + 2\alpha}{2T} \tag{38}$$

and

$$r = \frac{\lg_2 m}{m + 2\alpha} \tag{39}$$

The bandwidth separation requirements for the coherent and incoherent FSK modulation schemes are discussed in Appendix J. It is apparent from that discussion that the PSK and ASK systems are far more efficient than the FSK ones for increasing m. The probability of error, however, rapidly increases with m for the PSK and ASK systems while the reverse is true for the FSK. (See figures 18 and 19.) Thus the modulation schemes to be preferred depend on the criterion chosen as well as on m.

Another modulation method, the biorthogonal, should be mentioned. A biorthogonal signal set can be obtained from an orthogonal set by augmenting it with the negative of each orthogonal signal. The best application of biorthogonal signals is in the transmission of words of increasing lengths, i.e., word lengths of several bits. These signals are important here because the use of biorthogonal codes doubles the

number of available levels from those of orthogonal codes without increasing the required bandwidth. Therefore, a biorthogonal set provides the advantage of reducing by 50 percent the bandwidth requirements compared with an orthogonal signal set of the same number of levels. Moreover, this reduction is accomplished without increasing the probability of error. In fact, it can be shown that the biorthogonal code results in smaller mean probability of error than the orthogonal code (ref. 19). In the limit of large m, the probabilities of error for the orthogonal, biorthogonal, and transorthogonal (which is the optimum) codes approach the same level because for these codes the correlation coefficients between two signals approach zero for large m. For the orthogonal code it is zero by definition for all m.

In the context of bandwidth efficiency, the coherent FSK could be easily converted to a biorthogonal system with a consequent bandwidth requirement given by

$$B = \frac{m + 4a}{4T} \qquad m \geq 4 \tag{40}$$

and

$$r = \frac{2 \lg_2 m}{m + 4a} \tag{41}$$

For the case where m is equal to 2,

$$B = \frac{1 + a}{T} \tag{42}$$

Equation (42) gives the minimum bandwidth for transmission of a pulse of duration T. It is evident that the bandwidth for a binary biorthogonal signal set would be identical with that of binary PSK; in fact, the two sets are identical.

In Table 1 the signal-to-noise ratio in energy-per-bit per noise-spectral-density and bandwidth requirements are listed for the transmission of a four-bit word with an error probability (bound) of 10^{-4}. A constant data rate is assumed for all modulation schemes considered. Because of this assumption, the integration time for an m level symbol will be $(\lg_2 m)$ times larger than that for a binary symbol, with a consequent reduction of bandwidth for the m level symbol. The bandwidth B is given in

TABLE 1.— BANDWIDTH AND SIGNAL-TO-NOISE RATIO REQUIREMENTS FOR VARIOUS MODULATION SCHEMES

Modulation System	$E_b/2N_0$	B
PSK binary	10	6
PSK 4 level	9.5	3
PSK 16 level	50	1.5
FSK (incoherent)* binary	17.8	10
FSK (incoherent) 4 level	10	9
FSK (incoherent) 16 level	5.6	16.5
FSK (coherent) binary	17.8	6
FSK (coherent) 4 level	10	5
FSK (coherent) 16 level	5.6	8.5
Biorthogonal** binary (= PSK)	10	6
Biorthogonal 4 level	10	3
Biorthogonal 16 level	5.6	4.5
ASK (coherent) binary	16	6
ASK (coherent) 4 level	58	3
ASK (coherent) 16 level		1.5
DPSK binary	10.5	6
DPSK 4 level	16	3
DPSK 16 level		1.5

*The difference between signal-to-noise ratios required for coherent FSK and incoherent FSK has been ignored in these calculations.

**The biorthogonal set considered is an FSK (coherent) set augmented by the negatives of each orthogonal signal.

multiples of $1/T$, where T is the word duration. The value of α has been taken to be $1/2$, and E_b is the energy per bit.

As may be seen from the table, the lowest signal-to-noise ratio required is that of the 16-level orthogonal or biorthogonal set. The bandwidth requirement is lowest for the 4-level biorthogonal set and the 4 level PSK, DPSK, and ASK sets. If equal weight were given to signal-to-noise ratio and to bandwidth, the 16-level biorthogonal and 4-level PSK would be the optimum choices.

It may be claimed that the comparison in Table 1 between the various modulation systems is somewhat unfair to low level systems such as the binary. The reason for this apparent unfairness may be seen from the following considerations. Suppose a sequence of M 4-bit words is transmitted by means of both binary and 16 level systems. In the 16 level system, each symbol corresponds to one word. Consequently, each symbol error is also a word error. In the binary system, four symbols are required to complete a word. Therefore, in the binary system it is possible that four symbol errors could occur and still result in only one word error. For this reason the average word error is somewhat lower in the binary system than in the m-level system for equal symbol errors in each system. This superiority of the binary system from this viewpoint is really only apparent, however, since in general the errors will appear in random groupings; for very small probabilities of error, such as 10^{-4}, it is much more likely that each error in the binary system would occur in separate words, thereby resulting in a word error for each symbol error as in the 16 level code. Consequently, the apparent possible reduction of error probability of the low level codes due to these considerations has been ignored.

Relation between Signal-to-noise Ratio and Rms Phase Errors in Phase-locked Loops

In the presentation of the probability of error curves, it was assumed that the signal-to-noise ratio and rms phase errors were independent. This method of presentation was convenient because it did not require the postulation of a model for relating the two quantities.

In actual practice, $(E'/2N_0')$ and σ are not independent but are related in a manner that depends on the configuration and the parameters of the phase synchronizing loop. When the signal-to-noise ratio in the loop is high, the rms phase error will be small; and when the signal-to-noise ratio in the loop is small, the rms phase error can be significant. Charles and Lindsey (ref. 20) have investigated the relationship between loop signal-to-noise ratio $(P/2N_0B_L)$ and the rms phase error for a loop of the type shown in figure 20. The quantity B_L is the equivalent noise bandwidth of the tracking loop (one-sided); i.e., noise power is $2N_0B_L$, P_s is the power in the signal, and N_0 is the two-sided noise spectral density. The investigation indicates that for signal-to-noise ratios in the loop greater than 9 db, the probability density function of the phase error is gaussian with variance equal to the inverse of the loop signal-to-noise ratio.

As an illustration, a binary PSK system that uses the information signal squared to provide a phase reference (refs. 21, 22) was considered; the discussion is presented in Appendix K. In brief, the variance of the reference phase is given by

$$\sigma_\gamma^2 = B_L T \left(\frac{2N_0'}{E'}\right) \left[2 + (M+1) \frac{B_i T}{2}\left(\frac{2N_0'}{E'}\right)\right] \qquad (43)$$
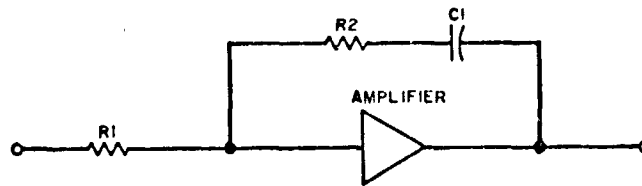
Figure 20.   Loop filter for proportional plus integral control.

where M is the number of elements in the array.   A graph of this equation is shown in figure 21a for two combinations of parameters.   It is evident that for combined signal-to-noise ratios of interest, the resulting rms phase errors are so small that they have little effect on the probability of error.   Thus, except for low signal-to-noise ratios, the system will operate very close to the zero phase error limit.

The preceding results are quite pessimistic in that it was assumed that the phase errors in the individual element signals and the phase error in the coherent detector were independent and, consequently, that their variances added directly.   However, this condition does not exist since the reference signal as well as the information signal is derived from the sum of the element outputs.   As a consequence, the reference signal has the same phase error as the information signal except for an additional error that results from noise in the sum signal.   This latter error is the only one that affects the detection process.   It may be computed directly from equation (K-6) in Appendix K.   The resulting rms phase error is shown in figure 21b.   It is evident that the rms value of the phase error is much smaller for this case than in the case in which the phase errors are assumed to be uncorrelated.

Analysis of a Specific Retrodirective System

The operating characteristics of a particular retrodirective configuration are presented in this section.   The analysis is given in Appendices L through O.   The system considered uses phase inversion by mixing and is shown in figure 22.   An incoming information signal and a pilot signal are converted to an intermediate frequency, amplified, and diplexed.   The pilot is amplified and used as a reference signal with which the information signal is mixed to yield a second intermediate frequency.   This last mixing operation removes the interelement phase shift.   The signals from all elements are then combined and fed to a common receiver.   The pilot signal is also mixed with the transmitter signal to superimpose on the transmitter signal the phase angle required to send the signal in the direction from which the pilot arrived.   The incident signal was assumed to
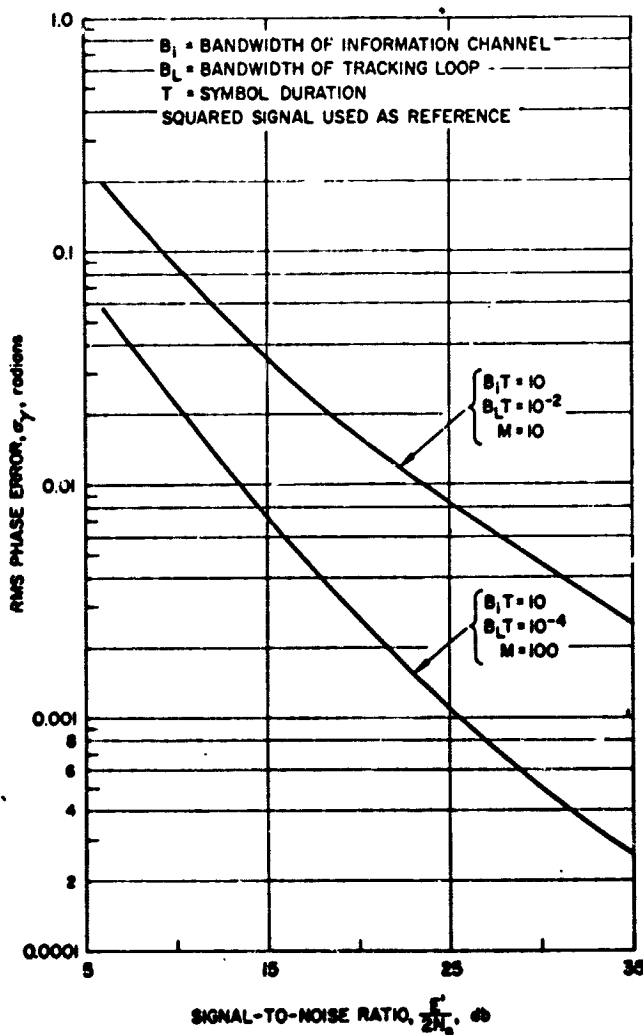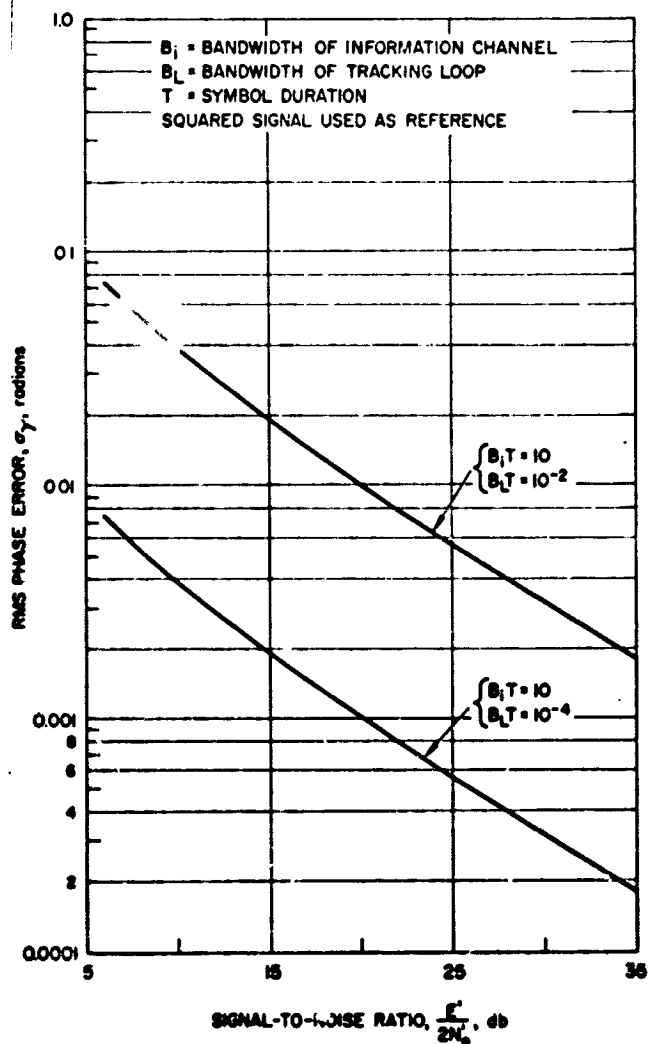
Figure 21. Expected rms phase errors from adaptive arrays.
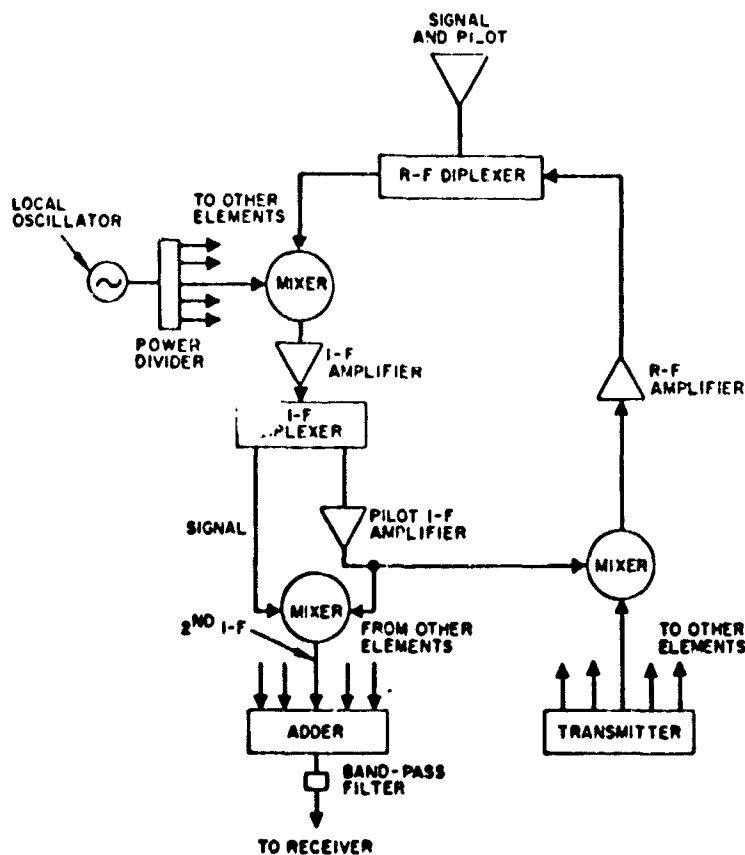
Figure 22. Retrodirective array using phase inversion by mixing and giving array gain on reception.

consist of an information signal that may be amplitude and phase modulated and an unmodulated pilot signal that is at a frequency near that of the information signal carrier frequency. The analysis assumed that the noise is random and gaussian with a flat spectrum over the frequency ranges of interest, that the noise in the information channel is independent of the noise in the pilot channel, and that the signal-to-noise ratios are established by the first i-f amplifier.

Error probability analysis of system using phase inversion by mixing. — The determination of the percentage of error in interpreting which of a number of possible messages was sent requires a knowledge of the joint probability density function of the pertinent message parameters. In the following sections the problem is considered for a system of the type described above.

For the consideration of error probabilities for a specific coding scheme, the signal out of the second mixer of the system in figure 22 must be examined. There is an added complication with phase inversion systems, however, in that the signal of interest contains products of pilot channel

noise and information channel noise. These products are not gaussi n.
Furthermore, they are not independent of the other nois(ter. is so that
the evaluation of the probability density functions is not a simple matter.
Some simplifications are possible. For example, the integrations of the
signals may be approximated by sums of te.ms which, if selected at the
proper sampling points, are independent.

When the interval of integration contains a large number of indepen-
dent sampling points, the probability density function of the integral
approaches a gaussian distribution. Furthermore, the noise terms consist
of the sums of the independent noise terms from M channels, further on-
tributing to the gaussian nature of the density function. The main departure
of the density function from a precisely gaussian function occurs in the tails
of the function. The region near the peak will be a good approximation to
a gaussian function. For low signal-to-noise ratios the error is determined
mainly by the region of the peak, and use of a gaussian approximation should
yield a reasonable estimate of the probability of error. Conversely, for
very high signal-to noise ratios, the tails of the density functions are
important in determination of error probabilities. However, in this case
the nongaussian terms in the signal become small and so have little effect
on the probability of error. Consequently, the assumption of a gauss in
density function for the noise terms should lead to a reasonable estimate
for the probabilities of error for systems of the phase-inversion-by-mixing
type.

The use of gaussian statistics for the noise outputs of the integrators
makes it possible to carry over the probability of error results already
obtained for the arrays with phase-locked loops and, with some modifica-
tion, apply them to phase-inversion arrays. The analysis is presented in
Appendix L and the results of analysis are summarized here.

For phase and/or frequency-modulated systems, the mean probabil-
ity of error may be determined merely by replacing E'/N_0' by B^2/σ^2 where
B^2 and σ^2 are given by

$$B^2 = \frac{A^2}{4}\left(\left[\sum_{n=1}^{M}\sqrt{E_{pn}E_{in}}\left(\cos\,\Phi_n - \Phi_{pn}\right)\right]^2 + \left[\sum_{n=1}^{M}\sqrt{E_{pn}E_{in}}\,\sin\left(\Phi_n - \Phi_{pn}\right)\right]^2\right)$$

(49a)

$$\sigma^2 = \frac{A^2}{4}N_0\left[\sum_{n=1}^{M}E_{in} + \sum_{n=1}^{M}E_{pn} + \frac{M}{4}N_0\alpha B_i T\right] \quad \begin{cases} \alpha B_i T \gg 1 \\ \alpha < 1 \end{cases}$$ (49b)

$$\sigma^2 = \frac{A^2}{4} N_0 \left[\sum_{n=1}^{M} E_{in} 2\alpha B_i T + \sum_{n=1}^{M} E_{pn} + \frac{M}{4} N_0 \alpha B_i T \right] \begin{cases} \alpha B_i T < 1/\pi \\ B_i T \gg 1 \end{cases} \quad (49c)$$

In these equations E_{in} is the energy per symbol in the nth element receiver and E_{pn} is the pilot signal energy in the same receiver during a symbol duration, T. The symbol α is the ratio of the pilot channel bandwidth, B_p, to information channel bandwidth, B_i.

In systems that use amplitude modulation, the value of E_i varies from symbol to symbol and consequently, because of the form of σ^2, it also varies from symbol to symbol. As a result care must be taken to use the correct values for σ^2 in computing the mean probability of error from the equations in the discussion of coherent and incoherent ASK modulation in the earlier analysis of systems that use phase-locked loops.

Comparison of phase-inversion systems and phase-locked systems. — For phase or frequency-modulated systems a comparison of the error performances of self-steering arrays that use phase inversion by mixing and those that use phase-locked loops is readily made by comparing the quantities E'/N_0' and B^2/σ^2 for similar operating conditions, i. e. , the same incident powers, the same array sizes, etc. It has been found that for operating conditions such that in the phase inversion system

$$\alpha < 1 \qquad (50a)$$

$$\alpha B_i T \gg 1 \qquad (50b)$$

then

$$B^2/\sigma^2 = \frac{1}{4} E'/N_0' \qquad (50c)$$

That is, for the conditions specified, about four times as much power must be provided to the phase inversion array as to the phase-locked loop array. For operating conditions such that

$$\alpha B_i T < \frac{1}{\pi} \qquad (51a)$$

$$B_i T \gg 1 \qquad (51b)$$

the performance of the phase inversion system approaches that of the phase-locked system.

<u>Signal-to-noise analysis of phase-inversion system.</u> — As an example of the values of B^2/σ^2 that might be obtained in an operational system, the following configuration was analyzed. The system consisted of a 20-watt C-band transmitter and a 4-foot transmitting array on an orbiting bus, and a one-foot-square aperture of retrodirective modules on a landing capsule. The number of modules assumed was sufficient to prevent formation of grating lobes when the required coverage angle was a cone of half angle θ_m. It is given by

$$M \approx \frac{A_e}{\lambda^2} (1 + \sin \theta_m)^2 \tag{52}$$

where A_e is the area of the array.

It was assumed that $\theta_m = 70$ degrees.

Transmission distances of 4,000 miles and 12,000 miles were used, and the output was divided between signal and pilot to maximize B^2/σ^2 at the capsule receiver. Receiver noise figures of 6 db, 8 db, and 10 db were used and a bit rate of 10^6 bits per second was assumed. At the frequency of interest (6 GHz) the wavelength, λ, is 0.164 foot. An effective receiving antenna element temperature of $100^\circ K$ and a transmitting array efficiency of 90 percent were assumed. The latter assumption yields a transmitting antenna gain of 37.2 db.

Figure 23 shows computed values of B^2/σ^2 for various values of m as a function of α. The curves are shown for $0 < \alpha < 10^{-3}$ but values of B^2/σ^2 are given for the limiting case in which the pilot bandwidth equals the information channel bandwidth ($\alpha \rightarrow 1$). The information bandwidth, B_i, was adjusted so that $B_i T = 5$, where T is the symbol duration. Since the bit rate was constant at 10^6 bits per second, T is given by

$$T = \lg_2(m) \, 10^{-6} \tag{53}$$

and consequently,

$$B_i = \frac{5 \times 10^6}{\lg_2 (m)} \tag{54}$$

For α between 0 and 10^{-3} these parametric values correspond to pilot channel bandwidths between 0 and 5000 Hz. Narrow pilot bandwidths can be used if the incident doppler is tracked by the local oscillator. It is evident that there is not a large change in B^2/σ^2 over the range of α from 0 to 10^{-3}, but for wide band pilot channels (i.e., $\alpha \rightarrow 1$) the degradation of B^2/σ^2 is significant. The improvement in B^2/σ^2 for increasing values of m results from the longer symbol duration obtainable for larger m since the bit rate is held constant. The curve of figure 23 can be used in
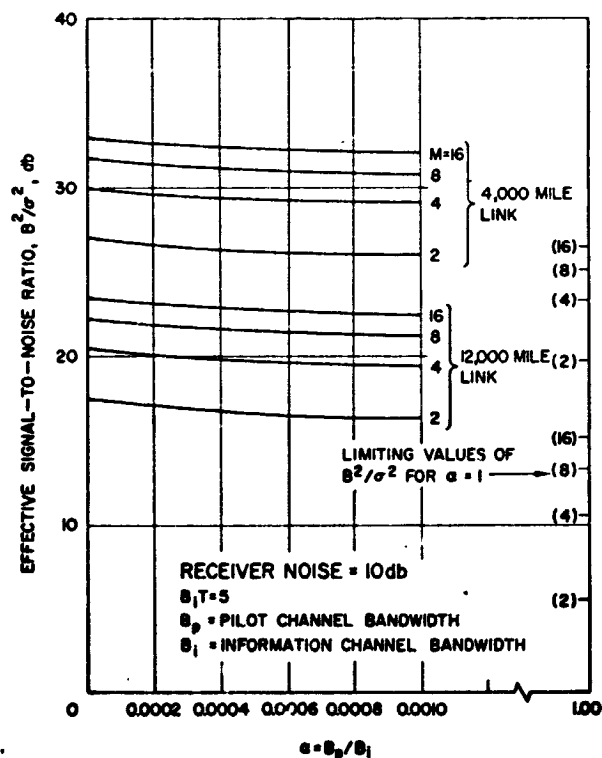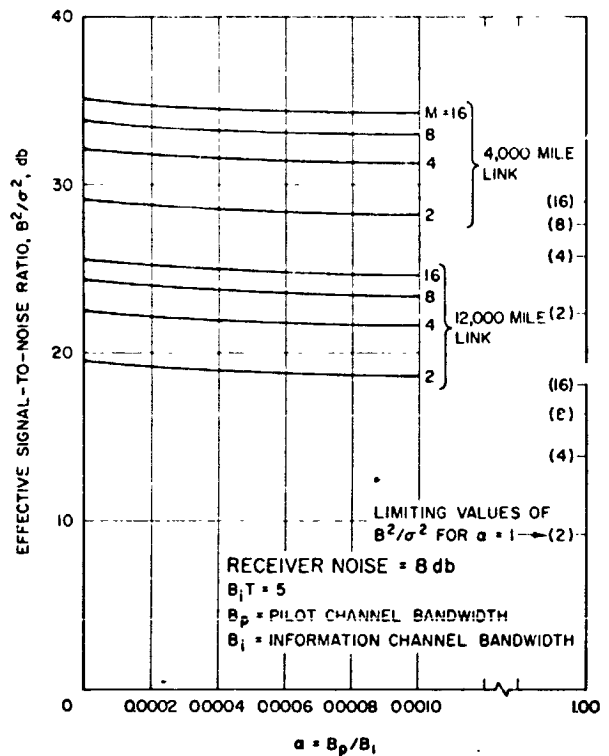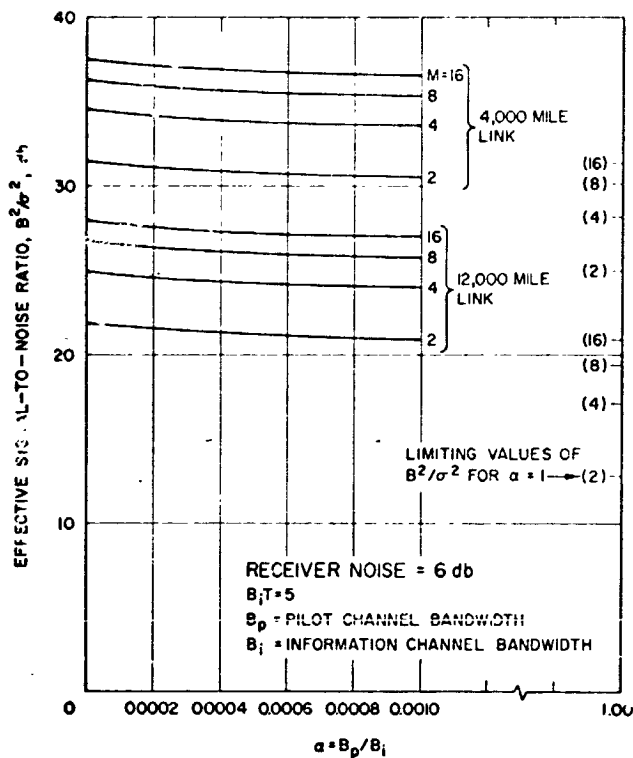
Figure 23. Effective signal-to-noise ratios as a function of pilot bandwidth of a phase-inversion system receiving m-ary digital modulated signals.

conjunction with the curves of figures 11 through 14, 16, and 17 to determine probability of error per symbol by replacing E'/N_0 in those figures with B^2/σ^2.

Signal-to-noise ratio of reradiated signal. — In retrodirective operation of the phase-inversion type, the signal-to-noise ratio of the transmitted signal will be affected by the signal-to-noise ratio of the received pilot when the system is operated as a linear device. An analysis of array operation was carried out for the derivation of an expression for the resulting signal-to-noise ratio of such a transmitted signal in terms of the properties of the system. From this analysis the following expression for transmitted signal and noise was obtained:

$$E_n = K'' \sum_n \sqrt{g_{en}(\theta, \varphi)}\; f_T(t) \left\{ \sqrt{g_{en}(\theta_i, \varphi_i)}\; K\lambda_p\, C \cos\left[\omega_T t + \phi(t) - \phi_{pn}(\theta_1, \varphi_1) - \zeta_n(\theta_1, \varphi_1) + \zeta_{Tn}(\theta, \varphi) + \phi_{Tn}(\theta, \varphi)\right] \right.$$

$$\left. + (a_n'' + c_n)\cos\left[\omega_T t + \zeta_{Tn}(\theta, \varphi) + \phi_T(\theta, \varphi)\right] + (b_n'' + d_n)\sin\left[\omega_T t + \zeta_{Tn}(\theta, \varphi) + \phi_{Tn}(\theta, \varphi)\right] \right\} \qquad (55)$$

This expression is necessary in evaluation of the performance of a communication link from the self-steering array back to the pilot source.

CONCLUSION

Analysis of Results

During the course of this study, the applicability of self-steering arrays to planetary probe missions has been considered. A consideration of possible mission requirements indicated that self-steering arrays that use phase inversion by mixing may be applicable to the lander-bus communication link because of the relatively short distance involved. Phase-locked loops with their extremely narrow noise bandwidths will probably be required for the bus-earth link because of the large transmission distances and corresponding low signal levels. Effort has been concentrated on determining the performance capabilities of both types of self-steering arrays when used with various digital modulation schemes.

An analysis was made of probability of error in the detection of m-ary digital modulation signals. The analysis included the effects on the error probabilities of additive gaussian noise and of phase errors in the incoming signal or in the reference oscillator. The modulation systems analyzed were m-ary coherent PSK, differentially coherent PSK, coherent and incoherent FSK, and coherent and incoherent ASK.

The analysis of the probability of error was extended to include the effects of arraying a number of channels through adaptive receivers, i. e. , the effects of an adaptive self-steering array. It has been shown that for large arrays the results for single channel systems can be simply modified to account for the effects of the array. The modifications are merely a change in the effective signal-to-noise ratio and a change in the rms phase error in the signal.

Curves showing the probabilities of error per symbol versus energy-per-symbol per noise-spectral-density were presented for all modulations except incoherent ASK. Computational difficulties have precluded accurate calculation for this modulation. As expected, in the absence of phase errors, binary coherent PSK modulation yields the smallest probability of error for all signal-to-noise ratios on the above basis of comparison. However, in the presence of phase errors that do not vary appreciably during the time duration of adjacent symbols, i. e. , slowly varying phase errors, DPSK appears to be the best. When rapid fluctuations occur, DPSK systems would be degraded more than incoherent systems. In that case binary incoherent FSK will become superior to DPSK.

These conclusions were based on the probability of error per symbol as a function of energy-per-symbol per noise-spectral-density. In the binary case this value is the same as the probability of error per bit. A more significant basis for comparison of modulation techniques is the probability of error per word for a given information rate. Use of this

parameter requires a consideration of coding techniques as well as of modulation techniques. Curves of word error probabilities versus energy-per-bit per noise-spectral-density were presented for 4-bit and 10-bit words transmitted using PSK coherent, DPSK, FSK coherent and incoherent, and ASK coherent modulations. The curves were computed on the basis of a fixed data rate. From the curves it appears that 16 level FSK coherent is the best in the absence of phase errors and FSK incoherent is the best in the presence of phase errors. However, consideration of bandwidth requirements may negate these findings since FSK requires a greater bandwidth than other modulations and bandwidth may be more important than power requirements. Therefore, a combination of power requirements and bandwidth requirements must be considered in the selection of the optimum system for any application. This consideration shows that of the cases considered, a 16-level biorthogonal FSK system appears to be quite attractive.

The problem of determining the probability of error when employing a system that uses phase inversion by mixing was examined for various digital modulations. It was shown that by proper modification of the ratio of the energy-per-symbol to noise-spectral density, the results of the analysis of adaptive arrays can be applied to the phase-inversion array. This result depends on making the approximation that in the phase-inversion system the noise is gaussianly distributed. The study showed that in the absence of fading and multipath propagation, the adaptive systems are generally superior to the phase-inversion systems with regard to error probabilities; the performance of the latter approaches that of the former when the pilot bandwidth can be made sufficiently small.

The signal-to-noise characteristics of a self-steering system that uses phase inversion by mixing were analyzed. The analysis considered a link from an orbiting bus to a landing capsule as the example for calculations. Transmission distances of 4000 and 12,000 miles were used. A self-steering array on the lander was taken to be 1-foot-square with element temperatures assumed to be $100^\circ K$. Correlation of element noise was neglected. Receiver noise figures of 6, 8, and 10 db were used for a system operating at 6 GHz. The transmitter on the bus supplied a total of 20 watts to a 4-foot diameter array that was assumed to be 90-percent efficient. The signal-to-noise ratios were computed for the system as the ratio of pilot channel bandwidth to information channel bandwidth was varied between zero and unity for an information rate of 10^6 bits per second.

An expression was also derived for the signal and noise radiated by the retrodirective system. The noise in the radiated signal results from the noise in the pilot signal which is used to steer the transmitted signal. The expression is necessary in evaluating the performance of a communication link from the self-steering array to the pilot terminal.

48.

Recommendations

As a result of the studie conducted on this contract, the basic operating characteristics of self-steering arrays of the adaptive type and the phase inversion type have been determined. Their applicability to planetary probe missions under favorable operating conditions has been established. However, in a typical mission environment, conditions may not always be favorable and the performance of the systems under more adverse conditions remains to be evaluated.

One of the most important items to be considered in the design of a planetary probe communications system is the multipath problem. In general, the signal proceeds along many different paths from transmitter to receiver so that the received signals on each path differ in all of their parameters, particularly in amplitude and in time delay. The two most significant effects on digital communications systems introduced by multipath transmission are selective fading and intersymbol interference. Selective fading occurs because the signals that have traveled the various paths add with different phases. Since the amplitudes and delays are time-varying, large variations of signal strength can be observed at a single frequency as a function of time, or equivalently, variations in signal strength can be observed at a given time as a function of frequency. Inter-symbol interference occurs because of the different time delays along the various paths in the multipath structure. The information-carrying modulation may, therefore, be badly distorted by the superposition of (already distorted) modulation waveforms with randomly varying time delays.

There is a growing literature concerning multipath problems, and in attempts to counteract the effects, a number of techniques have been devised. These include various modulating schemes such as single side-band transmission, synchronous modulation methods, various types of diversity reception, and coding. One of the most interesting and sophis-ticated methods employed has been the RAKE system (ref. 23). In this system, it is assumed that there is a discrete number of multipath channels and that the signals along each of these channels can be isolated in the receiver by the transmission of an appropriate wideband signal. The isolation is accomplished by means of techniques of correlation detection that tend to isolate wideband signals that have different delays. Each of these separate signals is processed in such a way that it is given an optimum weighting coefficient and phase shift or time delay so as to compensate for the medium effects. However, to accomplish this desirable objective, the system must measure the properties of the medium: i.e., it must determine the optimum weighting and appropriate delay from mea-surements of the response of the medium. If this determination is possible, then the RAKE system is probably close to optimum. However, reasonably high SNR's are required to yield the information rate needed to supply the necessary information regarding medium variations. It is quite possible that the information rate required to yield the necessary medium properties will exceed the information rate of the signal transmission (ref. 24).

If the signal-to-noise ratio is low, the information capacity of the channel becomes so small that the receiver is denied the required information concerning medium variations, and systems such as RAKE cannot operate properly.

In addition, deep space probe communications systems, particularly for planetary missions such as the Mars probe, have multipath problems which are uniquely different from those encountered in ordinary communications systems. One of the major differences concerns the communications system geometry. Not only is the communication link for space probes of great length, but the multipath problem itself is strongly affected by the presence of a planet adjacent to both the bus and lander. In ordinary communications systems, the multipath structure results from scattering, tropospheric stratification, ionospheric (plasma) effects, etc. In space probe communications systems, there is the principal additional earth-planet-bus path for the bus and the bus-planet-lander path for the lander. These additional paths may be of far greater significance than the large number of paths within an ordinary medium. Medium effects will occur because the transmitted signal must pass through the earth's and/or the planet's atmosphere, and they will occur on both the "primary" (i.e., earth-bus or bus-lander) path and the "secondary" (i.e., earth-planet-bus or bus-planet-lander) paths.

The secondary path yields a very complicated received signal because of the complicated character of the reflection from the planet's surface. A smooth surface yields a predominantly specular reflection while a rough surface yields a predominantly diffuse reflection. It is expected that the reflection from a planetary surface would have components of each type. Essentially all of the planet's surface that is capable of intercepting radiation from the transmitter will be illuminated. Although the planet will appear as a point to a transmitter on earth, it will appear to the receiver in the bus or lander as a very large, extended, reflecting surface containing multiple (nearly specular) reradiating sources superimposed on a noisy background arising from diffuse reflection from much of the planet.

The unusual, noisy, multipath structure as seen by the receiver is further complicated by the fact that the receiver is moving relative to both the planet and the transmitter. This relative motion gives rise to complicated doppler and other derivative effects. Indeed, depending on the orbit of the bus, it is possible that the direct path to the bus from the transmitter will be cut because the planet will intercept the line-of-sight between the earth and the bus. When this interruption occurs, some communications may continue for a short period as a result of diffraction effects as the bus disappears behind the planet. These effects, however, should be very small at the extremely high frequencies envisaged for use with such a system.

The conductivity, as well as the geometry, of the reflecting surface is also of importance in determination of the nature of secondary reflections. This conductivity is in general unknown, but probably will vary randomly as a function of the portion of the surface being illuminated.

Glenn and Lieberman (ref. 25) have compared several digital modulation schemes in single-channel systems operating in a fading and jamming environment. As might be anticipated, their results indicate that in severe fading and jamming environments, coherent systems suffer the greatest degradation and incoherent systems ultimately become superior in terms of probability of error. Since self-steering antenna systems may be affected differently by multipath environments, their performance under such conditions will be investigated during the second phase of the present contract.

The study will include a comparison of the relative performance of self-steering systems using the following modulations: m-ary PSK coherent, DPSK, FSK coherent, FSK incoherent, ASK coherent, ASK incoherent. The self-steering systems that will be studied include those that use phase inversion by mixing and those that use phase-locked loops or other similar techniques to obtain self-steering characteristics.

Since a self-adaptive system may be desirable for the bus receiver on the earth-bus link, it is important to determine the effect on the input to the tracking loop of the relationship between the probability distribution of the reference phase (in particular, its standard deviation) and the signal-to-noise ratio, multipath effects, etc. Although a number of analyses have been made of the effects of certain kinds of noise on frequency and phase tracking loops, the joint effect of noise and multipath effects of the type expected to be encountered by the probe requires investigation.

Once the loop is locked-on in its dependent variable (for example, frequency, phase, etc.), then the antenna array will automatically adjust its amplitudes and phases to lock-on to the transmitted antenna beam in space. The loop lock-on capability is a function of the same parameters as the loop tracking capabilities, and both problems should be investigated when the systems are operating in a multipath environment. Such things as lock-on probabilities and the probability of loss of lock will be considered.

A very important problem that is related to loop lock-on is the communications blackout that may occur when the lander enters the planetary atmosphere. The employment of high microwave frequencies or millimeter-wave frequencies on planetary probes would be advantageous since high-gain antennas could be used and would tend to alleviate the problem. Utilization of millimeter waves with self-steering systems is contingent on the implementation of self-steering techniques at these short wavelengths. Consequently, in order for a realistic assessment to be made of millimeter-wave self-steering arrays for application to planetary probes, it is necessary to study the trade-offs between the advantages of increased directive gain and improved capability to

withstand blackout during entry versus such characteristics as system weight, increased losses, higher receiver noise figures, and reduced power generating capabilities that are encountered at millimeter-wave frequencies.

Antenna Department, Aerospace Group
Hughes Aircraft Company
Culver City, California, 21 July 1967.

APPENDIX A. THE SIGNAL SPACE CONCEPTS

Any finite set of waveforms of duration T, say $S_1(t)$, $S_2(t)$, ..., $S_m(t)$, can be represented as a linear combination of k orthonormal waveforms $\varphi_1(t)$, $\varphi_2(t)$, ..., $\varphi_k(t)$, where $k \le m$ (ref. 16). Thus

$$S_i(t) = \sum_{j=1}^{k} a_{ij}\, \varphi_j(t) \qquad i = 1, 2, \ldots, m \qquad (A-1)$$

where

$$a_{ij} = \int_0^T S_i(t)\, \varphi_j(t)\, dt \qquad (A-2)$$

and

$$\int_0^T \varphi_i(t)\, \varphi_j(t)\, dt = \delta_{ij} \qquad (A-3)$$

where δ_{ij} is the Kronecker delta. The subscripts in equations (A-1) through (A-3) refer to coordinates in signal space, where the signal space is defined by a k-dimensional Euclidean orthogonal coordinate system. Thus, the numbers in equation (A-2), where j runs from 1 through k, are the k coordinate projections of the signal point S_i on a k-dimensional Euclidean space. The coefficients a_{ij} in equation (A-2) may be computed by means of a series of product integrators.

If each signal waveform is transmitted with equal probability and if the received signal is perturbed by additive, stationary, white, zero mean, gaussian noise, then for the case of coherent detection the decision rule which selects the message point closest to the received point minimizes the probability of error. The detector that makes use of this decision rule is

called a maximum likelihood detector. For coherent demodulation, a series of product demodulators and integrators followed by a maximum likelihood decision device will be employed.

The signal space technique is normally applied to systems in which the additive noise is white, that is, has a constant spectral density over all frequencies. It is, however, proved below that this technique can be applied when the noise has any spectrum, with the only requirements being that the mean of the noise is zero and that the noise process is stationary. This result is quite interesting because it shows that for the set of orthogonal functions chosen for the signal, the noise components of interest are independent, even though the signal orthogonal functions do not form a complete set for representing the noise function n(t).

The coefficients of the orthonormal functions in equation (A-1) are determined by equation (A-2). A set of product integrators can be used to compute these coefficients. The integrators can also be used as the first stage of a detector in a data transmission system. The second stage of such a detector decides, on the basis of the k outputs of the product integrators, what signal was actually sent. The transmitted signal, $S_i(t)$, is perturbed by additive, white, stationary, zero mean, gaussian noise. The received signal is therefore given by

$$y(t) = S_i(t) + n(t) \tag{A-4}$$

The output of the jth product integrator is, therefore, from equation (A-4).

$$\int_0^T y(t)\, \varphi_j(t)\, dt = a_{ij} + n_j \qquad\qquad j = 1, 2, \cdots k \tag{A-5}$$

where

$$a_{ij} = \int_0^T S_i(t)\, \varphi_j(t)\, dt \tag{A-6}$$

$$n_j = \int_0^T n(t)\, \varphi_j(t)\, dt \tag{A-7}$$

Since the noise model used is stationary and gaussian with zero mean, the probability that a noise perturbation n_j lies between a and b is given by

$$P(a \leq n_j < b) = \frac{1}{\sqrt{2\pi}\,\sigma_j} \int_a^b \exp\left[-\frac{y^2}{2\sigma_j^2}\right] dy \qquad (A-8)$$

where

$$\sigma_j^2 = \overline{n_j^2} = \int_0^T \int_0^T R_n(t_2 - t_1)\, \varphi_j(t_1)\, \varphi_j(t_2)\, dt_1\, dt_2 \quad j = 1, 2, \cdots, k \qquad (A-9)$$

and $R_n(t_2 - t_1)$ is the autocorrelation function of the noise. It is given by

$$R_n(t_2 - t_1) = \overline{n(t_1)\, n(t_2)} \qquad (A-10)$$

The noise may be expanded in an orthogonal expansion similar to that in equation (A-1). Thus,

$$n(t) = \sum_{i=1}^k n_i\, \varphi_i(t) + h(t) \qquad (A-11)$$

where $h(t)$ is a remainder term included to preserve the equality. With the use of equation (A-7), it follows from equation (A-11) that

$$\int_0^T n(t)\, \varphi_j(t)\, dt = n_j + \int_0^T h(t)\, \varphi_j(t)\, dt = n_j \qquad (A-12)$$

where

$$\int_0^T h(t)\, \varphi_j(t)\, dt = 0 \qquad (A-13)$$

Thus, the noise may be decomposed into two portions, the first, n_j, consisting of the projection of the noise on the signal space, and the second consisting of that portion of the noise which is orthogonal to the signal space. In other words, the n_1, n_2,..., n_k represent the k coordinate projections of the noise on the signal space and represent that portion of the noise which will interfere with the detection process.

From equation (A-7)

$$\overline{n_i\,n_j} = \iint_0^T \overline{n(t_1)\,n(t_2)}\; \varphi_i(t_1)\,\varphi_j(t_2)\,dt_1\,dt_2 \tag{A-14}$$

$$\overline{n_i\,n_j} = \iint_0^T R_n(\tau)\,\varphi_i(t_1)\,\varphi_j(t_2)\,dt_1\,dt_2 \tag{A-15}$$

where

$$\tau \equiv t_2 - t_1 \tag{A-16}$$

If it is assumed that the noise $n(t)$ is stationary and has zero mean, it follows that the function $R_n(\tau)$ is even. By means of a simple change of variable, equation (A-15) may be written as

$$\overline{n_i\,n_j} = \iint_{-T/2}^{T/2} R_n(\tau)\varphi_i(t_1 + \frac{T}{2})\,\varphi_j(t_2 + \frac{T}{2})\,dt_1\,dt_2 \tag{A-17}$$

For the digital modulations of interest, the φ_i can be selected as

$$\varphi_i = \sqrt{\frac{2}{T}} \cos \omega_i t \qquad i = 1,..\frac{k}{2} \tag{A-18a}$$

$$\varphi_i = \sqrt{\frac{2}{T}} \sin \omega_i t \qquad i = \frac{k}{2} + 1,\ldots k \tag{A-18b}$$

where ω_i is the angular frequency. As an example, if the modulation is PSK, DPSK, or ASK, the frequency is fixed and k equals 2. If the modulation is FSK, there must be a separate ω_i for each frequency of transmission so that k is 2n where n is the number of frequencies used. The

carrier frequencies ω_i are so chosen that the bit period T is an integral number of cycles, or so that $\omega_i T = 2k_i\pi$, where k_i is an integer. It therefore follows that

$$
\left.
\begin{aligned}
\cos \omega_i(t_1 + \frac{T}{2}) &= \cos (\omega_i t_1 + k_i\pi) = + \cos \omega_i t_1 \quad \text{for } k_i \text{ even} \\
&= - \cos \omega_i t_1 \quad \text{for } k_i \text{ odd} \\
\sin \omega_i(t_2 + \frac{T}{2}) &= \sin (\omega_i t_2 + k_i\pi) = + \sin \omega_i t_2 \quad \text{for } k_i \text{ even} \\
&= - \sin \omega_i t_2 \quad \text{for } k_i \text{ odd}
\end{aligned}
\right\}
\quad \text{(A-19)}
$$

Substitution of equation (A-19) into equation (A-17) gives

$$
\overline{n_i n_j} = \frac{2}{T}(-1)^{k_i + k_j} \iint_{-T/2}^{T/2} R_n(\tau) \begin{Bmatrix} \cos \omega_i t_1 \\ \sin \omega_i t_1 \end{Bmatrix} \begin{Bmatrix} \sin \omega_j t_2 \\ \cos \omega_j t_2 \end{Bmatrix} dt_1 \, dt_2
$$

$$(A-20)$$

Because $R_n(\tau)$ is even in τ, it may be seen that the integral vanishes when $1 \le i \le k/2$ and $(k/2 + 1) \le j \le k$. This amounts to saying that the coefficients of the in-phase and quadrature components of the expansion of the noise are independent, since they are gaussian and uncorrelated. When $1 \le i, j \le k/2$ or $(k/2 + 1) \le i, j \le k$, the integral does not vanish identically. However, in two important cases it does vanish. In one case the spectra of the noises for the ith frequency and the jth frequency are disjoint. Then the noises are independent and

$$
\overline{n_i \, n_j} = 0 \qquad \text{for all } i \ne j \qquad (A-21)
$$

In the second case the noise is white. Then

$$
\overline{n(t_1) \, n(t_2)} = N_0 \, \delta(t_2 - t_1) \qquad (A-22)
$$

and equation (A-14) reduces to

$$\overline{n_i \, n_j} = N_0 \int_0^T \varphi_j(t) \, \varphi_i(t) \, dt \qquad \text{(A-23a)}$$

$$\overline{n_i \, n_j} = N_0 \, \delta_{ij} \qquad \text{(A-23b)}$$

This result is quite interesting because it shows that for the set of orthogonal functions chosen for the signal, the noise components of interest are independent, even though the signal orthogonal functions do not form a complete set for representing the noise function, n(t). The fact that these noise components are independent greatly simplifies the computations in the body of the report. In particular, it shows that the additive noise need not necessarily be white. In fact, for PSK, DPSK, and ASK modulations, the additive noise may have any spectrum. The only requirement is that the mean of the noise be zero and that the noise be stationary.

APPENDIX B.   ANALYSIS OF m-ary COHERENT PSK MODULATING SYSTEM

Phase Shift Keying

In a coherent phase shift keyed scheme, the information is carried by digital modulation of the phase. The alphabet of transmitted waveforms is therefore

$$S_i(t) = \sqrt{\frac{2E}{T}} \cos \left(\omega_o t + \frac{2\pi i}{m} \right) [u(t)\, u(T - t)] \tag{B-1}$$

where

$i = 1, 2, \ldots, m$; $u(t)$ is the unit step function; E is the energy content of $S_i(t)$; T is the duration of the waveform; and ω_o is some integer multiple of $2\pi/T$. The desired received signal energy is proportional to E. The phase modulation in equation (B-1) represents m-ary phase shift keying. The phase modulation is therefore a random square wave in which the step changes in the wave occur after an integral number of bit durations T. It is assumed that the transmitter and coding are optimum so that each of the m levels is equally likely to occur. It is clear that equation (B-1) can be written as the sum of a sinusoid and a cosinusoid, and since these are orthogonal, a reasonable choice for the orthonormal functions $\varphi_j(t)$ is

$$\left. \begin{aligned} \varphi_1(t) &= \sqrt{\frac{2}{T}} \cos \omega_o t \\[2em] \varphi_2(t) &= \sqrt{\frac{2}{T}} \sin \omega_o t \end{aligned} \right\} \tag{B-2}$$

From equation (A-2), the coordinates of the message points are

$$a_{i1} = \int_0^T \sqrt{\frac{2E}{T}} \cos \left(\omega_o t + \frac{2\pi i}{m} \right) \sqrt{\frac{2}{T}} \cos \omega_o t \, dt = \sqrt{E} \cos \frac{2\pi i}{m}$$

$$a_{i2} = \int_0^T \sqrt{\frac{2E}{T}} \cos \left(\omega_o t + \frac{2\pi i}{m} \right) \sqrt{\frac{2}{T}} \sin \omega_o t \, dt = -\sqrt{E} \sin \frac{2\pi i}{m}$$

(B-3)

In the important case in which m = 2 (binary PSK), the two members of the signal alphabet are

$$S_i(t) = \sqrt{\frac{2E}{T}} \cos (\omega_o t + \pi i) = \sqrt{\frac{2E}{T}} \cos \omega_o t \cos \pi i \qquad (B-4)$$

Therefore,

$$a_{i2} = 0$$

(B-5)

$$a_{i1} = \sqrt{E} \cos \pi i$$

Thus, if the measured output phase angle lies between $\pi/2$ and $3\pi/2$, that is, in the left hand portion of the circle in figure B-1, it is assumed that the transmitted signal was S_1. If the received phase angle lies between $3\pi/2$ and $5\pi/2 = \pi/2$, that is, in the right side of the circle in figure B-1, it is assumed that the transmitted signal was S_2.

In coherent PSK, the received signal plus additive noise becomes

$$e(t) = \sqrt{\frac{2E}{T}} \cos \left[\omega_d t + \frac{2\pi i}{m} - \theta(t) \right] + n(t) \qquad (B-6)$$

where $\theta(t)$ is a phase uncertainty introduced by the coherent reference oscillator or by the propagation path. Since the frequency has been translated
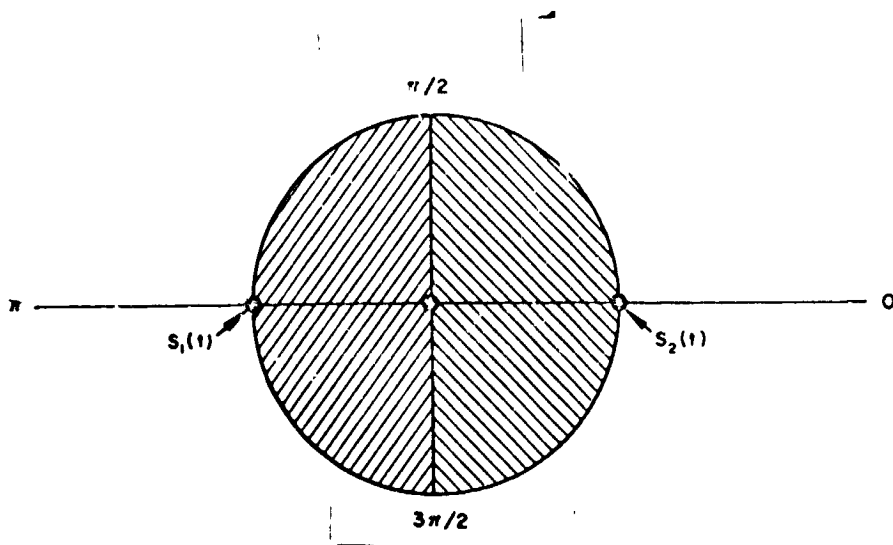
Figure B-1. Signal-space representation of binary PSK signal.

from the radio frequency ω_o to the intermediate frequency ω_d, the corresponding orthonormal functions are, from equation (B-2),

$$\left.\begin{array}{l} \varphi_1(t) = \sqrt{\dfrac{2}{T}} \cos \omega_d t \\[3mm] \varphi_2(t) = \sqrt{\dfrac{2}{T}} \sin \omega_d t \end{array}\right\}$$ (B-7)

The first stage in the optimum demodulation scheme is then to pass the signal in equation (B-6) through a set of product integrators as shown in figure B-2.
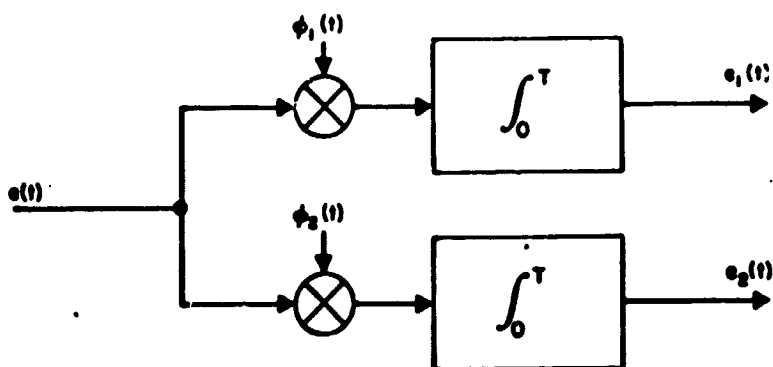
Figure B-2. Product integrators for optimum demodulation of coherent PSK.

The output of the jth product integrator becomes, after equation (B-6) is expanded and equation (B-4) is employed,

$$
\begin{aligned}
e_j &= \int_0^T e(t)\, \varphi_j(t)\, dt \\
&= \int_0^T dt\, \varphi_j(t) \sqrt{\frac{2E}{T}} \left\{ \cos\left(\omega_d t + \frac{2\pi i}{m}\right) \cos \vartheta\,(t) + \sin\left(\omega_d t + \frac{2\pi i}{m}\right) \sin \theta(t) \right\} \\
&\quad + \int_0^T n(t)\, \varphi_j(t)\, dt
\end{aligned} \tag{B-8}
$$

At this point, it is convenient to make the assumption that $\theta(t)$ does not vary appreciably during the bit period T. This assumption is a good one if the period T is short, as would normally be the case for fairly high bit rates, and/or in a slow fading environment. If θ is assumed to be constant during the period T and equations (A-2) and (B-3) are utilized,

$$
e_j = \cos\theta\, a_{ij} + \sin\theta\, b_{ij} + n_j \tag{B-9}
$$

where

$$
b_{ij} = \sqrt{\frac{2E}{T}} \int_0^T dt\, \varphi_j(t) \sin\left(\omega_d t + \frac{2\pi i}{m}\right) \tag{B-10}
$$

$$
n_j = \int_0^T dt\, \varphi_j(t)\, n(t) \tag{B-11}
$$

and a_{ij} is defined in general in equation (A-2) and in particular in equation (B-3). For the kind of noise, n(t), assumed, the statistics of n_j have been worked out in Appendix A. It is shown that n_j is a gaussian variable with zero mean and variance N_0, where N_0 is the spectral density of the noise (assumed to be

62

white). The noise outputs of the various product integrators are independent. The statistics for the random variable n_j may then be summarized as

$$\left.\begin{array}{c} \overline{n_j} = 0 \\[2em] \overline{n_j n_k} = N_0\ \delta_{jk} \end{array}\right\} \qquad (\text{B-12})$$

The coefficients b_{ij} arise from an alphabet of signals H_i given by

$$H_i = \sqrt{\frac{2E}{T}}\ \sin\left(\omega_d t + \frac{2\pi i}{m}\right) \qquad (\text{B-13})$$

The signals (B-13) are 90 degrees out of phase with the transmitted alphabet S_i and are not members of that alphabet. Since

$$H_i(t) = S_i\left(t - \frac{\pi}{2\omega_d}\right) \qquad (\text{B-14})$$

it follows that when S_i is specified, H_i is likewise specified.

Probability of Error Computations

If, in response to a transmitted signal S_j, the observed signal e does not lie in the region in observation space corresponding to S_j, the decision device identifies the signal incorrectly and an error has been made. If the proper region of the observation space for a transmitted signal S_i is R_i, then the conditional probability that e_i lies in the region R_i, given that S_i was transmitted, is the probability of correct detection for the signal S_i. The joint probability that e_i will lie in R_i and that S_i was sent is then given by the product of the conditional probability that e_i lies in R_i times the marginal probability of S_i being transmitted. The joint probability of correct detection is then found by summing this joint probability over the index i, thereby taking into account all possible transmitted signals S_i. The probability of error is then one minus this quantity.

The probability of error when all possible transmitted signals are considered is given by

$$
P_\epsilon = \sum_{i=1}^{m} P(S_i) P(e \notin R_i | S_i)
$$

$$
= \frac{1}{m} \sum_{i=1}^{m} P(e \notin R_i | S_i)
$$

(B-15)

The conditional probability in equation (B-15) is read as the probability that e is not an element of R_i, given that S_i was sent. $P(S_i)$ is read as the probability that S_i was sent. Since all S_i are all equally likely to be sent, $P(S_i)$ can be replaced by $1/m$. It remains to find the required conditional probability. To obtain the joint probability distribution of the four random variables in equation (B-9), it is necessary to find the relationship between a_{ij} and b_{ij}. It follows in equations (B-10), (B-13), and (B-14) that

$$
b_{ij} = \int_0^T dt\, \phi_j(t)\, H_i(t) = \int_0^\Gamma dt\, \phi_j(t)\, S_i \left(t - \frac{\pi}{2\omega_d} \right)
$$

$$
= \int_{-\frac{\pi}{2\omega_d}}^{T - \frac{\pi}{2\omega_d}} dt\, \phi_j \left(t + \frac{\pi}{2\omega_d} \right) S_i(t)
$$

(B-16)

From equation (B-16), it does not appear that there is an explicit relationship between b_{ij} and a_{ij} unless the form of ϕ_j is known. With the use of equation (B-14), the coefficients b_{i1} and b_{i2} are given, respectively, by

$$b_{i1} = \int_0^T \sqrt{\frac{2E}{T}} \sin \left(\omega_d t - \frac{2\pi i}{m} \right) \sqrt{\frac{2}{T}} \cos \omega_d t \; dt$$

$$= \frac{\sqrt{E}}{T} \int_0^T \left[\sin \left(2\omega_d t + \frac{2\pi i}{m} \right) + \sin \frac{2\pi i}{m} \right] dt \qquad \text{(B-17)}$$

$$= \sqrt{E} \sin \frac{2\pi i}{m} = - a_{i2}$$

$$b_{i2} = \int_0^T \sqrt{\frac{2E}{T}} \sin \left(\omega_d t + \frac{2\pi i}{m} \right) \sqrt{\frac{2}{T}} \sin \omega_d t \; dt$$

$$= \frac{\sqrt{E}}{T} \int_0^T \left[\cos \frac{2\pi i}{m} - \cos \left(2\omega_d t + \frac{2\pi i}{m} \right) \right] dt \qquad \text{(B-18)}$$

$$= \sqrt{E} \cos \frac{2\pi i}{m} = a_{i1}$$

In evaluation of equations (B-17) and (B-18), it has again been assumed that ω_d is some integer multiple of $(2\pi/T)$. Equations (B-17) and (B-18) show that the b's are equivalent to cross-coupling the product integrator outputs. The coefficients b_{ij} and a_{ij} can also be shown to be statistically uncorrelated. If the mean of the a's and b's is 0, then b_{ij} and a_{ij} are statistically orthogonal. When S_i is given, i is specified, and therefore a_{ij} and b_{ij} are specified. As a result, when e_j is conditioned on S_i, a_{ij} and b_{ij} are treated as constants. From equation (B-9), the conditional probability of e_j, given S_i and θ, is

$$p(e_j|S_i, \theta) = \int p(e_j|S_i, \theta, n_j)\, p(n_j)\, dn_j$$

$$= \int \delta(e_j - \cos\theta\, a_{ij} - \sin\theta\, b_{ij} - n_j)\, p(n_j)\, d_{nj} \qquad \text{(B-19)}$$

$$= P_{nj}(e_j - \cos\theta\, a_{ij} - \sin\theta\, b_{ij})$$

In equation (B-19) it has been assumed that n_j is independent of S_i and θ. It is certainly true that the additive noise is independent of the incoming signal. However, the angle θ is affected by the receiver noise. It is assumed here that the noise bandwidth of the reference signal is much narrower than the noise bandwidth of the received information-carrying signal. Since θ is the difference between the input signal phase which is not affected by receiver noise and the reference phase which presumably has a noise spectrum that is very narrow, the correlation between the noise associated with the signal, n_j, and the reference phase is negligible. The correlation between θ and n_j is therefore also negligible. There is no correlation between θ and S_i, because θ is not present in the transmitted signal S_i but arises as a consequence of phase variations in the transmission medium and the reference signal in the receiver. Since n_j is gaussian, it follows from equation (B-12) that

$$\cdot p(e|S_i, \theta) = \prod_{j=1}^{k} P_{nj}(e_j - \cos\theta\, a_{ij} - \sin\theta\, b_{ij}) \qquad \text{(B-20)}$$

In equation (B-20), e is a random vector whose components are e_1, e_2, ..., e_k. In this case, for which there are only two (k=2) orthonormal functions, equation (B-20) may be written

$$p(e|S_i, \theta) = P_{n1}(e_1 - a_{i1}\cos\theta - b_{i1}\sin\theta) \cdot P_{n2}(e_2 - a_{i2}\cos\theta - b_{i2}\sin\theta)$$

$$= \frac{1}{2\pi N_o} \exp\left\{ -\frac{1}{2N_o}\left[(e_1 - a_{i1}\cos\theta - b_{i1}\sin\theta)^2 \right.\right.$$

$$\left.\left. + (e_2 - a_{i2}\cos\theta - b_{i2}\sin\theta)^2 \right] \right\} \qquad \text{(B-21)}$$

66

From equations (B-17), (D-18), equation (B-21), the following expression may be written;

$$p\left(\underline{e}|S_1,\theta\right) = \frac{1}{2\pi N_0}\exp\left\{-\frac{1}{2N_0}\left[\left(e_1 - \sqrt{E}\cos\frac{2\pi i}{m}\cos\theta\right.\right.\right.$$

$$\left.\left.\left. - \sqrt{E}\sin\frac{2\pi i}{m}\sin\theta\right)^2 + \left(e_2 + \sqrt{E}\sin\frac{2\pi i}{m}\cos\theta - \sqrt{E}\cos\frac{2\pi i}{m}\sin\theta\right)^2\right]\right\}$$

$$= \frac{1}{2\pi N_0}\exp\left[-\frac{1}{2}\left\{\left[\frac{e_1}{\sqrt{N_0}} - \sqrt{\frac{E}{N_0}}\cos\left(\theta - \frac{2\pi i}{m}\right)\right]^2\right.\right.$$

$$\left.\left. + \left[\frac{e_2}{\sqrt{N_0}} - \sqrt{\frac{E}{N_0}}\sin\left(\theta - \frac{2\pi i}{m}\right)\right]^2\right\}\right] \qquad (B-22)$$

figure B-3 shows the geometrical situation. The probability that the vector $\underline{e}$ lies in the region R_i, given that S_i was transmitted and the reference angle is θ, is equal to the probability that the vector e lies in the crosshatched region shown in figure B-3. This probability must be independent of i. That it is independent can be shown by rotating the coordinate system in figure B-3 through the angle $\left(-\frac{2\pi i}{m}\right)$. From figure B-3 the probability that $\underline{e}$ is an element of R_i, given that S_i was transmitted and that the reference angle is θ, is

$$p\left(\underline{e}\in R_i|S_i,\theta\right) = \int_0^\infty de_1 \int_{e_1\tan\left(-\frac{2\pi i}{m}-\frac{\pi}{m}\right)}^{e_1\tan\left(-\frac{2\pi i}{m}+\frac{\pi}{m}\right)} p\left(e|S_i,\theta\right)de_2 \qquad (B-23)$$

The coordinates of figure B-3 are then rotated through $\left(-\frac{2\pi i}{m}\right)$ by means of the equations

$$e_1 = E_1\cos\frac{2\pi i}{m} + E_2\sin\frac{2\pi i}{m} \qquad E_1 = + e_1\cos\frac{2\pi i}{m} - e_2\sin\frac{2\pi i}{m}$$

$$e_2 = -E_1\sin\frac{2\pi i}{m} + E_2\cos\frac{2\pi i}{m} \qquad E_2 = + e_1\sin\frac{2\pi i}{m} + e_2\cos\frac{2\pi i}{m} \qquad (B-24)$$

Substituting equations (B-24) into equation (B-22) yields

$$p = (\underline{E} \mid S_i, \theta) = \frac{1}{2\pi N_0} \exp\left[-\frac{1}{2} \left\{ \frac{e_1^2 + e_2^2}{N_0} - \frac{2e_1 \sqrt{E}}{N_0} \cos\left(\theta - \frac{2\pi i}{m}\right) \right.\right.$$

$$\left.\left. -\frac{2e_2 \sqrt{E}}{N_0} \sin\left(\theta - \frac{2\pi i}{m}\right) + \frac{E}{N_0} \right\} \right]$$

$$= \frac{1}{2\pi N_0} \exp\left[-\frac{1}{2 N_0} \left\{ E_1^2 + E_2^2 - 2\sqrt{E} \cos\left(\theta - \frac{2\pi i}{m}\right)\right.\right.$$

$$\left(E_1 \cos\frac{2\pi i}{m} + E_2 \sin\frac{2\pi i}{m}\right) - 2\sqrt{E} \sin\left(\theta - \frac{2\pi i}{m}\right)$$

$$\left.\left.\left(- E_1 \sin\frac{2\pi i}{m} + E_2 \cos\frac{2\pi i}{m}\right) + E \right\} \right]$$

$$= \frac{1}{2\pi N_0} \exp\left[\frac{1}{2} \left\{ \left(\frac{E_1}{\sqrt{N_0}} - \sqrt{\frac{E}{N_0}} \cos\theta\right)^2 \right.\right.$$

$$\left.\left. + \left(\frac{E_2}{\sqrt{N_0}} - \sqrt{\frac{E}{N_0}} \sin\theta\right)^2 \right\} \right]$$

$$\left.\right\} \text{(B-25)}$$

Equations (B-25) show that the desired probability is indeed independent of i. When i is set equal to m in equation (B-22), equation (B-25) results.

The geometry in the new coordinate system is shown in figure B-4, and in this system equation (B-23) becomes

$$p(\underline{E} \in R_i \mid S_i, \theta) = \int_0^\infty dE_1 \int_{-E_1 \tan\frac{\pi}{m}}^{E_1 \tan\frac{\pi}{m}} dE_2 \, p(\underline{E} \mid S_i, \theta) \qquad \text{(B-26)}$$
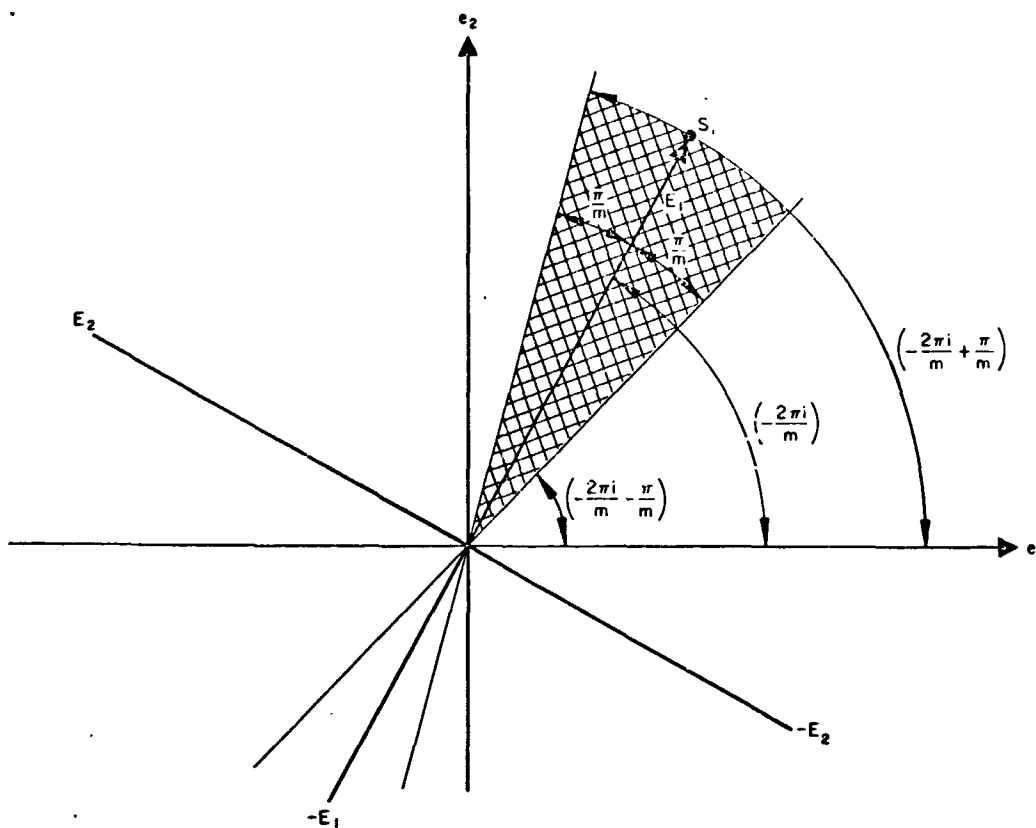
Figure B-3. Signal space representation of received signal.
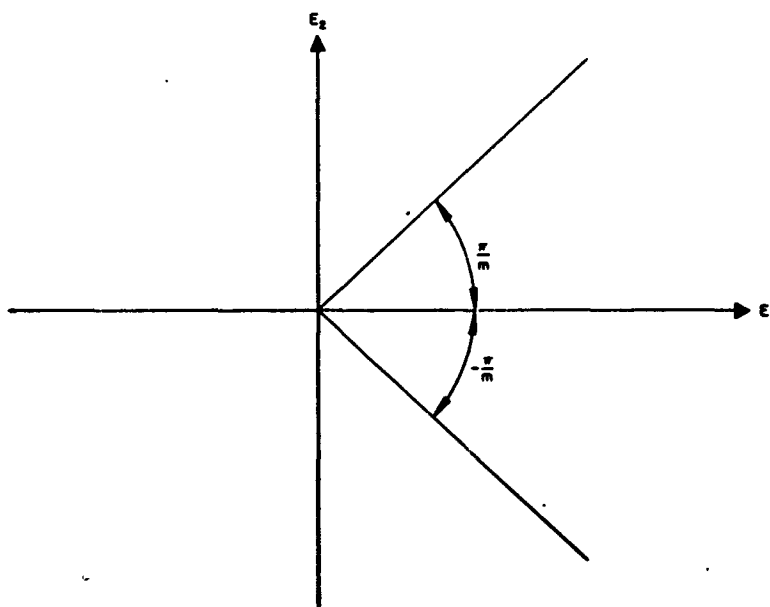
Figure B-4. Coordinate system of figure B-3 rotated
by $2\pi i/m$.

Let

$$x = \frac{E_1}{\sqrt{N_0}} - \sqrt{\frac{E}{N_0}} \cos \theta$$

$$\left. y = \frac{E_2}{\sqrt{N_0}} - \sqrt{\frac{E}{N_0}} \sin \theta \right\}$$ (B-27)

Since the probability in equation (B-26) is the same for each i and since the probability that S_i is sent is $\frac{1}{m}$, the probability of error is 1 minus the average of equation (B-25) over all θ. For this operation, the distribution of θ must be postulated. The coherent detection scheme and the analysis presented so far is most applicable when the rms fluctuation of θ is small. This condition is best satisfied when phase-locked loops are used to track the incoming phase and the demodulation is coherent. It is assumed that the distribution of θ is gaussian with zero mean and variance σ^2. The probability of error will then be found as a function of this variance. The variance of θ is a function of the signal-to-noise ratio on the input. Although the error arising from non-zero θ will be small if the signal-to-noise ratio is high, the signal-to-noise ratio to be expected when the signal is transmitted from the earth to Mars is quite low. In this case, the variance of θ may be sufficiently large to give a significant error. The distribution of θ is given by

$$p(\theta) = \frac{1}{\sqrt{2\pi\sigma^2}} \exp\left[-\frac{\theta^2}{2\sigma^2}\right]$$ (B-28)

It therefore follows that

$$P_e = 1 - \frac{1}{\sqrt{2\pi}\,\sigma} \int_{-\infty}^{\infty} d\theta \exp\left[-\frac{\theta^2}{2\sigma^2}\right] p\,(\underline{E} \in R_i | S_i, \theta)$$ (B-29)

Employing equations (B-25) and (B-27), equation (B-29) becomes

$$P_e = 1 - \frac{2}{(2\pi)^{3/2}\sigma} \int_0^\infty d\theta \exp\left[-\frac{\theta^2}{2\sigma^2}\right] \int_{-\sqrt{\frac{E}{N_0}}\cos\theta}^\infty dx \exp\left[-\frac{x^2}{2}\right]$$

$$\int_{-x\tan\frac{\pi}{m} - \frac{\sqrt{E/N_0}}{\cos \pi/m}\sin\left(\theta + \frac{\pi}{m}\right)}^{x\tan\frac{\pi}{m} - \frac{\sqrt{E/N_0}}{\cos \pi/m}\sin\left(\theta - \frac{\pi}{m}\right)} dy \exp\left[-\frac{y^2}{2}\right] \qquad (B-30)$$

In equation (B-30), the range of integration from $-\infty$ to ∞ on θ is replaced by two times the integral from 0 to ∞, since the integral (B-30) is even in θ. The bounds on y are the upper limit, y_u, and the lower limit y_ℓ, where

$$- \infty < y_\ell \leq - \sqrt{\frac{E}{N_0}}\sin\theta \leq y_u < \infty$$

$$- \sqrt{\frac{E}{N_0}}\cos\theta \leq x < \infty \qquad (B-31)$$

and where

$$y_u = x\tan\frac{\pi}{m} - \frac{\sqrt{E/N_0}}{\cos \pi/m}\sin\left(\theta - \frac{\pi}{m}\right)$$

$$y_\ell = -x\tan\frac{\pi}{m} - \frac{\sqrt{E/N_0}}{\cos \pi/m}\sin\left(\theta + \frac{\pi}{m}\right) \qquad (B-32)$$

The geometry of equation (B-30) is shown in figure B-5.

Equation (B-30) can be written as

$$P_e = 1 - \frac{1}{\sqrt{2\pi}\sigma}\int_{-\infty}^\infty \exp\left[-\frac{\theta^2}{2\sigma^2}\right] I(\theta)\, d\theta \qquad (B-33)$$
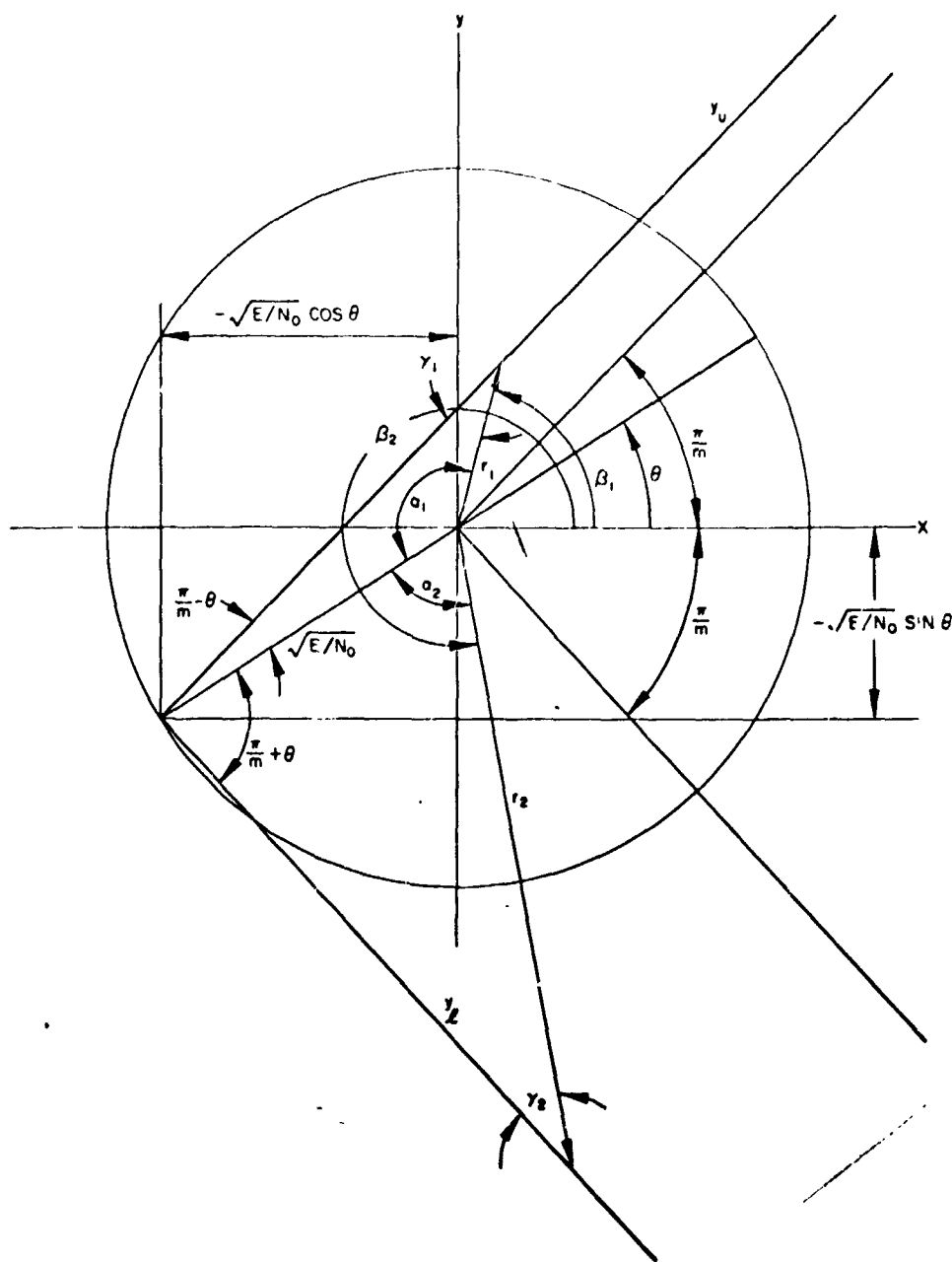
Figure B-5. Region of integration for $-\dfrac{\pi}{m} \le \theta \le \dfrac{\pi}{m}$

where

$$I(\theta) = \frac{1}{2\pi} \int_{-\sqrt{\frac{E}{N_0}}\cos\theta}^{\infty} dx\, \exp\left[-\frac{x^2}{2}\right] \int_{y_\ell}^{y_u} dy\, \exp\left[-\frac{y^2}{2}\right] \qquad (B\text{-}34)$$

Let

$$r = x^2 + y^2$$

$$dxdy = r \, dr \, d\beta$$

$$(B-35)$$

The area of interest is the wedge-shaped region in figure B-5 lying between y_ℓ and y_u. From the geometry depicted,

$$\frac{\sin \gamma_1}{\sqrt{E/N_0}} = \frac{\sin \left(\frac{\pi}{m} - \theta \right)}{r_1}$$

$$\frac{\sin \gamma_2}{\sqrt{E/N_0}} = \frac{\sin \left(\frac{\pi}{m} + \theta \right)}{r_2}$$

$$(B-36)$$

As can be seen,

$$\alpha_1 = \pi - \beta_1 + \theta \qquad \alpha_2 = \beta_2 - \pi - \theta$$

$$\gamma_1 = \beta_1 - \frac{\pi}{m} \qquad \gamma_2 = 2\pi - \frac{\pi}{m} - \beta_2$$

$$(B-37)$$

so that the three regions of integration are

$$0 \le r_1 \le \sqrt{E/N_0} \; \frac{\sin \left(\frac{\pi}{m} - \theta \right)}{\sin \left(\beta_1 - \frac{\pi}{m} \right)}$$

$$\frac{\pi}{m} \le \beta_1 \le \pi + \theta$$

$$(B-38)$$

$$0 \le r_2 \le - \sqrt{E/N_0} \ \frac{\sin\left(\frac{\pi}{m} + \theta\right)}{\sin\left(\frac{\pi}{m} + \beta_2\right)} \Bigg\} \tag{B-39}$$

$$\pi + \theta \le \beta_2 \le 2\pi - \frac{\pi}{m}$$

$$\left. \begin{array}{l} 0 \le r_3 < \infty \\[20pt] -\frac{\pi}{m} \le \beta_3 \le \frac{\pi}{m} \end{array} \right\} \tag{B-40}$$

The above bounds are valid for $-\pi/m \le \theta \le \pi/m$. The appropriate geometry for $\pi/m \le \theta \le 2\pi - \pi/m$ appears in figure B-6.
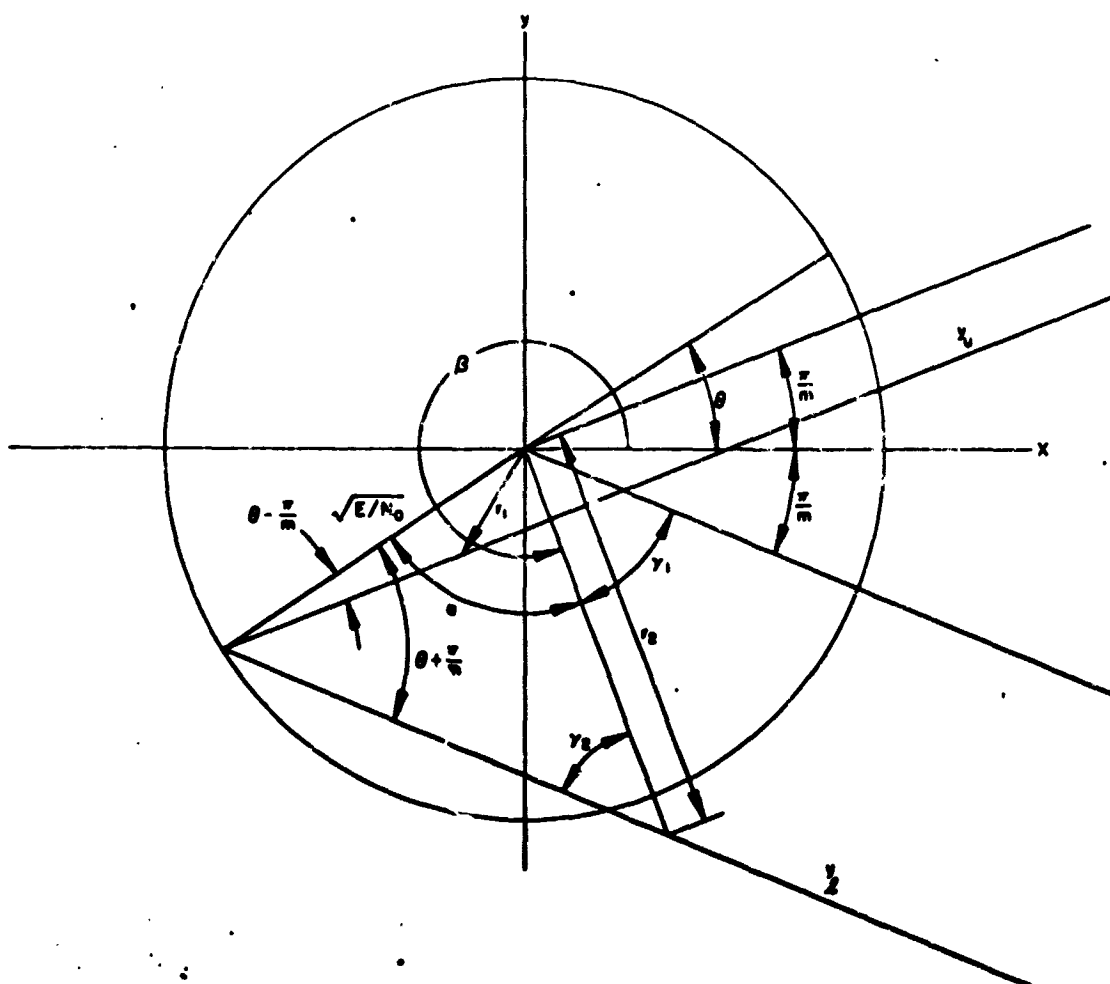
Figure B-6. Regions of integration for $\frac{\pi}{m} \le \theta \le 2\pi - \frac{\pi}{m}$

74

From the geometry in figure B-6.

$$\alpha = \beta - \pi - \theta \qquad\qquad \gamma_1 = 2\pi + \frac{\pi}{m} - \beta \left.\vphantom{\begin{array}{c}a\\b\end{array}}\right\} \qquad (\text{B-41})$$

$$\gamma_2 = 2\pi - \frac{\pi}{m} - \beta$$

$$\frac{\sin \gamma_1}{\sqrt{E/N_0}} = \frac{\sin (\theta - \pi/m)}{r_1} \left.\vphantom{\begin{array}{c}a\\b\\c\\d\end{array}}\right\}$$

$$(\text{B-42})$$

$$\frac{\sin \gamma_2}{\sqrt{E/N_0}} = \frac{\sin (\theta + \pi/m)}{r_2}$$

The regions of integration are the same as in figure B-5, except that equation (B-38) is replaced by

$$\theta \leq r_1 \leq \sqrt{E/N_0} \; \frac{\sin (\pi/m - \theta)}{\sin (\beta_1 - \pi/m)} \left.\vphantom{\begin{array}{c}a\\b\\c\end{array}}\right\}$$

$$(\text{B-43})$$

$$\pi + \theta \leq \beta_1 \leq 2\pi + \pi/m$$

The area whose bounds are given by equation (B-43) is subtracted from the other two areas rather than added as in figure B-5.

It follows from equations (B-38) through (B-40) and figure B-5, and from equations (B-34) and (B-35), that

$$I(\theta) = \frac{1}{2\pi} \left\{ \int_{\frac{\pi}{m}}^{\pi+\theta} d\beta \int_{0}^{\sqrt{E/N_0} \frac{\sin(\pi/m - \theta)}{\sin(\beta - \pi/m)}} \exp\left[-r^2/2\right] r\, dr \right.$$

$$+ \int_{\pi+\theta}^{2\pi-\pi/m} d\beta \int_{0}^{-\sqrt{E/N_0} \frac{\sin(\pi/m + \theta)}{\sin(\pi/m + \beta)}} \exp\left[-r^2/2\right] r\, dr$$

$$\left. + \int_{-\pi/m}^{\pi/m} d\beta \int_{0}^{\infty} \exp\left[-r^2/2\right] r\, dr \right\} \qquad (B\text{-}44)$$

$$= \frac{1}{2\pi} \left[2\pi - \int_{\pi/m}^{\pi+\theta} d\beta \exp\left[-\frac{E}{2N_0} \frac{\sin^2\left(\frac{\pi}{m} - \theta\right)}{\sin^2\left(\beta - \frac{\pi}{m}\right)} \right] \right.$$

$$\left. - \int_{\pi+\theta}^{2\pi - \frac{\pi}{m}} \exp\left[-\frac{E}{2N_0} \frac{\sin^2\left(\frac{\pi}{m} + \theta\right)}{\sin^2\left(\beta + \frac{\pi}{m}\right)} \right] d\beta \right]$$

It is interesting to compare this result with $I(\theta)$ found from equations (B-43), (B-39), and (B-40) and figure B-6. In this case,

$$I(\theta) = \frac{1}{2\pi} \left[-\int_{\pi+\theta}^{2\pi+\pi/m} d\beta \int_{0}^{\sqrt{E/N_0} \frac{\sin\left(\frac{\pi}{m} - \theta\right)}{\sin\left(\beta - \frac{\pi}{m}\right)}} \exp\left[-r^2/2\right] r\, dr \right.$$

$$\left. + \int_{\pi+\theta}^{2\pi-\pi/m} d\beta \int_{0}^{-\sqrt{E/N_0} \frac{\sin\left(\frac{\pi}{m} + \theta\right)}{\sin\left(\frac{\pi}{m} + \beta\right)}} \exp\left[-r^2/2\right] r\, dr + \int_{-\pi/m}^{\pi/m} d\beta \int_{0}^{\infty} \exp\left[-r^2/2\right] r\, dr \right]$$

$$(B\text{-}45)$$

Equation (B-44) can be written in the form of equation (B-45) by reversing the order of integration in the first integral in equation (B-44). This first integral can be written as

$$
\left.
\begin{aligned}
I_1 &= \int_{\pi/m}^{\pi+\theta} d\beta \int_0^{\sqrt{E/N_0}\,\frac{\sin(\pi/m-\theta)}{\sin(\beta-\pi/m)}} \exp[-r^2/2]\, r\,dr \\[2em]
&= -\int_{\pi+\theta}^{2\pi+\pi/m} d\beta \int_0^{\sqrt{E/N_0}\,\frac{\sin(\pi/m-\theta)}{\sin(\beta-\pi/m)}} \exp[-r^2/2]\, r\,dr
\end{aligned}
\right\} \tag{B-46}
$$

Since $m \geq 2$, $\pi/m < \pi + \theta$ for $\theta > 0$; hence, the upper bound on the second equation for I_1 is $2\pi + \pi/m$ rather than π/m in order that the area represented by the double integral be positive. This fact is also evident from the geometry in figures B-5 and B-6, in which the same area represented by I that is added in figure B-5 is subtracted in figure B-6. It therefore follows that equation (B-44) reduces to equation (B-45) in the range $2\pi - \pi/m \leq \theta \leq 2\pi + \pi/m$ so that equation (B-44) applies for all θ. Substituting equation (B-44) into equation (B-33) yields

$$
P_e = 1 - \frac{1}{\sqrt{2\pi}\sigma} \int_{-\infty}^{\infty} d\theta\, \exp\left[-\frac{\theta^2}{2\sigma^2}\right]\left[1 - \frac{1}{2\pi}\int_{\pi/m}^{\pi+\theta} \exp\left[-\frac{E}{2N_0}\frac{\sin^2(\pi/m-\theta)}{\sin^2(\beta-\pi/m)}\right]d\beta - \frac{1}{2\pi}\int_{\pi+\theta}^{2\pi-\pi/m} \exp\left[-\frac{E}{2N_0}\frac{\sin^2(\pi/m+\theta)}{\sin^2(\pi/m+\beta)}\right]d\beta\right]
$$

$$
= \frac{2}{(2\pi)^{3/2}\sigma}\int_0^{\infty} \exp\left[-\frac{\theta^2}{2\sigma^2}\right] \left\{\left[\int_{\pi/m}^{\pi+\theta} \exp\left[-\frac{E}{2N_0}\frac{\sin^2(\beta-\pi/m)}{\sin^2(\beta-\pi/m)}\right]d\beta + \int_{\pi+\theta}^{2\pi-\pi/m} \exp\left[-\frac{E}{2N_0}\frac{\sin^2(\beta+\pi/m)}{\sin^2(\beta+\pi/m)}\right]d\beta\right]\right\} \tag{B-47}
$$

Equation (B-47) is the integral to be computed to yield P_e for m-ary PSK. For m = 2, equation (B-47) simplifies as follows.

$$P_e = \frac{2}{(2\pi)^{3/2} \sigma} \int_0^\infty \exp\left[-\frac{\theta^2}{2\sigma^2}\right] I_0(\theta) \, d\theta \qquad (B-48)$$

where

$$
\begin{aligned}
I_0(\theta) &= \int_{\pi/2}^{3\pi/2} \exp\left[-\frac{E}{2N_0} \frac{\cos^2\theta}{\cos^2\beta}\right] d\beta = 2 \int_0^{\pi/2} \exp\left[-\frac{E}{2N_0} \frac{\cos^2\theta}{\cos^2\beta}\right] d\beta \\[2ex]
&= 2 \exp\left[-\frac{E}{2N_0} \cos^2\theta\right] \int_0^{\pi/2} \exp\left[-\frac{E}{2N_0} \cos^2\theta \tan^2\beta\right] d\beta \\[2ex]
&= 2 \exp\left[-\frac{E}{2N_0} \cos^2\theta\right] \int_0^\infty \exp\left[-\frac{E}{2N_0} \cos^2\theta \, z^2\right] \frac{dz}{1+z^2}
\end{aligned}
\qquad (B-49)
$$

But (ref. 26), equation (B-49) becomes

$$I_0(\theta) = \sqrt{2\pi} \int_{\sqrt{\frac{E}{N_0}} \cos\theta}^\infty \exp\left[-z^2/2\right] dz \qquad (B-50)$$

and, upon the substituting of equation (B-50) into equation (B-48),

$$P_e = \frac{2}{\sqrt{2\pi}\,\sigma} \int_0^\infty \exp\left[-\frac{\theta^2}{2\sigma^2}\right] d\theta \, \frac{1}{\sqrt{2\pi}} \int_{\sqrt{\frac{E}{N_0}} \cos\theta}^\infty \exp\left[-z^2/2\right] dz \qquad (B-51)$$

78

On employing the identity

$$\frac{1}{\sqrt{2\pi}} \int_{\psi}^{\infty} \exp\left[-z^2/2\right] dz = 1 - \frac{1}{\sqrt{2\pi}} \int_{-\infty}^{\psi} \exp\left[-z^2/2\right] dz \qquad (B-52)$$

equation (2) in the Discussion results.

The expansion of equation (1) of the Discussion for low signal-to-noise ratios may be derived from equations (B-25) and (B-26). First, E_1 and E_2 are converted to polar coordinates by the transformation

$$E_1 = r \cos \psi$$
$$\qquad (B-53)$$
$$E_2 = r \sin \psi$$

On using this relation in equation (B-25), equation (B-26) becomes

$$p(E \epsilon R_i | S_i, \theta) = \frac{1}{2\pi N_0} \int_0^{\infty} \int_{-\frac{\pi}{m}}^{\frac{\pi}{m}} \exp\left[\frac{1}{2}\left\{\left(\frac{r \cos \psi - \sqrt{E} \cos \theta}{\sqrt{N_0}}\right)^2\right.\right.$$

$$\left.\left. + \left(\frac{r \sin \psi - \sqrt{E} \sin \theta}{\sqrt{N_0}}\right)^2\right]\right] d\psi r\, dr$$

$$= \frac{1}{2\pi N_0} \int_0^{\infty} \int_{-\frac{\pi}{m}}^{\frac{\pi}{m}} \exp\left[-\frac{1}{2}\frac{E}{N_0}\sin^2(\psi-\theta)\right]$$

$$\exp\left[-\frac{1}{2}\frac{[r - \sqrt{E} \cos(\psi-\theta)]^2}{N_0}\right] d\psi r\, dr$$

$$= \frac{1}{2\pi N_0} \int_{-\frac{\pi}{m}}^{\frac{\pi}{m}} \exp\left[-\frac{1}{2}\frac{E}{N_0}\sin^2(\psi-\theta)\right]$$

$$\int_{-\sqrt{E}\cos(\psi-\theta)}^{\infty} [t + \sqrt{E} \cos(\psi-\theta)] \exp\left[-\frac{1}{2}\frac{t^2}{N_0}\right] d\psi dt$$

$$= \frac{1}{m} \exp\left[-\frac{E}{2N_0}\right] + \frac{1}{2\sqrt{\pi}}\sqrt{\frac{E}{2N_0}} \int_{-\frac{\pi}{m}}^{\frac{\pi}{m}} \cos(\psi-\theta)$$

$$\exp\left[-\frac{E}{2N_0}\sin^2(\psi-\theta)\right] dx + \frac{\sqrt{E}}{2\pi N_0}$$

$$\int_{-\frac{\pi}{m}}^{\frac{\pi}{m}} \cos(\psi-\theta) \exp\left[-\frac{E}{2N_0}\sin^2(\psi-\theta)\right] \int_0^{\sqrt{E}\cos(\psi-\theta)} \exp(-\frac{t^2}{2N_0}) dt d\psi$$

If this last form of equation (B-54) is expanded in power of $\sqrt{\frac{E}{2N_0}}$ and averaged over θ and m, the mean probability of a correct decision results. Equation (3) is just one minus this value. The limiting value of probability of error for high signal-to-noise ratios may also be from the third form of equation (B-54). In this equation the integral over t approaches either zero, when $\psi - \theta$ is in the second or third quadrant, or $\sqrt{2\pi N_0}$ when $\psi - \theta$ lies in the first or fourth quadrant. If the substitution

$$u = \sin(\psi - \theta) \tag{B-55}$$

is made, the region of integration is as shown in figure B-7.
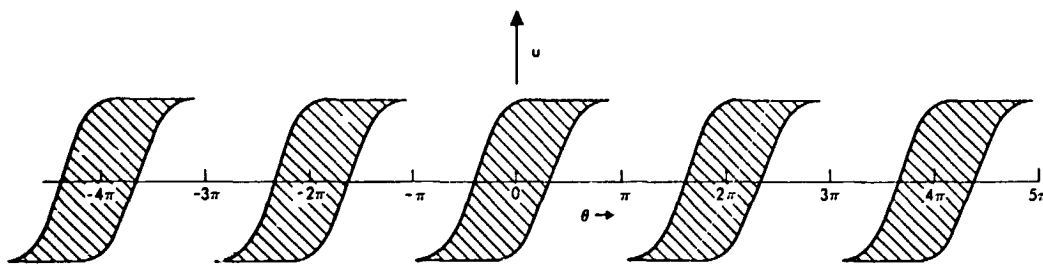
Figure B-7. Region of integration for large signal-to-noise ratios.

However, as E/N_0 becomes large, only the regions of integration that include $u = 0$ contribute significantly to the integral. These regions include only the ranges of θ given by

$$2n\pi - \frac{\pi}{m} \leq \theta \leq 2n\pi + \frac{\pi}{m} \tag{B-56}$$

and in these ranges the integration over u may be extended to $\pm\infty$. Consequently,

$$p(E \epsilon R_i | S_i, \theta) = 1 \qquad 2n\pi - \frac{\pi}{m} < \theta < 2n\pi + \frac{\pi}{m}$$

$$= 0 \qquad \text{elsewhere} \tag{B-57}$$

The probability of error is then

$$P_e \longrightarrow \frac{1}{\sqrt{2\pi}\sigma_\theta} \sum_{n=-\infty}^{\infty} \int_{2n\pi - \frac{\pi}{m}}^{2n\pi + \frac{\pi}{m}} \exp\left[-\frac{\theta^2}{2\sigma_\theta^2} \right] d\theta \tag{B-58}$$

and equation (4) in the Discussion follows immediately.

80

APPENDIX C. EFFECT OF BANDWIDTH ON THE PROBABILITY OF ERROR IN THE DETECTION OF BINARY COHERENT PHASE SHIFT KEY MODULATION

General Derivation

In this appendix the effect of channel bandwidth on probability of error is considered. A binary PSK signal with gaussian additive noise is assumed. The signal is detected using a noiseless coherent reference signal and is then integrated over a bit duration, T. The integrator is an integrate-and-dump type and is synchronized with the bit timing. The signals are assumed to be band-limited so that there will be some intersymbol influence at the integrator input. It is assumed that this influence is restricted to adjacent bits only. The adjacent bits into the filter look somewhat as in figure C-1.

Adjacent bits are equally likely to be of the same sign or of opposite signs. The signal into the filter may be written as

$$f_1(t) = f_0(t) \pm f_0(t+T) \pm f_0(t-T) \qquad 0 < t < T \qquad \text{(C-1)}$$

where $f_0(t)$ is the basic waveform of the phase detected bit. The probability density function for $f_1(t)$ is

$$P_1(f_1) = \frac{1}{4} \delta \left(f_1(t) - \left[f_0(t) - f_0(t+T) - f_0(t-T) \right] \right)$$

$$+ \frac{1}{4} \delta \left(f_1(t) - \left[f_0(t) - f_0(t+T) + f_0(t-T) \right] \right)$$

$$+ \frac{1}{4} \delta \left(f_1(t) - \left[f_0(t) + f_0(t+T) - f_0(t-T) \right] \right)$$

$$+ \frac{1}{4} \delta \left(f_1(t) - \left[f_0(t) + f_0(t+T) + f_0(t-T) \right] \right) \qquad \text{(C-2)}$$
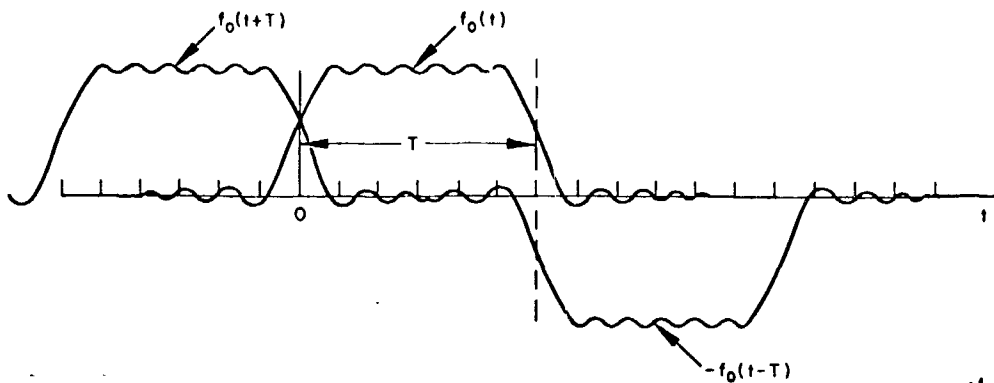
Figure C-1. Illustration of effect of finite bandwidth on rectangular waveshapes.

The total filter input is

$$v(t) = f_1(t) + n(t) \tag{C-3}$$

where n is a gaussian random variable with zero mean and variance σ_n^2.

$$p_n(n) = \frac{1}{\sqrt{2\pi}\,\sigma_n} \exp\left(-\frac{n^2}{2\,\sigma_n^2}\right) \tag{C-4}$$

The output of the integrator may be written as

$$y(T) = \int_0^T v(t)\,dt = \int_0^T f_0(t)\,dt \pm \int_0^T f_0(t+T)\,dt$$

$$\pm \int_0^T f_0(t-T)\,dt + \int_0^T n(t)\,dt \tag{C-5a}$$

$$= F_0 \pm F_1 \pm F_2 + \int_0^T n(t)\,dt \tag{C-5b}$$

$$y(T) = F + \int_0^T n(t)\,dt = F + z \tag{C-5c}$$

where the definitions of the capital F's are obvious. The probability density functions of F and z are

$$P_F(F) = \frac{1}{4} \delta \left(F - \left[F_0 - F_1 - F_2 \right] \right) + \frac{1}{4} \delta \left(F - \left[F_0 - F_1 + F_2 \right] \right)$$

$$+ \frac{1}{4} \delta \left(F - \left[F_0 + F_1 - F_2 \right] \right) + \frac{1}{4} \delta \left(F - \left[F_0 + F_1 + F_2 \right] \right) \quad \text{(C-6)}$$

and

$$P_z(z) = \frac{1}{\sqrt{2 \pi} \, \sigma_z} \exp \left[- \frac{z^2}{2 \sigma_z^2} \right] \quad \text{(C-7)}$$

where

$$\left. \begin{array}{l} \sigma_z^2 = \overline{\left[\int_0^T n(t) \, dt \right]^2} = \overline{\int_0^T \int_0^T n(t_2) \, n(t_1) \, dt_2 \, dt_1} \\[4mm] \sigma_z^2 = \int_0^T \int_0^T \overline{n(t_2) \, n(t_1)} \, dt_2 \, dt_1 = \int_0^T \int_0^T R_n(\tau) \, dt_2 \, dt_1 \end{array} \right\} \quad \text{(C-8)}$$

where $R_n(\tau)$ is the autocorrelation function of the noise (stationary). The transformation

$$\left. \begin{array}{l} t_2 = t_1 + \tau \\[3mm] t = t_1 \end{array} \right\} \quad \text{(C-9)}$$

gives

$$\sigma_z^2 = \int_0^T \int_{t-T}^t R_n(\tau) \, d\tau \, dt = \int_{-T}^T R_n(\tau) \, g(-\tau) \, d\tau \quad \text{(C-10)}$$

w' ˈrc

$$g(\tau) = \tau + T \qquad\qquad -T < \tau < 0$$

$$g(\tau) = T - \tau \qquad\qquad 0 < \tau < T$$

(C-11)

The last form was derived by using the relation between the autocorrelation function and the spectral density, together with the convolution theorem for Fourier transforms. The probability density function of y is given by

$$p_y(y) = \int_{-\infty}^{\infty} p_F(F)\, p_z(y - F)\, dF$$

$$= \frac{1}{4\sqrt{2\pi}\,\sigma_z}\left\{ \exp\left[-\frac{\left(y - \left[F_0 - F_1 - F_2\right]\right)^2}{2\,\sigma_z^2} \right] \right.$$

$$+ \exp\left[-\frac{\left(y - \left[F_0 - F_1 + F_2\right]\right)^2}{2\,\sigma_z^2} \right] + \exp\left[-\frac{\left(y - \left[F_0 + F_1 - F_2\right]\right)^2}{2\,\sigma_z^2} \right]$$

$$+ \exp\left[-\frac{\left(y - \left[F_0 + F_1 + F_2\right]\right)^2}{2\,\sigma_z^2} \right] \right\}$$

(C-12)

If it is assumed that $F_0 > 0$, then the probability of error in interpreting the received signal is

$$P_e = \int_{-\infty}^{0} p_y(y)\, dy$$

(C-13)

84

This relation gives

$$P_e = \frac{1}{4\sqrt{2\pi}\,\sigma_z} \left\{ \int_{-\infty}^{0} \exp\left[-\frac{\left(y-\left[F_0-F_1-F_2\right]\right)^2}{2\sigma_z^2}\right] dy \right.$$

$$+ \int_{-\infty}^{0} \exp\left[-\frac{\left(y-\left[F_0-F_1+F_2\right]\right)^2}{2\sigma_z^2}\right] dy$$

$$+ \int_{-\infty}^{0} \exp\left[-\frac{\left(y-\left[F_0+F_1-F_2\right]\right)^2}{2\sigma_z^2}\right] dy + \int_{-\infty}^{0} \exp\left[-\frac{\left(y-\left[F_0+F_1+F_2\right]\right)^2}{2\sigma_z^2}\right] dy \right\}$$

$$(C-14)$$

But

$$\int_{-\infty}^{0} \exp\left[-\frac{(\alpha-a)^2}{b}\right] dx = \sqrt{b}\int_{a/\sqrt{b}}^{\infty} \exp\left[-u^2\right] du = \frac{\sqrt{\pi b}}{2}\,\mathrm{erfc}\left(\frac{a}{\sqrt{b}}\right)$$

$$(C-15)$$

and the probability of error integral becomes

$$P_e = \frac{1}{8}\left\{ \mathrm{erfc}\left(\frac{F_0-F_1-F_2}{\sqrt{2}\,\sigma_z}\right) + \mathrm{erfc}\left(\frac{F_0-F_1+F_2}{\sqrt{2}\,\sigma_z}\right) + \mathrm{erfc}\left(\frac{F_0+F_1-F_2}{\sqrt{2}\,\sigma_z}\right) \right.$$

$$\left. + \mathrm{erfc}\left(\frac{F_0+F_1+F_2}{\sqrt{2}\,\sigma_z}\right) \right\}$$

$$(C-16)$$

Special Case of a Rectangular Passband

The input signal is assumed to be a square waveshape given by

$$f_{oo}(t) = A \left[U(t - t_0) - U(t - t_0 - T) \right] \qquad \text{(C-17)}$$

Its Fourier transform is

$$\left. \begin{aligned} \mathscr{F}_{oo}(\omega) &= A \int_{t_0}^{t_0 + T} \exp(-j\omega t)\, dt \\[2em] \mathscr{F}_{oo}(\omega) &= A T \exp\left[-j\omega \left(t_0 + \frac{T}{2} \right) \right] \frac{\sin\left(\dfrac{\omega T}{2}\right)}{\left(\dfrac{\omega T}{2}\right)} \end{aligned} \right\} \qquad \text{(C-18)}$$

The passband is assumed to be uniform from $-\Omega$ to Ω where $\Omega = 2\pi f_c$ (f_c = cutoff frequency). The transfer function of the input filter is then

$$\mathscr{N}(\omega) = \left[U(\omega + \Omega) - U(\omega - \Omega) \right] \exp(-j\omega T_d) \qquad \text{(C-19)}$$

where T_d is the signal time delay through the filter.

Then

$$\left. \begin{aligned} f_0(t) &= \frac{1}{2\pi} \int_{-\infty}^{\infty} \mathscr{F}_{oo}(\omega)\, \mathscr{N}(\omega) \exp(j\omega t)\, d\omega \\[2em] f_0(t) &= \frac{A}{\pi} \left[\text{Si}\left(\Omega[t - t_0 - T_d]\right) - \text{Si}\left(\Omega[t - t_0 - T_d - T]\right) \right] \end{aligned} \right\} \qquad \text{(C-20)}$$

where Si is the sine integral.

It is easily seen that

$$f_0(t + T) = \frac{A}{\pi} \left[\text{Si}\left(\Omega[t + T - t_0 - T_d]\right) - \text{Si}\left(\Omega[t - t_0 - T_d]\right) \right] \qquad \text{(C-21a)}$$

and

$$f_0(t-T) = \frac{A}{\pi} \left[Si(\Omega [t-T-t_0-T_d]) - Si(\Omega [t-2T-t_0-T_d]) \right] \qquad (C-21b)$$

$$F_0 = \int_{t_1}^{t_1+T} f_0(t) \, dt$$

$$
\begin{aligned}
F_0 = \frac{A}{\pi} &\left\{ (T+t_1-t_0-T_d) \, Si \left[\Omega(T+t_1-t_0-T_d) \right] - 2(t_0+T_d-t_1) \, Si \left[\Omega(t_0+T_d-t_1) \right] \right. \\
&+ (t_0+T_d+T-t_1) \, Si \left[\Omega(t_0+T_d+T-t_1) \right] - \frac{2\cos \Omega(t_0+T_d-t_1)}{\Omega} \\
&+ \left. \frac{\cos \Omega(T+t_1-t_0-T_d)}{\Omega} + \frac{\cos \Omega(t_0+T_d+T-t_1)}{\Omega} \right\}
\end{aligned}
$$

$$(C-22)$$

In a similar manner the following expressions are obtained.

$$
\begin{aligned}
F_1 = \int_{t_1}^{t_1+T} f_0(t+T) \, dt = \frac{A}{\pi} &\left\{ (2T+t_1-t_0-T_d) \, Si \left[\Omega(2T+t_1-t_0-T_d) \right] \right. \\
&-2(t_0+T_d-t_1-T) \, Si \left[\Omega(t_0+T_d-t_1-T) \right] + (t_0+T_d-t_1) \, Si \left[\Omega(t_0+T_d-t_1) \right] \\
&- \frac{2\cos \Omega(t_0+T_d-t_1-T)}{\Omega} + \frac{\cos \Omega(2T+t_1-t_0-T_d)}{\Omega} \\
&+ \left. \frac{\cos \Omega(t_0+T_d-t_1)}{\Omega} \right\}
\end{aligned}
$$

$$(C-23)$$

and

$$F_2 = \int_{t_1}^{t_1+T} f_0(t-T) \, dt$$

$$= \frac{A}{\pi} \left\{ (t_1-t_0-T_d) \, \mathrm{Si} \left[\Omega(t_1-t_0-T_d) \right] - 2(t_0+T_d+T-t_1) \, \mathrm{Si} \left[\Omega(t_0+T_d+T-t_1) \right] \right.$$

$$+ (t_0+T_d+2T-t_1) \, \mathrm{Si} \left[\Omega(t_0+T_d+2T-t_1) \right] - \frac{2 \cos \Omega(t_0+T_d+T-t_1)}{\Omega}$$

$$\left. + \frac{\cos \Omega(t_1-t_0-T_d)}{\Omega} + \frac{\cos \Omega(t_0+T_d+2T-t_1)}{\Omega} \right\} \tag{C-24}$$

When $t_1 = t_0 + T_d$, the integrator is synchronized with the symbol occurrence and F_0 is maximum. Then

$$F_0 = \frac{2A}{\pi} \left\{ T \, \mathrm{Si}[\Omega T] + \frac{\cos \Omega T - 1}{\Omega} \right\} \tag{C-25a}$$

$$F_1 = \frac{2A}{\pi} \left\{ T \left[\mathrm{Si}(2\Omega T) - \mathrm{Si}(\Omega T) \right] - \frac{\cos \Omega T}{\Omega} + \frac{1 + \cos \Omega 2T}{2\Omega} \right\} \tag{C-25b}$$

$$F_2 = \frac{2A}{\pi} \left\{ T \left[\mathrm{Si}(2\Omega T) - \mathrm{Si}(\Omega T) \right] - \frac{\cos \Omega T}{\Omega} + \frac{1 + \cos 2\Omega T}{2\Omega} \right\} = F_1 \tag{C-25c}$$

For the rectangular passband from $-\Omega$ to Ω, the noise spectrum in that region will be identical with the input noise spectrum

$$S(w) = N_0 \left[U(w+\Omega) - U(w-\Omega) \right] \tag{C-26}$$

88

where

$$N_0 = \frac{\pi}{\Omega} \sigma_n^2 \qquad \text{(C-27)}$$

then

$$\left. \begin{aligned} R(\tau) &= \frac{1}{2\pi} \int_{-\infty}^{\infty} S(\omega) \exp(j\omega\tau)\, d\omega \\[2em] R(\tau) &= \frac{N_0 \Omega}{\pi} \frac{\sin \Omega\tau}{\Omega\tau} \end{aligned} \right\} \qquad \text{(C-28)}$$

Then

$$\sigma_z^2 = \int_0^T \int_{t-T}^t R(\tau)\, d\tau\, dt = \frac{2 N_0}{\pi} T\, Si(\Omega T) \qquad \text{(C-29)}$$

If Ω is increased so that $\Omega T >> 1$, then eventually

$$F_0 \rightarrow AT \qquad \text{(C-30a)}$$

$$F_1 \text{ and } F_2 \rightarrow 0 \qquad \text{(C-30b)}$$

$$\sigma_z^2 \rightarrow N_0 T \qquad \text{(C-30c)}$$

Then the probability of error becomes

$$P_e \rightarrow \frac{1}{2} \text{erfc}\left(\frac{A\sqrt{T}}{\sqrt{2 N_0}} \right) = \frac{1}{2} \text{erfc}\left(\sqrt{\frac{E}{2 N_0}} \right) \qquad \text{(C-31)}$$

where $E(= A^2 T)$ is the energy per bit. This result is the one that is usually quoted.

When Ω or T is decreased so that $\Omega T \ll 1$, then

$$Si(\Omega T) \rightarrow \Omega T \qquad (C\text{-}32a)$$

and

$$F_0 \rightarrow \frac{A}{\pi} \Omega T^2 \qquad (C\text{-}33a)$$

$$F_1 \rightarrow \frac{A}{\pi} \Omega T^2 \qquad (C\text{-}33b)$$

$$F_2 \rightarrow \frac{A}{\pi} \Omega T^2 \qquad (C\text{-}33c)$$

$$\sigma_z^2 \rightarrow \frac{2}{\pi} N_0 \Omega T^2 \qquad (C\text{-}33d)$$

The probability of error then becomes

$$P_e \rightarrow \frac{1}{8} \left\{ \text{erfc}\left(-\frac{A}{2}\sqrt{\frac{\Omega}{N_0 \pi}}\, T\right) + 2\,\text{erfc}\left(\frac{A}{2}\sqrt{\frac{\Omega}{N_0 \pi}}\, T\right) + \text{erfc}\left(\frac{3A}{2}\sqrt{\frac{\Omega}{N_0 \pi}}\, T\right) \right\}$$

$$(C\text{-}34)$$

The energy in a single bit is $A^2 T = E$ and, when the relation $\Omega = 2\pi f_c$ is used, there results

$$P_e \rightarrow \frac{1}{8}\left\{ \text{erfc}\left(-\sqrt{\frac{E f_c T}{2 N_0}}\right) + 2\,\text{erfc}\left(\sqrt{\frac{E f_c T}{2 N_0}}\right)\right.$$

$$\left. + \text{erfc}\left(3\sqrt{\frac{E f_c T}{2 N_0}}\right)\right\} \qquad 2\pi f_c T \ll 1 \qquad (C\text{-}35)$$

As f_c or $T \rightarrow 0$, the value approaches $\frac{1}{2}$.

Numerical Example

Let the bandwidth of the filter be $2 f_c = \frac{1}{T}$. Then $\Omega T = \pi$, and the probability of error becomes

$$P_e = \frac{1}{8} \left\{ \text{erfc}\left(0.336 \sqrt{\frac{E}{N_0}}\right) + 2 \text{ erfc}\left(0.504 \sqrt{\frac{E}{N_0}}\right) + \text{erfc}\left(0.672 \sqrt{\frac{E}{N_0}}\right) \right\}$$

(C-36)

This result is to be compared with the case in which $\Omega T >> 1$. For this latter case

$$P_e = \frac{1}{2} \left\{ \text{erfc}\left(0.707 \sqrt{\frac{E}{N_0}}\right) \right\}$$

(C-37)

It is evident that, since each value of erfc in the equation (C-36) is greater than the value of the erfc in equation (C-37), the average value of their sum, i.e., the error probability, is greater than that given by equation (C-37) for all values of E/N_0.

APPENDIX D. ANALYSIS OF m-ary DIFFERENTIALLY COHERENT PHASE SHIFT KEY MODULATING SYSTEM

In a system that uses differentially coherent PSK, the coherent reference is obtained by delaying the received signal by the duration of one character and by noting the change in phase between the delayed signal and the incoming signal. The ith character of an m-ary alphabet is transmitted by phase shifting the signal by an amount $i\, 2\pi/m$ over that of the previous signal. The detection consists of computing the angular difference between adjacent received signals. The set of orthonormal functions for expression of the received signal is

$$\varphi_1(t) = \sqrt{\frac{2}{T}} \ \cos \omega t \qquad\qquad (D\text{-}1a)$$

$$\varphi_2(t) = \sqrt{\frac{2}{T}} \ \sin \omega t \qquad\qquad (D\text{-}1b)$$

The signal alphabet consists of functions of the form

$$S_{ik}(t) = \sqrt{\frac{2E}{T}} \ \cos\left(\omega t + \frac{2\pi i}{m} + \zeta_k\right)\left[U(t)\ U(T-t)\right] \qquad (D\text{-}2)$$

where the subscript ik denotes that the transmitted symbol is the ith symbol, provided that the previously transmitted symbol was the kth symbol whose phase is given by ζ_k. The received signals will be the transmitted signals plus additive noise. The outputs of the product integrators are of the form

$$x_{ik} = \sqrt{\frac{2}{T}} \int_0^T \left[S_{ik}(t) + n(t)\right] \cos\left(\omega t - \vartheta(t)\right) dt \qquad (D\text{-}3a)$$

$$y_{ik} = \sqrt{\frac{2}{T}} \int_0^T \left[S_{ik}(t) + n(t)\right] \sin\left(\omega t - \theta(t)\right) dt \qquad (D\text{-}3b)$$

where $\theta(t)$ represents a random phase variation of the reference generator. The outputs of the product integrators for the received symbol and for the delayed previously received symbol are given by

$$x_{ik} = \frac{\sqrt{E}}{T} \cos\left(\frac{2\pi i}{m} + \zeta_k\right) \int_0^T \cos\theta(t)\,dt + \frac{1}{\sqrt{2T}} \int_0^T a(t)\cos\theta(t)\,dt$$

<div align="right">(D-4a)</div>

$$- \frac{\sqrt{E}}{T} \sin\left(\frac{2\pi i}{m} + \zeta_k\right) \int_0^T \sin\theta(t)\,dt + \frac{1}{\sqrt{2T}} \int_0^T b(t)\sin\theta(t)\,dt$$

$$y_{ik} = -\frac{\sqrt{E}}{T} \sin\left(\frac{2\pi i}{m} + \zeta_k\right) \int_0^T \cos\theta(t)\,dt + \frac{1}{\sqrt{2T}} \int_0^T b(t)\cos\theta(t)\,dt$$

<div align="right">(D-4b)</div>

$$- \frac{\sqrt{E}}{T} \cos\left(\frac{2\pi i}{m} + \zeta_k\right) \int_0^T \sin\theta(t)\,dt - \frac{1}{\sqrt{2T}} \int_0^T a(t)\sin\theta(t)\,dt$$

$$x_{kj} = \frac{\sqrt{E}}{T} \cos\zeta_k \int_0^T \cos\theta(t-T)\,dt + \frac{1}{\sqrt{2T}} \int_0^T a(t-T)\cos\theta(t-T)\,dt$$

$$- \frac{\sqrt{E}}{T} \sin\zeta_k \int_0^T \sin\theta(t-T)\,dt + \frac{1}{\sqrt{2T}} \int_0^T b(t-T)\sin\theta(t-T)\,dt$$

<div align="right">(D-4c)</div>

$$y_{kj} = -\frac{\sqrt{E}}{T} \sin\zeta_k \int_0^T \cos\theta(t-T)\,dt + \frac{1}{\sqrt{2T}} \int_0^T b(t-T)\cos\theta(t-T)\,dt$$

$$- \frac{\sqrt{E}}{T} \cos\zeta_k \int_0^T \sin\theta(t-T)\,dt - \frac{1}{\sqrt{2T}} \int_0^T a(t-T)\sin\theta(t-T)\,dt$$

<div align="right">(D-4d)</div>

The representation for noise centered about ω is given as

$$n(t) = a(t) \cos \omega t + b(t) \sin \omega t \qquad (D-5)$$

where a (t) and b (t) are, respectively, the in-phase and quadrature components of the additive noise.

One limiting case can be readily analyzed; the case in which θ (t) is essentially constant over the duration of two adjacent symbols. Since the statistics of the terms containing noise are unchanged by the mixing, equations (D-4) may be rewritten as

$$x_{ik} = \sqrt{E} \cos\left(\frac{2\pi i}{m} + \zeta_k + \theta\right) + n_{11} \qquad (D-4a')$$

$$y_{ik} = -\sqrt{E} \sin\left(\frac{2\pi i}{m} + \zeta_k + \theta\right) + n_{12} \qquad (D-4b')$$

$$x_{kj} = \sqrt{E} \cos(\zeta_k + \theta) + n_{21} \qquad (D-4c')$$

$$y_{kj} = -\sqrt{E} \sin(\zeta_k + \theta) + n_{22} \qquad (D-4d')$$

where the n_{ij} are independent gaussian random variables with zero mean and variance N_0. The angular separation between these signals as represented on a polar plot may be written as $\psi = 2\pi i/m + \zeta_2 - \zeta_1$ where ζ_2 and ζ_1 represent the angular uncertainty in the two signals that results from the additive noise. A decision is made by selecting the multiple of $2\pi/m$ that lies nearest to ψ. A correct decision results if and only if

$$\eta \equiv \left| \zeta_2 - \zeta_1 \right| < \frac{\pi}{m}$$

This decision criterion is in fact the optimum one to use. The random variable, η, depends nonlinearly on the independent gaussian random variables, n_{11}, n_{12}, n_{21}, and n_{22}. The probability density function of η has been derived by Fleck and Trabka (ref. 27). It is given as

$$p(\eta) = \frac{1}{\pi} \int_{\psi=0}^{\pi/2} \sin\psi \left[1 + \frac{E}{2N_0}(1 + \cos\eta \sin\psi)\right] \exp\left[-\frac{E}{2N_0}(1 - \cos\eta \sin\psi)\right] d\psi \quad \eta > 0$$

$$(D-6)$$

Since an error occurs if and only if $\pi/m < \eta \le \pi$, the mean probability of error is

$$P_e = \frac{1}{\pi} \int_{\eta=\pi/m}^{\pi} \int_{\psi=0}^{\pi/2} \sin \psi \left[1 + \frac{E}{2N_0} (1 + \cos \eta \sin \psi) \right] \exp \left[-\frac{E}{2N_0} (1 - \cos \eta \sin \psi) \right] d\psi \, d\eta$$

$$(D-7)$$

The probability of error per symbol may be evaluated in closed form for binary DPSK modulation. In this case an error occurs only when

$$|\varphi_2 - \varphi_1| > \frac{\pi}{2} \qquad (D-8)$$

That is,

$$P_e = \frac{1}{2} P (z \in R_1 | S_2) + \frac{1}{2} P (z \in R_2 | S_1) \qquad (D-9)$$

Since the additive gaussian noise is distributed uniformly in phase, the component along the received signal z_1 (transmitted signal, S_1, plus noise), in figure D-1 is gaussian with zero mean and variance N_0. If the next received
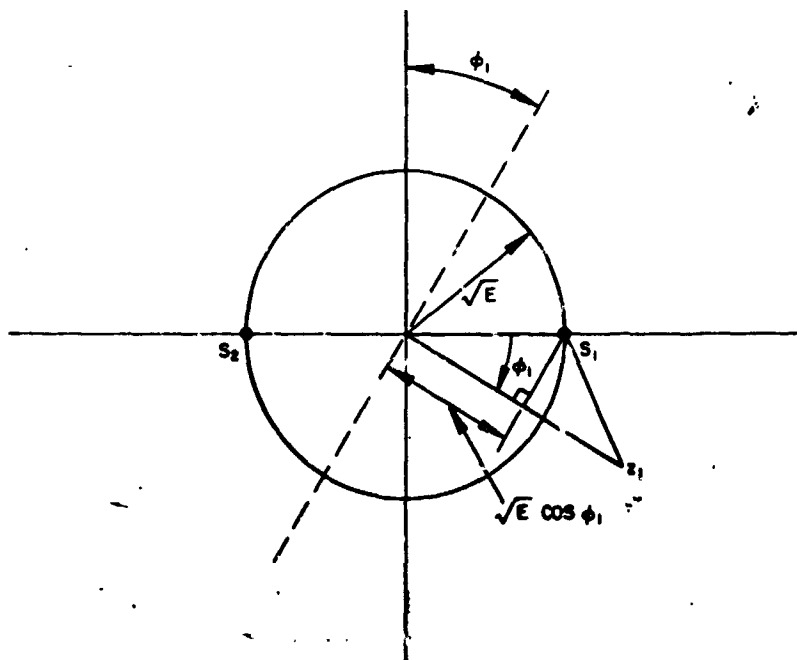
Figure D-1. Illustration of binary DPSK signal space.

signal is also S_1, there will be an error in interpreting it if, and only if, the noise voltage is less than $-E \cos \varphi_1$. If, on the other hand, the next signal is S_2 there will be an error in interpretation if, and only if, the noise exceeds $+E \cos \varphi_1$. The probability of error, given φ_1, may be written as

$$P_e(\varphi_1) = \frac{1}{2\sqrt{2\pi}} \int_{-\infty}^{-\sqrt{\frac{E}{N_0}}\cos\varphi_1} \exp\left(-\frac{x^2}{2}\right) dx + \frac{1}{2\sqrt{2\pi}} \int_{\sqrt{\frac{E}{N_0}}\cos\varphi_1}^{\infty} \exp\left(-\frac{x^2}{2}\right) dx$$

(D-10a)

$$P_e(\varphi_1) = \frac{1}{\sqrt{2\pi}} \, \Phi\left(-\sqrt{\frac{E}{N_0}}\cos\varphi_1\right)$$

(D-10b)

Arthurs and Dym (ref. 18) give the probability density function for φ_1 as

$$p(\varphi_1) = \frac{1}{2\pi} \int_0^\infty \nu \exp\left(-\frac{1}{2}\left[\nu^2 - 2\nu\sqrt{\frac{E}{N_0}}\cos\varphi_1 + \frac{E}{N_0}\right]\right) d\nu$$

(D-11)

By completing the square in this equation, the mean probability of error may be written

$$P_e = \int_{-\pi}^{\pi} P_e(\varphi_1)\, p(\varphi_1)\, d\varphi_1$$

(D-12a)

$$P_e = \frac{1}{\pi} \int_{\varphi=0}^{\pi} \Phi\left(\sqrt{\frac{E}{N_0}}\cos\varphi\right)\left[\exp\left(-\frac{E}{2N_0}\right) + \sqrt{\frac{E}{N_0}}\cos\varphi\,\Phi\left(\sqrt{\frac{E}{N_0}}\cos\varphi\right)\right] d\varphi$$

(D-12b)

$$P_e = \frac{\exp\left(-\frac{E}{2N_0}\right)}{\pi} \int_{\varphi=0}^{\frac{\pi}{2}}\left[\Phi\left(-\sqrt{\frac{E}{N_0}}\cos\varphi\right) + \Phi\left(\sqrt{\frac{E}{N_0}}\cos\varphi\right)\right] d\varphi = \frac{1}{2}\exp\left(-\frac{E}{2N_0}\right)$$

(D-12c)

APPENDIX E. ANALYSIS OF COHERENT m-ary FREQUENCY SHIFT KEY MODULATING SYSTEM

In the FSK scheme, the ith character of the signal alphabet corresponds to a signal at a corresponding angular frequency ω_i. The signal alphabet is then characterized by

$$S_i = \sqrt{\frac{2E}{T}} \cos \omega_i t \qquad (E-1)$$

The corresponding orthonormal functions are

$$\varphi_i = \sqrt{\frac{2}{T}} \cos \omega_i t \qquad (E-2)$$

The signal processing consists of mixing the received signal with a set of coherent local oscillators, one at each frequency ω_i, and integrating the resulting signals over a symbol period. The decision consists of deciding that the received signal is that corresponding to the largest integrator output. The reference oscillators contain independent gaussian random phase errors denoted by θ_k.

The detected signal coordinates are then

$$z_k = \int_0^T \left[\sqrt{\frac{2E}{T}} \cos \omega_k t + n(t) \right] \sqrt{\frac{2}{T}} \cos(\omega_k t - \theta_k) \, dt \qquad (E-3a)$$

$$z_k = \begin{cases} n_k & k \neq i \\ \sqrt{E} \cos \theta_i + n_i & k = i \end{cases} \qquad (E-3b)$$

It is assumed that the noise signals in the separate frequency bands are independent so that, as in the previous cases, the n_k are independent, gaussian, random variables with zero mean and variance N_0. The decision criterion used is the decision that $S_i(t)$ was received if

$$z_k < z_i \quad \text{for all } k \neq i \tag{E-4}$$

Since the n_k are independent, gaussian, random variables with zero mean, the joint probability density function of the z_k, conditioned on θ_i and S_i, is given by

$$p(z_1, z_2, z_i, \ldots z_m \mid \theta_i, S_i) = \frac{1}{\left(2\pi N_0\right)^{m/2}} \exp\left[\frac{-\left(z_i - \sqrt{E}\cos\theta_i\right)^2}{2N_0}\right] \prod_{\substack{k=1 \\ k \neq i}}^{m} \exp\left[\frac{-z_k^2}{2N_0}\right] \tag{E-5}$$

By the stated decision criterion, the probability of error given θ_i is

$$P_e(\theta_i, S_i) = 1 - \frac{1}{\left(2\pi N_0\right)^{m/2}} \int_{-\infty}^{\infty} \exp\left[\frac{-\left(z - \sqrt{E}\cos\theta_i\right)^2}{2N_0}\right]\left[\int_{-\infty}^{z} \exp\left[\frac{-u^2}{2N_0}\right]du\right]^{m-1} dz \tag{E-6}$$

The probability of error averaged over all possible values of θ_i and over all S_i is given by

$$P_e = 1 - \frac{1}{\left(2\pi N_0\right)^{m/2}} \int_{-\infty}^{\infty} \frac{\exp\left[-\frac{\theta^2}{2\sigma_\theta^2}\right]}{\sqrt{2\pi}\,\sigma_\theta^2} \int_{-\infty}^{\infty} \exp\left[\frac{-\left(z - \sqrt{E}\cos\theta\right)^2}{2N_0}\right]\left[\int_{-\infty}^{z} \exp\left[\frac{-u^2}{2N_0}\right]du\right]^{m-1} dz\, d\theta \tag{E-7}$$

98

For the case of binary coherent FSK modulation, the expression for the probability of error per symbol may be obtained from equation (E-7). The triple integral in that equation can be transformed to a double integral which is much more convenient for computational purposes. Consider the integral

$$I = \int_{-\infty}^{\infty} \frac{\exp\left(\frac{-(y - \sqrt{E}\cos\theta)^2}{2N_0}\right)}{\sqrt{2\pi N_0}} \int_{-\infty}^{y} \frac{\exp\left(-x^2/2N_0\right)}{\sqrt{2\pi N_0}}\, dx\, dy \quad (E\text{-}8)$$

The change of variables, $z = y - \sqrt{\frac{E}{2}}\cos\theta$, can be used so that

$$y - \sqrt{E}\cos\theta = z - (\sqrt{2} - 1)\sqrt{\frac{E}{2}}\cos\theta, \quad dy = dz \quad (E\text{-}9)$$

Then

$$I = \int_{-\infty}^{\infty} \frac{\exp\left(-\frac{\left[z - (\sqrt{2}-1)\sqrt{\frac{E}{2}}\cos\theta\right]^2}{2N_0}\right)}{\sqrt{2\pi N_0}} \int_{-\infty}^{z+\sqrt{\frac{E}{2}}\cos\theta} \frac{\exp\left(-x^2/2N_0\right)}{\sqrt{2\pi N_0}}\, dx\, dz$$

$$(E\text{-}10)$$

and with the change of variables

$$\left. \begin{array}{l} u = x - z \\[4pt] du = dx \end{array} \right\} \quad (E\text{-}11)$$

then

$$I = \int_{-\infty}^{\infty} \frac{\exp\left(-\frac{\left[z - (\sqrt{2}-1)\sqrt{\frac{E}{2}}\cos\theta\right]^2}{2N_0}\right)}{\sqrt{2\pi N_0}} \int_{-\infty}^{\sqrt{\frac{E}{2}}\cos\theta} \frac{\exp\left(-\frac{(u+z)^2}{2N_0}\right)}{\sqrt{2\pi N_0}}\, du\, dz$$

$$(E\text{-}12)$$

The order of integration is interchanged to give

$$
I = \int_{u=-\infty}^{\sqrt{\frac{E}{2}}\cos\theta} \int_{z=-\infty}^{\infty} \frac{\exp\left\{-\left[u^2+2uz+z^2+z^2-2(\sqrt{2}-1)\sqrt{\frac{E}{2}}(\cos\theta)z+(\sqrt{2}-1)^2\frac{E}{2}\cos^2\theta\right]\Big/2N_0\right\}}{2\pi N_0} \, dz \, du
$$

(E-13a)

$$
I = \int_{u=-\infty}^{\sqrt{\frac{E}{2}}\cos\theta} \int_{z=-\infty}^{\infty} \frac{\exp\left\{-\left[2z^2+4z\left(\frac{u}{2}-\frac{\sqrt{2}-1}{2}\sqrt{\frac{E}{2}}\cos\theta\right)+2\left(\frac{u^2}{2}+\frac{(\sqrt{2}-1)^2}{2}\frac{E}{2}\cos^2\theta\right)\right]\Big/2N_0\right\}}{2\pi N_0} \, dz \, du
$$

(E-13b)

Then by completing the square in z, the following expression may be written

$$
I = \int_{u=-\infty}^{\sqrt{\frac{E}{2}}\cos\theta} \int_{z=-\infty}^{\infty} \frac{1}{2\pi N_0} \exp\left\{-2\left\{\left[z^2+2z\left(\frac{u}{2}-\frac{\sqrt{2}-1}{2}\sqrt{\frac{E}{2}}\cos\theta\right)+\left(\frac{u}{2}-\frac{\sqrt{2}-1}{2}\sqrt{\frac{E}{2}}\cos\theta\right)^2\right]\right.\right.
$$

$$
\left.\left.+\left[\frac{u^2}{4}+\frac{u}{2}(\sqrt{2}-1)\sqrt{\frac{E}{2}}\cos\theta+\left(\frac{\sqrt{2}-1}{2}\right)^2\frac{E}{2}\cos^2\theta\right]\right\}\Big/2N_0\right\} \, du \, dz
$$

$$
= \int_{u=-\infty}^{\sqrt{\frac{E}{2}}\cos\theta} \frac{\exp\left(-\frac{2\left(\frac{u}{2}+\frac{\sqrt{2}-1}{2}\sqrt{\frac{E}{2}}\cos\theta\right)^2}{2N_0}\right)}{\sqrt{2\pi N_0}} \cdot \frac{1}{\sqrt{2}}\int_{z=-\infty}^{\infty} \frac{\exp\left(-\frac{\left(z+\frac{u}{2}-\frac{\sqrt{2}-1}{2}\sqrt{\frac{E}{2}}\cos\theta\right)^2}{2(N_0/2)}\right)}{\sqrt{2\pi N_0/2}} \, dz \, du
$$

(E-14)

Since the integral over z is just the infinite integral over a gaussian probability density function, its value is unity. So,

$$
I = \int_{u=-\infty}^{\sqrt{\frac{E}{2}}\cos\theta} \frac{\exp\left(-\left(\frac{u}{\sqrt{2}}+\frac{\sqrt{2}-1}{\sqrt{2}}\sqrt{\frac{E}{2}}\cos\theta\right)^2\Big/2N_0\right)}{\sqrt{2\pi N_0}} \frac{du}{\sqrt{2}}
$$

(E-15)

Let $v = u/\sqrt{2}$. Then

$$I = \int_{v=-\infty}^{\sqrt{\frac{E}{4}}\cos\theta} \frac{\exp\left(-\dfrac{\left(v+\dfrac{\sqrt{2}-1}{\sqrt{2}}\sqrt{\dfrac{E}{2}}\cos\theta\right)^2}{2N_0}\right)}{\sqrt{2\pi N_0}}\,dv \qquad\text{(E-16)}$$

Finally, letting $t = v + \dfrac{\sqrt{2}-1}{2}\sqrt{\dfrac{E}{2}}\cos\theta$ and $dt = dv$, there results

$$\left.\begin{aligned}
I &= \int_{t=-\infty}^{\sqrt{\frac{E}{4}}\cos\theta + \frac{\sqrt{2}-1}{\sqrt{2}}\sqrt{\frac{E}{2}}\cos\theta} \frac{\exp\left(-t^2/2N_0\right)}{\sqrt{2\pi N_0}}\,dt \\[2em]
&= \int_{t=-\infty}^{\sqrt{\frac{E}{2}}\cos\theta} \frac{\exp\left(-t^2/2N_0\right)}{\sqrt{2\pi N_0}}\,dt
\end{aligned}\right\} \qquad\text{(E-17)}$$

$$I = \Phi\left(\sqrt{\frac{E}{2N_0}}\cos\theta\right) \qquad\text{(E-18)}$$

So the mean error probability is

$$\left.\begin{aligned}
P_e &= 1 - \int_{-\infty}^{\infty} \frac{\exp(-\theta^2/2\sigma_\theta^2)}{\sqrt{2\pi}\,\sigma_\theta}\,\Phi\left(\sqrt{\frac{E}{2N_0}}\cos\theta\right)d\theta \\[2em]
P_e &= \int_{-\infty}^{\infty} \frac{\exp(-\theta^2/2\sigma_\theta^2)}{\sqrt{2\pi}\,\sigma_\theta}\,\Phi\left(-\sqrt{\frac{E}{2N_0}}\cos\theta\right)d\theta
\end{aligned}\right\} \qquad\text{(E-19)}$$

APPENDIX F. ANALYSIS OF m-ary INCOHERENT FREQUENCY SHIFT KEY MODULATING SYSTEM

Under conditions in which the phase of the incoming FSK signal is not known a priori, squared envelope correlation detection minimizes the probability of error. A system for such detection is shown in figure 7 in the discussion.

If z_i^2 is the greatest signal, then it is assumed that S_i was transmitted. This criterion is the optimum one to use. The alphabet of transmitted signals is given by

$$S_i = \sqrt{\frac{2E}{T}} \cos (\omega_i t + \zeta_i) \qquad \text{(F-1)}$$

where ζ_i is unknown.

The local oscillator outputs are given by

$$\varphi_{1k} = \sqrt{\frac{2}{T}} \cos (\omega_k t - \theta_k) \qquad \text{(F-2a)}$$

$$\varphi_{2k} = \sqrt{\frac{2}{T}} \sin (\omega_k t - \theta_k) \qquad \text{(F-2b)}$$

where the θ_k are as previously defined. Then if S_i is transmitted the output signals of the correlators are

$$x_k = \int_0^T z(t)\, \varphi_{1k}(t)\, dt = \begin{cases} n_{xk} & k \neq i \\ \sqrt{E} \cos (\zeta_i + \theta_i) + n_{xi} & k = i \end{cases} \qquad \text{(F-3a)}$$

$$y_k = \int_0^T z(t)\, \varphi_{2k}(t)\, dt = \begin{cases} n_{yk} & k \neq i \\ -\sqrt{E} \sin (\zeta_i + \theta_i) + n_{xi} & k = i \end{cases} \qquad \text{(F-3b)}$$

102

where, as before, the n_{xk} and n_{yk} are independent, gaussian, random variables with zero mean and variance N_0. Define ν_k as follows

$$\nu_k \equiv \frac{|z_k|}{|N_0|} \qquad (F\text{-}4)$$

when $k \neq i$, the probability density function of ν is Rayleigh (ref. 28) and is given by

$$p_{\nu_k}(\nu_k) = \nu_k \exp\left(-\frac{\nu_k^2}{2}\right) \qquad \nu_k > 0 \quad j \neq i \qquad (F\text{-}5)$$

The probability density function ν_1 is modified Rayleigh (ref. 28) and is given by

$$p_{\nu i}(\nu_i) = \nu_i I_0\left(\nu_i\sqrt{\frac{E}{N_0}}\right) \exp\left[-\frac{1}{2}\left(\nu_i^2 + \frac{E}{N_0}\right)\right] \qquad (F\text{-}6)$$

and is independent of θ or ζ. When the stated decision criterion is applied,

$$P_e = 1 - \int_0^\infty p_{\nu i}(\nu_i)\left[\int_0^{\nu_i} p_{\nu k}(\nu_k)\,d\nu_k\right]^{m-1} d\nu_i \qquad (F\text{-}7a)$$

$$P_e = 1 - \int_0^\infty \nu_i I_0\left(\nu_i\sqrt{\frac{E}{N_0}}\right)\exp\left[-\frac{1}{2}\left(\nu_i^2 + \frac{E}{N_0}\right)\right]\left[1 - \exp\left(-\frac{\nu_i^2}{2}\right)\right]^{m-1} d\nu_i$$

$$(F\text{-}7b)$$

On expansion of the term in the last parenthesis by the binomial theorem and evaluation of the resulting integral, there results

$$P_e = \frac{1}{m} \exp \left[-\frac{E}{4N_0} \right] \sum_{k=2}^{m-1} \binom{m}{k} (-1)^k \exp \left[\frac{E(2-k)}{4N_0 k} \right] \qquad \text{(F-8)}$$

For the special case of m = 2, this expression simplifies to

$$P_e = \frac{1}{2} \exp \left[-\frac{E}{4N_0} \right] \qquad \text{(F-9)}$$

APPENDIX G.   ANALYSIS OF m-ary COHERENT AMPLITUDE SHIFT KEY MODULATING SYSTEM

In the m-ary ASK scheme, information is transmitted by assigning each of m different signal amplitudes to a particular symbol.   The signal alphabet is composed of m sinusoidally varying signals of different amplitudes as shown in the following equation.

$$S_i(t) = \sqrt{\frac{2 E_i}{T}} \cos \omega t \qquad (G-1)$$

It is assumed the E_1 is the lowest level and E_m is the highest level.

The set of orthonormal functions in this case is composed of a single function φ_1 given by

$$\varphi_1(t) = \sqrt{\frac{2}{T}} \cos \omega t \qquad (G-2)$$

As in the other coherent systems, the incoming signal is mixed with a local oscillator signal and integrated over a symbol period as illustrated in figure 8 of the Discussion.   The local oscillator is assumed to have a phase uncertainty, θ.   Its signal is given by

$$\varphi(t) = \sqrt{\frac{2}{T}} \cos (\omega t - \theta) \qquad (G-3)$$

When the transmitted signal is S_i, the output of the detector is

$$z_i = \int_0^T [S_i(t) + n(t)] \sqrt{\frac{2}{T}} \cos (\omega t - \theta) \, dt \qquad (G-4a)$$

$$z_i = \sqrt{E_i} \cos \theta + n \qquad\qquad \text{(G-4b)}$$

where θ and n are gaussian with zero means and variances σ_θ^2 and N_0, respectively. The conditional probability density function of z_i given θ is given by

$$P_z(z_i|\theta) = \frac{1}{\sqrt{2\pi N_0}} \exp\left[\frac{-(z_i - \sqrt{E_1}\cos\theta)^2}{2 N_0}\right] \qquad\qquad \text{(G-5)}$$

If σ_θ is zero, equal spacing between levels yields an optimum system. This spacing is assumed here. It is also assumed that E_1 is equal to zero. Therefore,

$$\sqrt{E_{k+1}} - \sqrt{E_k} = \Delta \qquad\qquad \text{for all } k = 1, \ldots, (k-1) \qquad\qquad \text{(G-6)}$$

And if

$$\sqrt{E_i} - \frac{\Delta}{2} < z < \sqrt{E_i} + \frac{\Delta}{2} \qquad\qquad 1 < i < m \qquad\qquad \text{(G-7)}$$

it will be assumed that S_i was transmitted. For $i = 1$, it will be assumed that S_1 was transmitted if

$$z < \frac{\Delta}{2} \qquad\qquad \text{(G-8)}$$

and for $i = m$ it will be assumed that S_m was transmitted if

$$z > \sqrt{E_m} - \frac{\Delta}{2} \qquad\qquad \text{(G-9)}$$

106

The various probabilities of error, given θ, may now be written:

$$P_e(S_1, \theta) = P(z \notin R_1 | S_1, \theta) = \int_{\frac{\Delta}{2}}^{\infty} p_z(z_1 | \theta)\, dz_1 = \Phi\left(-\frac{\Delta}{2\sqrt{N_0}}\right)$$

(G-10a)

$$P_e(S_i, \theta) = P(z \notin R_i | S_i, \theta) = 1 - \int_{\sqrt{E_i} - \frac{\Delta}{2}}^{\sqrt{E_i} + \frac{\Delta}{2}} p_z(z_i | \theta)\, dz_i \quad 1 < i < m$$

(G-10b)

$$P_e(S_m, \theta) = P(z \notin R_m | S_m, \theta) = \int_{-\infty}^{\sqrt{E_m} - \frac{\Delta}{2}} p_z(z_m | \theta)\, dz_m$$

(G-10c)

The mean probability of error, given θ, is then

$$P_e = \frac{1}{m} \sum_1^m P_e(S_i | \theta)$$

(G-11)

The mean probability of error averaged over all possible values of θ is

$$P_e = \frac{1}{\sqrt{2\pi}\,\sigma_\theta} \int_{-\infty}^{\infty} \left\{ \frac{1}{m}\Phi\left(-\frac{\Delta}{2\sqrt{N_0}}\right) + \frac{m-2}{m} - \frac{1}{m} \sum_{i=2}^{m-1} \int_{\sqrt{E_i} - \frac{\Delta}{2}}^{\sqrt{E_i} + \frac{\Delta}{2}} p_z(z_i | \theta)\, dz_i \right.$$

$$\left. + \frac{1}{m} \int_{-\infty}^{\sqrt{E_m} - \frac{\Delta}{2}} p_z(z_m | \theta)\, dz_m \right\} \exp\left(\frac{-\theta^2}{2\sigma_\theta^2}\right)\, d\theta$$

(G-12)

For the binary case this expression reduces to

$$P_e = \frac{1}{2\sqrt{2\pi}\,\sigma_\theta} \int_{-\infty}^{\infty} \left\{ \Phi\left(-\frac{\Delta}{2\sqrt{N_0}}\right) + \int_{-\infty}^{\sqrt{E_2}-\frac{\Delta}{2}} p_z(z_2|\theta)\,dz_2 \right\} \exp\left[\frac{-\theta^2}{2\sigma_\theta^2}\right] d\theta$$

$$(G-13a)$$

$$= \frac{1}{2}\Phi\left(-\frac{1}{2}\sqrt{\frac{E_2}{N_0}}\right) + \frac{1}{2\sqrt{2\pi}\,\sigma_\theta} \int_{-\infty}^{\infty} \Phi\left(-\sqrt{\frac{E_2}{N_0}}\left[\cos\theta - \frac{1}{2}\right]\right) \exp\left(\frac{-\theta^2}{2\sigma_\theta^2}\right) d\theta$$

$$(G-13b)$$

From equation (G-6) it is evident that $\sqrt{E_k} = (k-1)\Delta$. It is convenient to express Δ in terms of E, the average energy per symbol:

$$E = \frac{1}{m}\sum_1^m E_k = \frac{\Delta^2}{m}\sum_1^m (k-1)^2 = \frac{\Delta^2}{m}\sum_1^{m-1} n^2 \qquad (G-14a)$$

$$E = \frac{\Delta^2}{6}(m-1)(2m-1) \qquad (G-14b)$$

so that

$$\Delta = \sqrt{\frac{6E}{(m-1)(2m-1)}} \qquad (G-14c)$$

With E_k expressed in terms of Δ and with the explicit expressions for the probability density functions, equation (G-12) may be written

$$P_e = \frac{1}{m}\Phi\left(-\frac{\Delta}{2N_0}\right) + \frac{m-2}{m}\cdot\frac{1}{m}\sum_{k=1}^{m-2}\int_{-\infty}^{\infty}\frac{1}{2\pi\sigma_\theta\sqrt{N_0}}\int_{\left(k-\frac{1}{2}\right)\Delta}^{\left(k+\frac{1}{2}\right)\Delta}\exp\left[\frac{-(z-k\Delta\cos\theta)^2}{2N_0}\right]dz\,\exp\left(\frac{-\theta^2}{2\sigma_\theta^2}\right)d\theta$$

$$+ \frac{1}{m}\int_{-\infty}^{\infty}\frac{1}{2\pi\sigma_\theta\sqrt{N_0}}\int_{-\infty}^{\left(m-\frac{3}{2}\right)\Delta}\exp\left[\frac{-(z-(m-1)\Delta\cos\theta)^2}{2N_0}\right]dz\,\exp\left(\frac{-\theta^2}{2\sigma_\theta^2}\right)d\theta \qquad (G-15a$$

108

$$P_e = \frac{1}{m} \, \Phi \left(-\frac{\Delta}{2N_0} \right) + \frac{m-2}{m}$$

$$- \frac{1}{m\sqrt{2\pi}\,\sigma_\theta} \int_{-\infty}^{\infty} \sum_{k=1}^{m-2} \Phi\left(\frac{k\Delta}{\sqrt{N_0}} \left[1 + \frac{1}{2k} - \cos\theta \right] \right) \exp\left(\frac{-\theta^2}{2\sigma_\theta^2} \right) d\theta$$

$$+ \frac{1}{m\sqrt{2\pi}\,\sigma_\theta} \int_{-\infty}^{\infty} \sum_{k=1}^{m-1} \Phi\left(\frac{k\Delta}{\sqrt{N_0}} \left[1 - \frac{1}{2k} - \cos\theta \right] \right) \exp\left(\frac{-\theta^2}{2\sigma_\theta^2} \right) d\theta$$

<div align="right">(G-15b)</div>

The limiting value for P_e as the signal-to-noise ratio increases without limit may readily be obtained from equation (G-15b) since, as Δ/N_0 increases, only the last series is non-vanishing and then only when

$$\cos\theta < 1 - \frac{1}{2k} \tag{G-16}$$

Therefore, as $E/N_0 \to \infty$ the probability of error becomes

$$\lim_{E/N_0 \to \infty} P_e = \frac{1}{m\sqrt{2\pi}\,\sigma_\theta} \sum_{k=1}^{m-1} \int_{\theta:\cos\theta<1-\frac{1}{2k}} \exp\left(\frac{-\theta^2}{2\sigma_\theta^2} \right) d\theta \tag{G-17}$$

For low signal-to-noise ratios one may expand Φ in a power series as

$$\Phi(x) \approx \frac{1}{2} - \frac{x}{\sqrt{2\pi}} \tag{G-18}$$

When this approximation is used, equation (G-15b) reduces to

$$P_e \approx \left(\frac{m-1}{m} \right) \left[1 - \sqrt{\frac{3E}{\pi(m-1)(2m-)N_0}} \exp\left(-\frac{\sigma_\theta^2}{2} \right) \right] \tag{G-19}$$

APPENDIX H. ANALYSIS OF m-ary INCOHERENT AMPLITUDE SHIFT KEY MODULATING SYSTEM

When the phase of the incoming signal is not known a priori, an incoherent system must be used for detection of ASK modulation. The signal alphabet is given by

$$S_i(t) = \sqrt{E_i} \cos(\omega t + \zeta) \qquad \text{(H-1)}$$

where ζ is an unknown phase angle uniformly distributed from 0 to 2π. The detection system is a squared envelope detector as shown in figure 9 in the Discussion. Following Arthurs and Dym (ref. 18), the decision rule adopted is to assume that the signal transmitted is that of the value of $\sqrt{E_i}$ closest to the value of $|z|$. This decision criterion approaches optimum as the signal-to-noise ratio increases. Therefore, if $\sqrt{E_1}$ is assumed to be zero and all $\sqrt{E_i}$ are assumed equally spaced as in the coherent case, it will be decided that S_i was transmitted if, and only if,

$$0 < |z| < \frac{\Delta}{2} \qquad\qquad i = 1 \qquad\qquad \text{(H-2a)}$$

$$\left(i - \frac{3}{2}\right)\Delta < |z| < \left(i - \frac{1}{2}\right)\Delta \qquad i = 2, \ldots, (m-1) \qquad \text{(H-2b)}$$

$$\left(i - \frac{3}{2}\right)\Delta < |z| \qquad\qquad i = m \qquad\qquad \text{(H-2c)}$$

The local oscillator signals are of the form

$$\varphi_1 = \sqrt{\frac{2}{T}}\cos(\omega t - \theta) \qquad\qquad \text{(H-3a)}$$

$$\varphi_2 = \sqrt{\frac{2}{T}}\sin(\omega t - \theta) \qquad\qquad \text{(H-3b)}$$

110

where θ is a random variable uniformly distributed from 0 to 2π. In analogy to previous cases, the received signal coordinates are

$$x = \int_0^T z(t) \varphi_1(t) \, dt = \sqrt{E_i} \cos (\zeta + \theta) + n_1 \qquad (\text{II } 4a)$$

$$y = \int_0^T z(t) \varphi_2(t) \, dt = - \sqrt{E_i} \sin (\zeta + \theta) + n_2 \qquad (\text{II-4b})$$

where n_1 and n_2 are independent, gaussian variables with zero mean and variance N_0. The probability density function of the variable ν_k, defined in equation (F-4), is a modified Rayleigh and is given by equation (F-6). The probability of a correct decision when $S_i(t)$ is sent is

$$P(z \epsilon R_i \mid S_i) = \int_{\left(i-\frac{3}{2}\right)\frac{\Delta}{\sqrt{N_0}}}^{\left(i-\frac{1}{2}\right)\frac{\Delta}{\sqrt{N_0}}} \nu I_0 \left(\nu \frac{(i-1)\Delta}{\sqrt{N_0}} \right) \exp \left[-\frac{1}{2} \left(\nu^2 + \frac{E_i}{N_0} \right) \right] d\nu \quad i=2,\dots,(m-1)$$

$$(\text{H-5a})$$

$$P(z \epsilon R_1 \mid S_1) = \int_0^{\frac{\Delta}{2\sqrt{N_0}}} \nu \exp \left(-\frac{\nu^2}{2} \right) d\nu = 1 - \exp \left(-\frac{\Delta^2}{8 N_0} \right) \qquad (\text{H-5b})$$

$$P(z \epsilon R_m \mid S_m) = \int_{\left(m-\frac{3}{2}\right)\frac{\Delta}{\sqrt{N_0}}}^{\infty} \nu I_0 \left(\nu \frac{(m-1)\Delta}{\sqrt{N_0}} \right) \exp \left[-\frac{1}{2} \left(\nu^2 + \frac{(m-1)^2 \Delta^2}{N_0} \right) \right] d\nu$$

$$(\text{H-5c})$$

The mean probability of error is then

$$P_e = 1 - \frac{1}{m} \sum_{i=1}^{m} P(z \epsilon R_i \mid S_i) \qquad (\text{H-6})$$

For the binary case, equation (H-6) reduces to

$$P_e = \frac{1}{2} \exp\left(-\frac{\Delta^2}{8 N_0}\right) + \frac{1}{2}\left[1 - \exp\left(-\frac{\Delta^2}{2 N_0}\right)\int_{\frac{\Delta}{2\sqrt{N_0}}}^{\infty} \nu\, I_0\left(\nu\,\frac{\Delta}{\sqrt{N_0}}\right)\exp\left(-\frac{\nu^2}{2}\right) d\nu\right]$$

(H-7)

In terms of average symbol energy, E, Δ is given by equation (G-14c). When this equation is substituted into equation (H-7), the following expression results.

$$P_e = \frac{1}{2} \exp\left(-\frac{E}{4 N_0}\right) + \frac{1}{2}\left[1 - \exp\left(-\frac{E}{N_0}\right)\int_{\sqrt{\frac{E}{2 N_0}}}^{\infty} \nu\, I_0\left(\nu\,\sqrt{\frac{2E}{N_0}}\right)\exp\left(-\frac{\nu^2}{2}\right) d\nu\right]$$

(H-8)

112

APPENDIX I. RELATION BETWEEN SINGLE ELEMENT ANTENNA AND ARRAY PERFORMANCE USING PHASE-LOCKED LOOPS

The array is assumed to operate on an incoming signal $S_i(t)$ of the form

$$S_i(t) = \sqrt{\frac{2 E_i}{T}} \cos(\omega_i t + \zeta_i) \tag{I-1}$$

where, depending on the type of modulation being used, the amplitude, frequency, or phase contains the information. The resulting signal into the detection and decision device is given by

$$s = \sum_{k=1}^{M} A_k \cdot \left[\sqrt{\frac{2 E_i}{T}} \cos(\omega_i t + \zeta_i + \beta_k) + n_k(t) \right] \tag{I-2a}$$

$$= \sum_{k=1}^{M} A_k \sqrt{\frac{2 E_i}{T}} \cos(\omega_i t + \zeta_i + \beta_k) + m(t) \tag{I-2b}$$

where

$$m(t) = \sum_{k=1}^{M} A_k n_k(t) \tag{I-2c}$$

Since the n_k are independent, $m(t)$ is flat gaussian noise with spectral density M_0 given by

$$M_0 = N_0 \sum_{k=1}^{M} A_k^2 \tag{I-3}$$

The A_k are positive weighting coefficients that account for any array excitation taper that might be employed. They are normalized so that

$$\sum_{k=1}^{M} A_k = 1 \tag{I-4}$$

Exact analysis of the probabilities of error can be carried out for all systems, but the results are in the form of multiple integrals and so are not very useful for purposes of computation. In any practical operating situation, it is expected that the adaptive receivers maintain the β_k at small values so that an approximate theory of the effects of the arrays can be worked out.

It is convenient to rewrite equation (I-2) as

$$s = \left[\sum_k \sum_\ell A_k A_\ell \exp j(\beta_k - \beta_\ell) \right]^{1/2} \sqrt{\frac{2 E_i}{T}} \cos(\omega_i t + \zeta_i + \xi) + m(t) \tag{I-5a}$$

where

$$\xi \equiv \tan^{-1} \frac{\Sigma A_k \sin \beta_k}{\Sigma A_k \cos \beta_k} \tag{I-5b}$$

When the β_k are small, equation (I-5b) becomes approximately

$$\xi \approx \frac{\Sigma A_k \beta_k}{\Sigma A_k} = \sum_{k=1}^{M} A_k \beta_k \tag{I-6}$$

where equation (I-4) has been used. Since the β_k have been assumed to be independent gaussian variables with zero mean and variance σ_β^2, ξ is also gaussian with zero mean and variance σ_ξ^2, which is related to σ_β^2 by

$$\sigma_\xi^2 = \sigma_\beta^2 \sum_1^{M} A_k^2 < \sigma_\beta^2 \tag{I-7}$$

For an example, when the A_k are all equal (uniform array illumination),

$$\sigma_\xi^2 = \frac{\sigma_\beta^2}{M} \tag{I-8}$$

One result of the arraying is, therefore, to reduce the effect of individual phase errors on the total signal phase error. This effect is common to all arraying techniques and is not peculiar to adaptive arrays. The adaptive array property is that of automatically minimizing the individual phase errors.

The effect of the β_k on the amplitude of the signal is also of interest. The amplitude squared term will be denoted by ϵ. Thus

$$\epsilon \equiv \sum_{k=1}^{M} \sum_{\ell=1}^{M} A_k A_\ell \exp\left[j(\beta_k - \beta_\ell)\right] \tag{I-9}$$

The expectation of ϵ, denoted by μ_ϵ, is given by

$$\mu_\epsilon = \exp(-\sigma_\beta^2) + \left[1 - \exp(-\sigma_\beta^2)\right] \sum_{k=1}^{M} A_k^2 \tag{I-10}$$

The variance of ϵ is a measure of the departure of ϵ from its average value. Since the derivation of the variance is quite tedious, only the results are given:

$$\sigma_\epsilon^2 = 2\left(\sum_{i=1}^{M} A_i^2\right)^2 \exp(-\sigma_\beta^2)\left[1 - \exp(-\sigma_\beta^2)\right] + 4 \exp(-\sigma_\beta^2)\left(\sum_{i=1}^{M} A_i^2\right) \sum_{i=1}^{M} \sum_{k=i+1}^{M} A_i A_k \left[1 - \exp(-\sigma_\beta^2)\right]$$

$$+ 2\left[1 - \exp(-2\sigma_\beta^2)\right]^2 \sum_{i=1}^{M} \sum_{k=i+1}^{M} A_i^2 A_k^2 \tag{I-11}$$

$$+ 2 \exp(-\sigma_\beta^2)\left[1 - \exp(-\sigma_\beta^2)\right]^2 \left(\sum_{i=1}^{M} \sum_{m=1}^{M} \sum_{k=G\binom{m+1}{i+1}}^{M} A_i A_m A_k^2 + \sum_{i=1}^{M} \sum_{k=i+1}^{M} \sum_{n=i+1}^{M} A_i^2 A_k A_n\right)$$
$$\quad\quad i \neq m \quad\quad\quad\quad\quad\quad\quad\quad k \neq n$$

where $G \begin{vmatrix} a \\ b \end{vmatrix}$ means the greater of a or b. When this expression is evaluated for uniform illumination, each A_i is equal to $1/M$: equation (I-11) reduces to

$$\sigma_\epsilon^2 = \frac{1}{M^2} \left[1 - \exp(-\sigma_\beta^2) \right]^2 + \frac{(M-1)}{M^3} \left[1 - \exp(-2\sigma_\beta^2) \right]^2$$

$$+ \frac{4}{3} \frac{(M-1)(M-2)}{M^3} \exp(-\sigma_\beta^2) \left[1 - \exp(-\sigma_\beta^2) \right]^2$$

(I-12)

As M becomes large and/or σ_β becomes small, σ_ϵ becomes small so that the variation of signal level about the mean is also very small. For example, for σ_β = 0.175 radian (10-degree rms phase error) and M = 10, the value of σ_ϵ is 0.0112. Even for a two-element array, σ_ϵ is only 0.033. Therefore, for sufficiently large arrays, the amplitude squared value does not vary appreciably about its average value as given by equation (I-10) and which, for uniformly illuminated arrays, reduces to

$$\mu_\epsilon = \exp(-\sigma_\beta^2) + \frac{1}{M} \left[1 - \exp(-\sigma_\beta^2) \right]$$

(I-13)

For arrays of ten elements or more this value is approximately

$$\mu_\beta = \exp(-\sigma_\beta^2)$$

(I-14)

For tapered arrays similar results hold, but the lower bounds on M to make the approximations valid are greater than for uniform arrays. The increase in the bounds depends on the taper and no general result can be given. It may be concluded that for large arrays and reasonable limits on the rms value of the individual phase errors, the major effects of the phase errors on the system operation are a modification of the signal-to-noise ratio and the introduction of an additional random phase error ξ with zero mean and variance given by equation (I-7) or (I-8). The resulting phase error is then a new gaussian, random variable ($\gamma = \theta + \xi$) with zero mean and variance σ_γ^2 such that

$$\sigma_\gamma^2 = \sigma_\theta^2 + \sigma_\xi^2$$

(I-15)

The results of the single element case may, therefore, be carried over to arrays of moderate and large size merely by replacing (E/N_0), the signal-to-noise ratio in the line between a single element and the summing point, with E'/N_0' where

$$\frac{E}{N_0} \left(\frac{\exp(-\sigma_\beta^2)}{\sum\limits_{i=1}^{M} A_i^2} + \left[1 - \exp(-\sigma_\beta^2) \right] \right) \equiv \frac{E'}{N_0'}, \qquad (I-16)$$

and replacing σ_θ with σ_γ where

$$\sigma_\gamma^2 = \sigma_\theta^2 + \sigma_\beta^2 \sum\limits_{i=1}^{M} A_i^2 \qquad (I-17a)$$

and the A_i satisfy equation (I-4). $\qquad\qquad\qquad$ (I-17b)

The results for the single channel cases can, therefore, be carried over directly to arrays when M is large and/or σ_β is sufficiently small.

APPENDIX J. BANDWIDTH SEPARATION REQUIREMENTS FOR COHERENT AND INCOHERENT FREQUENCY SHIFT KEY MODULATING SCHEMES

The bandwidth separation requirements for the coherent and incoherent FSK schemes may be obtained as follows. Two incoming signals can be considered with frequencies f_1 and f_2 and phases θ_1 and θ_2, respectively. The correlation between the two signals with respect to an integration time T is given by

$$\int_0^T \cos(\omega_1 t + \theta_1) \cos(\omega_2 t + \theta_2)\, dt = \frac{1}{\omega_1 - \omega_2}\left\{ \sin\left[(\omega_1 - \omega_2)T + (\theta_1 - \theta_2)\right] - \sin(\theta_1 - \theta_2)\right\}$$

(J-1)

where the double frequency terms are assumed to be filtered out. The right side of equation (J-1) will vanish if

$$(\omega_1 - \omega_2)T = 2n\pi \qquad n = 1, 2, \ldots \qquad (J-2)$$

or

$$f_1 - f_2 = \frac{n}{T} \qquad n = 1, 2, \ldots \qquad (J-3)$$

For a coherent system, $\theta_1 = \theta_2$ by the definition of coherence, and it is sufficient that

$$(\omega_1 - \omega_2)T = n\pi \qquad n = 1, 2, \ldots \qquad (J-4)$$

or

$$f_1 - f_2 = \frac{n}{2T} \qquad (J-5)$$

118

APPENDIX K. USE OF INFORMATION SIGNAL SQUARED
TO PROVIDE A PHASE REFERENCE

Stiffler (ref. 21) and Van Trees (ref. 22) have investigated the optimum division of power between information signals and phase synchronizing signals for specific configurations of systems that use binary PSK modulation. Their results indicate that, for the systems considered, the type that uses only the information signal squared to provide a phase reference gives the least probability of error for a given total signal power. They also use a gaussian probability density function for the phase error in the tracking loop but because of the squaring of the information signal used to obtain the phase reference, there are noise-noise products in the loop so that the rms phase error may be written

$$\sigma_\theta^2 = B_L T \left(\frac{2N_0}{E}\right)\left[1 + \left(\frac{B_i T}{2}\right)\left(\frac{2N_0}{E}\right)\right] \qquad (K\text{-}1)$$

To insure faithful reproduction of the stepped phase modulation, it is assumed that $B_i T \gg 1$.

The ranges of values of rms phase error that could be expected can be illustrated in the following situation. A uniform adaptive array of M elements receives a binary PSK signal. The phase reference is obtained from the squared signal. The configuration is shown in figure K-1. The signal-to-noise ratio of the combined output is $E'/(2N_0')$ so that the signal-to-noise ratio at the individual elements is approximately

$$\frac{E}{2N_0} = \frac{E'}{M 2N_0'} \qquad \sigma_\beta^2 < 0.1 \text{ rad}^2 \qquad (K\text{-}2)$$

The variance of the reference phase error is then given by

$$\sigma_\beta^2 = B_L T M \left(\frac{2N_0'}{E'}\right)\left[1 + \frac{B_i T}{2} M \left(\frac{2N_0'}{E'}\right)\right] \qquad \sigma_\beta^2 < 0.1 \text{ rad}^2 \qquad (K\text{-}3)$$
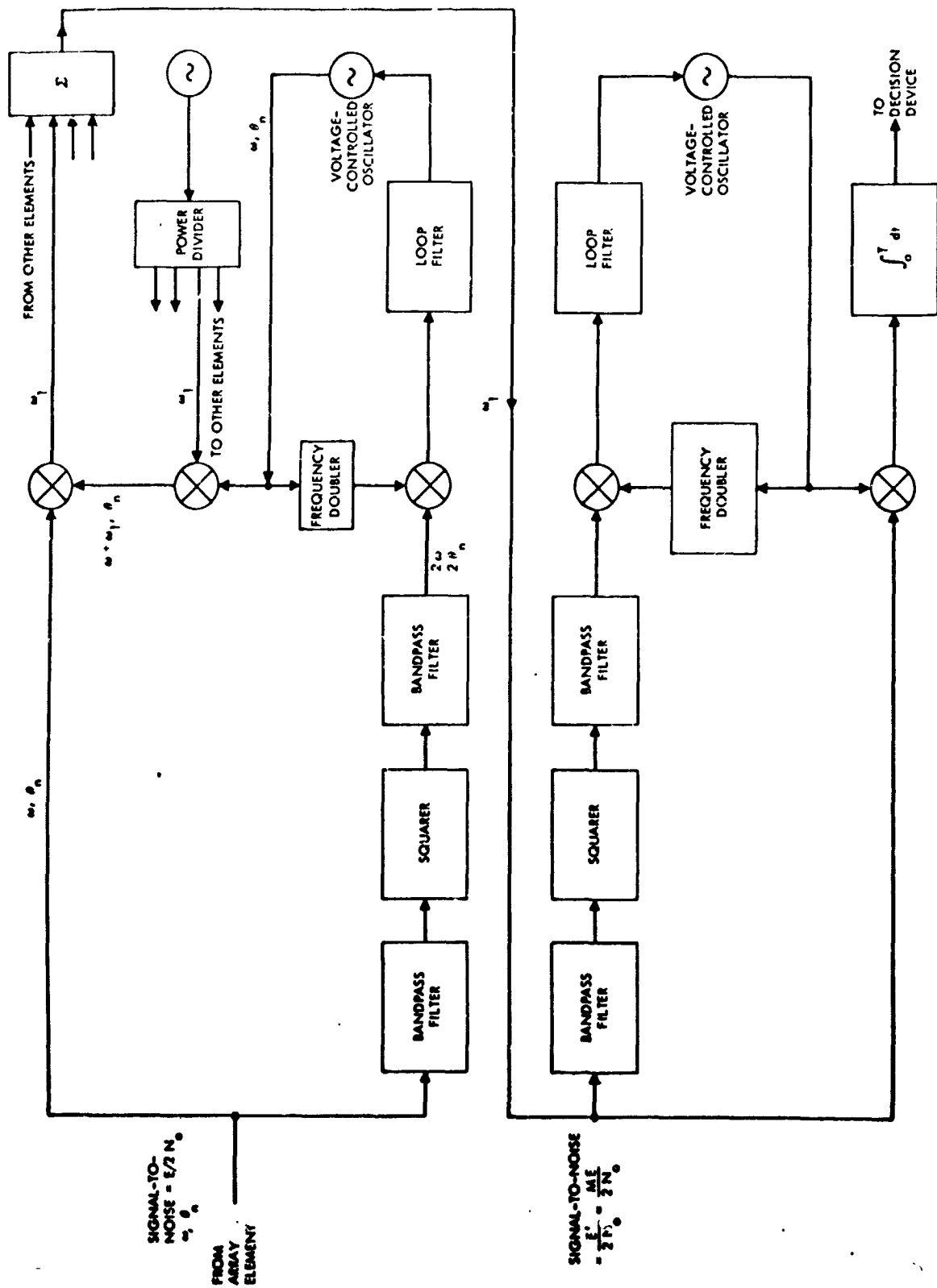
Figure K-1. Adaptive array configuration that uses a squared signal to obtain phase reference.

120

If it is assumed that $B_i = 10$, the above equation becomes

$$\sigma_\beta^2 = B_L TM\left(\frac{2N_0'}{E'}\right)\left[1 + 5M\left(\frac{2N_0'}{E'}\right)\right] \qquad \sigma_\beta^2 < 0.1 \text{ rad}^2 \qquad (K-4)$$

As indicated in Appendix I, the total rms phase error is given by

$$\sigma_\gamma^2 = \sigma_\theta^2 + \frac{\sigma_\beta^2}{M} \qquad (K-5)$$

where σ_γ is the rms phase error in the loop used to detect the combined signal and σ_θ is given by

$$\sigma_\theta^2 = B_L T\left(\frac{2N_0'}{E'}\right)\left[1 + \frac{B_i T}{2}\left(\frac{2N_0'}{E'}\right)\right] \qquad \sigma_\theta^2 < 0.1 \text{ rad}^2 \qquad (K-6)$$

Therefore, σ_γ^2 is given by

$$\sigma_\gamma^2 = B_L T\left(\frac{2N_0'}{E'}\right)\left[2 + (M+1)\frac{B_i T}{2}\left(\frac{2N_0'}{E'}\right)\right] \qquad \left.\begin{array}{c}\sigma_\theta^2 \\ \sigma_\beta^2\end{array}\right\} < 0.1 \text{ rad}^2 \qquad (K-7)$$

This result is plotted as a function of signal-to-noise ratio in figure 21 of the Discussion.

APPENDIX L. ANALYSIS OF RETRODIRECTIVE SYSTEM THAT USES PHASE INVERSION BY MIXING

Signal and Noise Considerations

An array of elements with the circuitry shown in figure L-1 is considered. The elements are located at $\bar{r}_n$ relative to an origin of coordinates. Interest here is in the signal and noise behavior of the system. All noise is assumed to be gaussian and flat over the bandwidths of interest. Noise in the pilot channel is assumed to be statistically independent of that in the information channel.
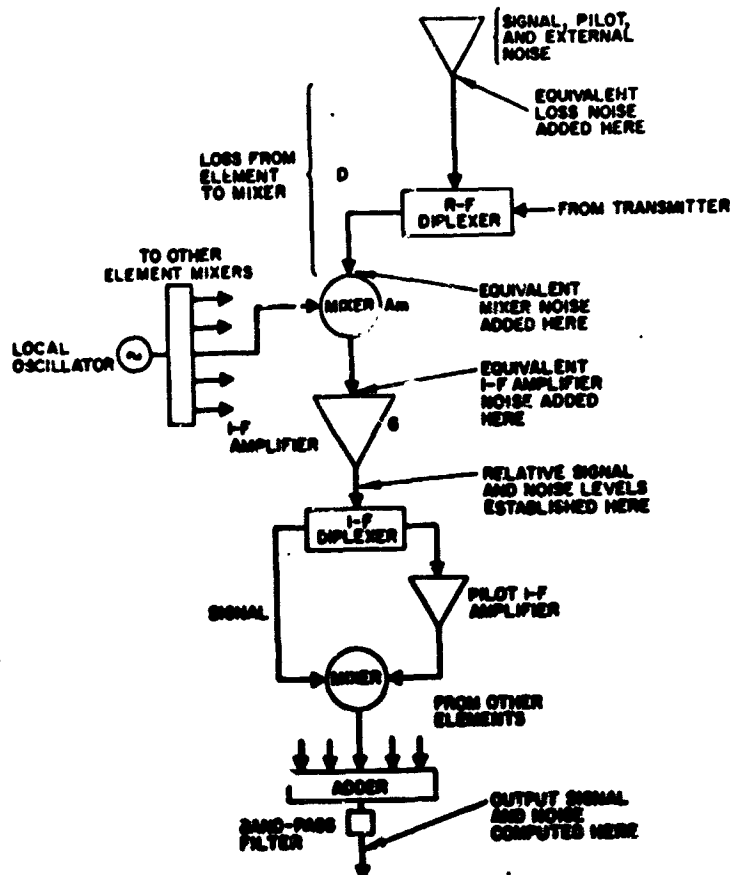

Figure L-1. Portion of retrodirective array that illustrates signal and noise performance of the system.

The noise in the information channel and in the pilot i-f channel will arise from several sources. There will be externally generated noise that is correlated from element to element and internally generated noise arising in the mixer and amplifier as well as stemming from dissipation. The noise sources are indicated in figure L-1. All the internally generated noise will be grouped together. The externally generated noise is kept separate. The internally generated noise voltage in the nth information channel translated to the first i-f frequency may be represented as

$$v_{in}(t) = a_n'(t) \cos (\omega_c - \omega_o) t + b_n'(t) \sin (\omega_c - \omega_o) t \qquad (L-1)$$

while that in the nth pilot channel is

$$v_{pn}(t) = a_n''(t) \cos (\omega_p - \omega_o) t + b_n''(t) \sin (\omega_p - \omega_o) t \qquad (L-2)$$

where ω_c is the information channel angular frequency, ω_p is the pilot angular frequency, and ω_o is the local oscillator angular frequency. The $a_n(t)$ and $b_n(t)$ are sample functions of a stationary gaussian process and at any instant of time are uncorrelated. Their expectations are zero and their variances are equal. Thus,

$$\overline{a_n' b_m'} = \overline{a_n' b_m''} = \overline{a_n'' b_m'} = \overline{a_n'' b_m''} = \overline{a_n' a_m''} = \overline{b_n' b_m''} = 0 \qquad (L-3a)$$

$$\overline{a_n' a_m'} = \overline{b_n' b_m'} = \sigma'^2 \delta_{mn} \qquad (L-3b)$$

$$\overline{a_n'' a_m''} = \overline{b_n'' b_m''} = \sigma''^2 \delta_{mn} \qquad (L-3c)$$

where δ_{mn} is the Kronecker delta. The bars denote ensemble averages. The externally generated noise voltage received by the nth element may be represented as

$$n_{in}(t) \propto \oiint \sqrt{g_{e_n} (\theta, \phi)} \left[X_i(\theta, \phi, t) \cos\left([\omega_c - \omega_o] t + \psi_n + \xi_n \right) \right.$$

$$\left. + Y_i(\theta, \phi, t) \sin\left([\omega_c - \omega_o] t + \psi_n + \xi_n \right) \right] d\Omega \qquad (L-4)$$

in the information channel and as

$$n_{pn}(t) \propto \oiint \sqrt{g_{e_n}(\theta, \phi)} \left[X_p(\theta, \phi, t) \cos \left[\omega_p - \omega_o \right] t + \psi_{pn} + \xi_n \right)$$

$$+ Y_p(\theta, \phi, t) \sin \left(\left[\omega_p - \omega_o \right] t + \psi_{pn} + \xi_n \right) \right] d\Omega \qquad (L\text{-}5)$$

where g_{e_n} is the effective element gain function and ξ_n a phase function of the element, referred to its location. The phases ψ_n and ψ_{pn} are due to the relative positions of the elements and are given by

$$\psi_n = \frac{\omega_c}{\nu} r_n \left[\sin \theta \sin \theta_n \cos (\phi - \phi_n) + \cos \theta \cos \theta_n \right] \qquad (L\text{-}6a)$$

$$\psi_{pn} = \frac{\omega_p}{\nu} \left[\sin \theta \sin \theta_n \cos (\phi - \phi_n) + \cos \theta \cos \theta_n \right] \qquad (L\text{-}6b)$$

where ν is the velocity of light. The terms X and Y are measures of the incident noise wave. They are also sample functions of a stationary gaussian process. They are assumed to be statistically independent and satisfy the conditions

$$\overline{X^2} = \overline{Y^2} \equiv \sigma^2 \qquad (L\text{-}7)$$

The received pilot signal is given by

$$s_{pn}(t) = K \sqrt{g_{e_n}} \lambda_p C \cos \left[(\omega_p - \omega_o)t + \Phi_{pn} - \zeta + \xi_n \right] \qquad (L\text{-}8)$$

and the received information signal may be written as

$$s_{in}(t) = K \sqrt{g_{e_n}} \lambda_c f(t) \cos \left[(\omega_c - \omega_o) t + \Phi_n + \Phi(t) - \zeta + \xi_n \right] \qquad (L\text{-}9)$$

where the symbols Φ_{pn} and Φ_n indicate the values of ψ_{pn} and ψ_n for the angle of incidence of the pilot and information signals, respectively. The voltages in the two channels are

$$V_{in}(t) = v_{in} + n_{in} + s_{in} \qquad (L\text{-}10a)$$

$$V_{pn}(t) = v_{pn} + n_{pn} + s_{pn} \qquad (L\text{-}10b)$$

124

The 2nd mixer output at the difference frequency is

$$v_{on}(t) = \frac{1}{2} K^2 g_{e_n} \lambda_c \lambda_p C f(t) \cos\left[(\omega_p - \omega_c) t + \Phi_{pn} - \Phi_n - \Phi(t)\right]$$

$$+ \frac{1}{2} K \sqrt{g_{e_n}} \lambda_c f(t) \oint \sqrt{g_{e_n}} X_p \cos\left[(\omega_p - \omega_c) t + \psi_{pn} + \xi_n(\theta, \phi) - \xi_n(\theta_1, \phi_1) - \Phi_n - \Phi(t)\right] d\Omega$$

$$- \frac{1}{2} K \sqrt{g_{e_n}} \lambda_c f(t) \oint \sqrt{g_{e_n}} Y_p \sin\left[(\omega_p - \omega_c) t + \psi_{pn} + \xi_n(\theta, \phi) - \xi_n(\theta_1, \phi_1) - \Phi_n - \Phi(t)\right] d\Omega$$

$$+ \frac{1}{2} K \sqrt{g_{e_n}} \lambda_c f(t) a''_n \cos\left[(\omega_p - \omega_c) t - \Phi_n - \Phi(t) + \zeta - \xi_n\right]$$

$$+ \frac{1}{2} K \sqrt{g_{e_n}} \lambda_c f(t) b''_n \sin\left[(\omega_p - \omega_c) t - \Phi_n - \Phi(t) + \zeta - \xi_n\right]$$

$$+ \frac{1}{2} K \sqrt{g_{e_n}} \lambda_p C \oint \sqrt{g_{e_n}} X_i \cos\left[(\omega_p - \omega_c) t + \Phi_{pn} - \psi_n + \xi_n(\theta_1, \phi_1) - \xi_n(\theta, \phi)\right] d\Omega$$

$$- \frac{1}{2} K \sqrt{g_{e_n}} \lambda_p C \oint \sqrt{g_{e_n}} Y_i \sin\left[(\omega_p - \omega_c) t + \Phi_{pn} - \psi_n + \xi_n(\theta_1, \phi_1) - \xi_n(\theta, \phi)\right] d\Omega$$

$$+ \frac{1}{2} \oint \oint \sqrt{g_{e_n}(\theta, \phi) g_{e_n}(\theta', \phi')} X_p(\theta, \phi) X_i(\theta', \phi') \cos\left[(\omega_p - \omega_c) t + \psi_{pn}(\theta, \phi) - \psi_n(\theta', \phi') + \xi_n(\theta, \phi) - \xi_n(\theta', \phi')\right] d\Omega d\Omega'$$

$$+ \frac{1}{2} \oint \oint \sqrt{g_{e_n}(\theta, \phi) g_{e_n}(\theta', \phi')} Y_p(\theta, \phi) Y_i(\theta', \phi') \cos\left[(\omega_p - \omega_c) t + \psi_{pn}(\theta, \phi) - \psi_n(\theta', \phi') + \xi_n(\theta, \phi) - \xi_n(\theta', \phi')\right] d\Omega d\Omega'$$

$$+ \frac{1}{2} \oint \oint \sqrt{g_{e_n}(\theta, \phi) g_{e_n}(\theta', \phi')} [Y_p(\theta, \phi) X_i(\theta', \phi') - X_p(\theta, \phi) Y_i(\theta, \phi)] \sin\left[(\omega_p - \omega_c) t + \psi_{pn}(\theta, \phi) - \psi_n(\theta', \phi') + \xi_n(\theta, \phi) - \xi_n(\theta', \phi')\right] d\Omega d\Omega'$$

$$+ \frac{1}{2} \oint \sqrt{g_{e_n}} [a''_n X_i + b''_n Y_i] \cos\left[(\omega_p - \omega_c) t - \psi_n(\theta, \phi) - \xi_n(\theta, \phi)\right] d\Omega$$

$$+ \frac{1}{2} \oint \sqrt{g_{e_n}} [b''_n X_i - a''_n Y_i] \sin\left[(\omega_p - \omega_c) t - \psi_n(\theta, \phi) - \xi_n(\theta, \phi)\right] d\Omega$$

$$+ \frac{1}{2} K \sqrt{g_{e_n}} \lambda_p C a'_n \cos\left[(\omega_p - \omega_c) t + \Phi_{pn} - \zeta + \xi_n\right]$$

$$- \frac{1}{2} K \sqrt{g_{e_r}} \lambda_p C b'_n \sin\left[(\omega_p - \omega_c) t + \Phi_{pn} - \zeta + \xi_n\right]$$

$$+ \frac{1}{2} \oint \sqrt{g_{e_n}} [a'_n X_p + b'_n Y_p] \cos\left[(\omega_p - \omega_c) t + \psi_{pn} + \xi_n\right] d\Omega$$

$$+ \frac{1}{2} \oint \sqrt{g_{e_n}} [a'_n Y_p - b'_n X_p] \sin\left[(\omega_p - \omega_c) t + \psi_{pn} + \xi_n\right] d\Omega$$

$$+ \frac{1}{2} (a''_n a'_n + b''_n b'_n) \cos(\omega_p - \omega_c) t + \frac{1}{2} (b''_n a'_n - a''_n b'_n) \sin(\omega_p - \omega_c) t \qquad \text{(L-11)}$$

where $K^2 = \dfrac{D A_m G}{4 \pi \eta}$. The letter D is the power transmission coefficient from the antenna element to the input to the first mixer, A_m is the mixer power transfer function, G is the power gain of the first i-f amplifier, and η is the impedance of free space. All system components are assumed to be matched.

Probability of Error

The signal in equation (L-11) is quite similar to the corresponding signal in the systems using the phase-locked loops except that, because the pilot signal is mixed with the information signal, the noise terms are not all gaussian nor are their spectra flat. (See Appendix O.) It is assumed that the same detection and decision methods are used in this system as in the adaptive system. In the subsequent treatment it is also assumed that the noises in the various channels are independent. This assumption neglects the effect of the correlated externally generated noise as compared with other noise sources, but this procedure is consistent with the treatment of phase-locked systems. The question of the correlation of externally generated noise is discussed in Appendix N.

125

With the assumptions concerning external noise in the previous paragraph, the signal from the second mixer may be written as

$$v_{on}(t) = \frac{1}{2} K^2 g_{en} \lambda_c \lambda_p C f(t) \cos \left[(\omega_p - \omega_c) t + \Phi_{pn} - \Phi_n - \Phi(t) \right]$$

$$+ \frac{1}{2} K \sqrt{g_{en}} \lambda_c f(t) a_n''(t) \cos \left[(\omega_p - \omega_c) t - \Phi_n - \Phi(t) + \zeta - \xi_n \right]$$

$$+ \frac{1}{2} K \sqrt{g_{en}} \lambda_c f(t) b_n''(t) \sin \left[(\omega_p - \omega_c) t - \Phi_n - \Phi(t) + \zeta - \xi_n \right]$$

$$+ \frac{1}{2} K \sqrt{g_{en}} \lambda_p C a_n' \cos \left[(\omega_p - \omega_c) t + \Phi_{pn} - \zeta + \xi_n \right]$$

$$- \frac{1}{2} K \sqrt{g_{en}} \lambda_p C b_n' \sin \left[(\omega_p - \omega_c) t + \Phi_{pn} - \zeta + \xi_n \right]$$

$$+ \frac{1}{2} (a_n'' a_n' + b_n'' b_n') \cos (\omega_p - \omega_c) t + \frac{1}{2} (b_n'' a_n' - a_n'' b_n') \sin (\omega_p - \omega_c) t \tag{L-12}$$

where the external noise is now included in the a's and b's which are independent, gaussian, random variables with zero means and variances $2 B_{i, p} N_0$; B_i is the bandwidth of the information channel; and B_p is the bandwidth of the pilot channel in Hz.

The signals from the various elements are next combined and, depending on the type of modulation and detection scheme used, are mixed with local oscillators whose outputs have the form

$$A \cos (\omega t + \theta) \tag{L-13a}$$

$$A \sin (\omega t + \theta) \tag{L-13b}$$

The low frequency components of the resulting signals are integrated over a symbol duration, T. The resulting signals are of the forms

$$v_1(T) = \frac{A}{4} K^2 \lambda_c \lambda_p C\, f(0^+) \sum_n g_{en} T \cos\left[\Phi(0^+) + \Phi_n - \Phi_{pn} + \theta\right]$$

$$+ \frac{A}{4} K \lambda_c\, f(0^+) \sum_n \sqrt{g_{en}} \cos\left[\Phi(0^+) + \Phi_n + \xi_n - \zeta + \theta\right] \int_0^T a_n''(t)\, dt$$

$$- \frac{A}{4} K \lambda_c\, f(0^+) \sum_n \sqrt{g_{en}} \sin\left[\Phi(0^+) + \Phi_n + \xi_n - \zeta + \theta\right] \int_0^T b_n''(t)\, dt$$

$$+ \frac{A}{4} K \lambda_p C \sum_n \sqrt{g_{en}} \cos\left[\theta - \Phi_{pn} + \zeta - \xi_n\right] \int_0^T a_n'(t)\, dt$$

$$+ \frac{A}{4} K \lambda_p C \sum_n \sqrt{g_{en}} \sin\left[\theta - \Phi_{pn} + \zeta - \xi_n\right] \int_0^T b_n'(t)\, dt$$

$$+ \frac{A}{4} \cos\theta \sum_n \int_0^T (a_n'' a_n' + b_n' b_n'')\, dt - \frac{A}{4} \sin\theta \sum_n \int_0^T \left[b_n'' a_n' - a_n'' b_n'\right] dt$$

(L-14a)

$$v_2(t) = \frac{A}{4} K^2 \lambda_c \lambda_p C f(0^+) \sum_n g_{en} T \sin\left[\Phi(0^+) + \Phi_n - \Phi_{pn} + \theta\right]$$

$$+ \frac{A}{4} K \lambda_c f(0^+) \sum_n \sqrt{g_{en}} \sin\left[\Phi(0^+) + \Phi_n - \zeta + \xi_n + \theta\right] \int_0^T a_n''(t)\ dt$$

$$+ \frac{A}{4} K \lambda_c f(0^+) \sum_n \sqrt{g_{en}} \cos\left[\Phi(0^+) + \Phi_n - \zeta + \xi_n + \theta\right] \int_0^T b_n''(t)\ dt$$

$$+ \frac{A}{4} K \lambda_c C \sum_n g_{en} \sin\left[\theta - \Phi_{pn} + \zeta - \xi_n\right] \int_0^T a_n'(t)\ dt$$

$$- \frac{A}{4} K \lambda_p C \sum_n g_{en} \cos\left[\theta - \Phi_{pn} + \zeta - \xi_n\right] \int_0^T b_n'(t)\ dt$$

$$+ \frac{A}{4} \sin\theta \sum_n \int_0^T \left[a_n'' a_n' + b_n'' b_n' \right] dt + \frac{A}{4} \cos\theta \sum_n \int_0^T \left[b_n'' a_n' - a_n'' b_n' \right] dt$$

$$(L-14b)$$

The evaluation of the probability of error requires the determination of the joint probability density functions of the signal parameters, just as for the adaptive systems. There is an added complication here, however, in that the last two terms in the equations result from products of pilot channel noise and information channel noise and are not gaussian. Furthermore, although they are not correlated with other noise terms, they are not independent of the other noise terms so that the evaluation of the probability density functions is not a simple matter. Some simplifications are possible. For example, the integrals may be approximated by sums of terms which, if selected at the proper sampling points, are independent.

When the interval of integration contains a large number of independent sampling points, the probability density function of the integral approaches a gaussian distribution. Furthermore, the noise terms consist of the sums of the independent noise terms from M channels, further contributing to the gaussian nature of the density function. The main departure of the density function from a precisely gaussian function occurs in the tails of the density function. The region near the peak will be a good approximation to a gaussian function. For low signal-to-noise ratios the error is determined

mainly by the region of the peak, and use of a gaussian approximation should yield a reasonable estimate of the probability of error. Conversely, for very high signal-to-noise ratios, the tails of the density functions are important in determination of error probabilities. However, in this case the nongaussian terms in equation (L-14) become small and so have little effect on the probability of error. Consequently, the assumption of a gaussian density function for the noise terms should lead to a reasonable estimate for the probabilities of error for systems of the phase-inversion-by-mixing type.

After the gaussian approximation for the noise distribution has been used, the only problem remaining is the evaluation of the second moment of the distributions. Once this value has been determined, all the results of the calculations for adaptive systems may be applied. Of course, when the results are expressed in terms of carrier and pilot energies and the noise spectral densities in carrier and pilot channels, they will differ in form from the results for the adaptive systems. Evaluation of the second moments is carried out next.

Evaluation of Second Moments of Noise Distributions

The signals and noise that come from the integrators are given by equation (L-14). As discussed above, the probability density functions of these outputs, given θ and given that the kth symbol was transmitted, are approximately gaussian and are given by

$$p(v_1 | \theta, S_k) = \frac{1}{\sqrt{2\pi}\,\sigma} \exp\left[-\frac{\left(v_1 - \mu_1^{(k)}\right)^2}{2\sigma^2} \right] \qquad (L-15a)$$

$$p(v_2 | \theta, S_k) = \frac{1}{\sqrt{2\pi}\,\sigma} \exp\left[-\frac{\left(v_1 - \mu_2^{(k)}\right)^2}{2\sigma^2} \right] \qquad (L-15b)$$

The mean values $\mu_1^{(k)}$ and $\mu_2^{(k)}$ are the correct signal voltages and are given by

$$\mu_1^{(k)} = \frac{A}{2} \sum_{n=1}^{M} \sqrt{E_{pn} E_{in}^{(k)}} \cos\left[\Phi^{(k)}(0^+) + \Phi_n - \Phi_{pn} + \theta \right]$$

$$= B^{(k)} \cos\left[\Psi^{(k)} + \Phi^{(k)}(0^+) + \theta \right] \tag{L-16a}$$

$$\mu_2^{(k)} = \frac{A}{2} \sum_{n=1}^{M} \sqrt{E_{pn} E_{in}^{(k)}} \sin\left[\Phi^{(k)}(0^+) + \Phi_n - \Phi_{pn} + \theta \right]$$

$$= B^{(k)} \sin\left[\Psi^{(k)} + \Phi^{(k)}(0^+) + \theta \right] \tag{L-16b}$$

where

$$B^{(k)} = \frac{A}{2} \sqrt{ \left[\sum_{n=1}^{M} \sqrt{E_{pn} E_{in}^{(k)}} \cos(\Phi_n - \Phi_{pn}) \right]^2 + \left[\sum_{n=1}^{M} \sqrt{E_{pn} E_{in}^{(k)}} \sin(\Phi_n - \Phi_{pn}) \right]^2 }$$

$$\tag{L-17a}$$

and

$$\tan \Psi^{(k)} = \frac{ \displaystyle\sum_{n=1}^{M} \sqrt{E_{pn} E_{in}^{(k)}} \sin(\Phi_n - \Phi_{pn}) }{ \displaystyle\sum_{n=1}^{M} \sqrt{E_{pn} E_{in}^{(k)}} \cos(\Phi_n - \Phi_{pn}) } \tag{L-17b}$$

130

The variances of the received signals, given θ and $S_{\downarrow}$, are given by the following expressions.

$$\sigma^{(k)2} = \frac{A^2}{4} N_0 \left[\sum_{n=1}^{M} E_{in}^{(k)} + \sum_{n=1}^{M} E_{pn} + \frac{M}{4} N_0 \alpha B_i T \right] \qquad \begin{cases} \alpha B_i T \gg 1 \\ \alpha < 1 \end{cases}$$
(L-18a)

$$\sigma^{(k)2} = \frac{A^2}{4} N_0 \left[\sum_{n=1}^{M} E_{in}^{(k)} 2\alpha B_i T + \sum_{n=1}^{M} E_{pn} + \frac{M}{4} N_0 \alpha B_i T \right] \qquad \begin{cases} \alpha B_i T < 1/\pi \\ B_i T \gg 1 \end{cases}$$
(L-18b)

In equations (L-16) through (L-18), $E_{in}^{(k)}$ is the energy of the kth symbol received in the nth channel, and E_{pn} is the energy of the pilot signal received in the nth channel during the symbol duration, T. The $E_{in}^{(k)}$ and the E_{pn} are related to the symbols of equations (L-14) by

$$E_{in}^{(k)} = \frac{1}{2} K^2 g_{en} \lambda_c^2 (f^{(k)})^2 T$$
(L-19a)

$$E_{pn}^{(k)} = \frac{1}{2} K^2 g_{en} \lambda_p^2 C^2 T$$
(L-19b)

The symbol α is the ratio of pilot channel bandwidth, B_p, to information channel bandwidth B_i (Hz). The superscript (k) denotes the symbol being transmitted. The derivation of equations (L-18) is given in Appendix O. If the modulation is phase modulation, all signal amplitudes are fixed and the information is contained in $\Phi^{(k)}(0^+)$. If the modulation is frequency modulation, all signals are zero except the signal out of the kth filter, and if the modulation is amplitude modulation, $E_{in}^{(k)}$ varies from symbol to symbol. In the case of amplitude modulation, therefore, the value of $\sigma^{(k)2}$ varies from symbol to symbol.

The phase angle $\theta + \Psi$ is a random variable that includes the phase, θ, of the reference oscillators and the phase of the incoming signal exclusive of phase modulation. In incoherent systems the phase is irrelevant. In coherent systems the reference oscillator is phase-locked to the incoming signal

so that $\theta + \Psi$ will have a zero mean and a variance σ_γ^2 that includes the rms value of the reference oscillator phase error plus the rms value of any incoming phase uncertainties that are not tracked by the reference oscillator and that also vary slowly with respect to the symbol length. Therefore $\theta + \Psi$ may be considered as a single variable γ. The probability of error, given S_k, is then obtained directly from the expressions already obtained by replacing E'/N_0' with $\left(B^{(k)2}\right)/\left(\sigma^{(k)2}\right)$. The mean probability of error is then computed by summing the error probability over the m equally probable symbols and dividing by m. For phase and/or frequency-modulated systems, the ratio $\left(B^{(k)2}\right)/\left(\sigma^{(k)2}\right)$ is independent of (k). With amplitude-modulated signals, it is dependent on (k).

Consequently, a comparison of phase inversion systems and adaptive systems for phase or frequency modulations may be made by a direct comparison of B^2/σ^2 and E'/N_0'. For amplitude modulations, however, the mean probabilities of error must be computed and compared. In fact, since $\sigma^{(k)}$ as well as $E_{in}^{(k)}$ varies from symbol to symbol, the optimum decision rule may be different for the amplitude-modulated systems that use phase inversion by mixing than it is for amplitude-modulated systems that use adaptive techniques.

Comparison of Systems That Use Phase-Locked Loops and Systems That Use Phase Inversion by Mixing

As stated above, phase or frequency-modulated systems of the self-phased and adaptive types can be compared directly by comparing E'/N_0' and B^2/σ^2. For the adaptive E'/N_0' is given by

$$\frac{E'}{N_0'} = \frac{E}{N_0}\left(\frac{\exp\left(-\sigma_\beta^2\right)}{\displaystyle\frac{M}{\sum_{n=1}^{M} A_n^2}} + \left[1 - \exp\left(-\sigma_{\beta'}^2\right)\right]\right) \qquad (L-20)$$

132

To facilitate the comparisons, the arrays will be assumed to be uniform arrays of identical elements. In this case the expression may be written

$$\frac{E'}{N_0'} = \frac{EM}{N_0}\left(\exp\left(-\sigma_\beta^2\right) + \frac{1}{M}\left[1 - \exp\left(-\sigma_\beta^2\right)\right]\right) \tag{L-21}$$

For the phase inversion type of uniform rectangular array, B^2/σ^2 is given by

$$\frac{B^2}{\sigma^2} = \frac{E_i M}{N_0}\left[\frac{\sin^2\left(N_x \frac{d_x \pi \Delta f}{\lambda_c f_i} \sin\theta\cos\varphi\right)\sin^2\left(N_y \frac{d_y \pi \Delta f}{\lambda_c f_i}\sin\theta\sin\varphi\right)}{M^2 \sin^2\left(\frac{d_x \pi \Delta f}{\lambda_c f_i}\sin\theta\cos\varphi\right)\sin^2\left(\frac{d_y \pi \Delta f}{\lambda_c f_i}\sin\theta\sin\varphi\right)}\right] \tag{L-22a}$$

$$\cdot \left[\frac{1}{1 + \frac{E_i}{E_p} + \frac{1}{4}\frac{aN_0 B_i T}{E_p}}\right]$$

for

$$\begin{cases} a < 1 \\ aB_i T \gg 1 \end{cases} \tag{L-22b}$$

and

$$\frac{B^2}{\sigma^2} = \frac{E_i M}{N_0}\left[\frac{\sin^2\left(N_x \frac{d_x \pi \Delta f}{\lambda_c f_i}\sin\theta\cos\varphi\right)\sin^2\left(N_y \frac{d_y \pi \Delta f}{\lambda_c f_i}\sin\theta\sin\varphi\right)}{M^2 \sin^2\left(\frac{d_x \pi \Delta f}{\lambda_c f_i}\sin\theta\cos\varphi\right)\sin^2\left(\frac{d_y \pi \Delta f}{\lambda_c f_i}\sin\theta\sin\varphi\right)}\right] \tag{L-23a}$$

$$\cdot \left[\frac{1}{1 + 2\frac{E_i}{E_p}aB_i T + \frac{N_0}{4E_p}aB_i T}\right]$$

for

$$\begin{cases} \alpha B_i T < \dfrac{1}{\pi} \\ \\ B_i T \gg 1 \end{cases} \qquad (L\text{-}23b)$$

The available energy E must be divided optimally between E_i and E_p so that B^2/σ^2 is maximized. Equation (L-22a) is maximized when $E_i = E_p = E/2$ and has the value

$$\left(\frac{B^2}{\sigma^2}\right) = \frac{EM}{4N_0} \left[\frac{\sin^2\left(N_x \dfrac{d_x \pi \Delta f}{\lambda_c f_i} \sin\theta \cos\varphi\right) \sin^2\left(N_y \dfrac{d_y \pi \Delta f}{\lambda_c f_i} \sin\theta \sin\varphi\right)}{M^2 \sin^2\left(\dfrac{d_x \pi \Delta f}{\lambda_c f_i} \sin\theta \cos\varphi\right) \sin^2\left(\dfrac{d_y \pi \Delta f}{\lambda_c f_i} \sin\theta \sin\varphi\right)} \right] \qquad (L\text{-}24a)$$

$$\cdot \left[\frac{1}{1 + \dfrac{N_0 B_i T}{4E}} \right]$$

for

$$\begin{cases} \alpha < 1 \\ \\ \alpha B_i T \gg 1 \end{cases} \qquad (L\text{-}24b)$$

For high signal-to-noise ratios and with

$$\frac{\Delta f}{f_i} \ll \frac{\lambda_c}{N_x d_x \sin\theta \cos\varphi} \qquad (L\text{-}25a)$$

$$\frac{\Delta f}{f_i} \ll \frac{\lambda_c}{N_y d_y \sin\theta \sin\varphi} \qquad (L\text{-}25b)$$

Equation (L-24a) reduces to

$$\frac{B^2}{\sigma^2} \approx \frac{EM}{4N_0} \qquad (L-26)$$

This result is about 6 db worse than for an adaptive system; i.e., approximately four times the energy per symbol is required to obtain the same error probability as would be obtained with an adaptive array. At low signal-to-noise ratios, the comparison is less favorable still. This comparison holds when the pilot channel bandwidth is essentially the same as the signal channel bandwidth. Such a situation would occur when the system must handle large doppler shifts (equal to or greater than the signal bandwidth) without a doppler tracking loop or when there are other significant frequency uncertainties. The addition of a frequency tracking loop for the local oscillator would reduce the required bandwidth in the pilot channel so that α could be significantly less than one and equation (L-23a) would apply. In this case the energy division between E_i and E_p is different for maximum B^2/σ^2. When the maximization process is carried out, the following values for E_i and E_p are reached.

$$E_i = \frac{E + DC - \sqrt{(E+DC)^2 - E(1-D)(E+DC)}}{1 - D} \qquad (L-27a)$$

$$E_p = E - E_i \qquad (L-27b)$$

$$E_p = \frac{-D(E+C) + \sqrt{(E+DC)^2 - E(1-D)(E+DC)}}{1 - D} \qquad (L-27c)$$

where

$$D \equiv 2\alpha B_i T \qquad (L-28a)$$

$$C \equiv \frac{N_0}{8} \qquad (L-28b)$$

As α gets sufficiently small, equation (L-27) may be approximated by

$$E_i \approx E\left[1 - \sqrt{1 + \frac{N_0}{8E}} \sqrt{2\alpha B_i T}\right] \qquad \text{(L-29a)}$$

$$E_p \approx E\left[\sqrt{1 + \frac{N_0}{8E}} \sqrt{2\alpha B_i T}\right] \qquad \text{(L-29b)}$$

so that

$$\frac{B^2}{\sigma^2} \approx \frac{EM}{N_0}\left[\frac{\sin^2\left(N_x \frac{d_x \pi \Delta f}{\lambda_c f_i} \sin\theta \cos\varphi\right) \sin^2\left(N_y \frac{d_y \pi \Delta f}{\lambda_c f_i} \sin\theta \sin\varphi\right)}{M^2 \sin^2\left(\frac{d_x \pi \Delta f}{\lambda_c f_i} \sin\theta \cos\varphi\right) \sin^2\left(\frac{d_y \pi \Delta f}{\lambda_c f_i} \sin\theta \sin\varphi\right)}\right]$$

$$\cdot \left[1 - 2\sqrt{1 + \frac{N_0}{8E}} \sqrt{2\alpha B_i T}\right] \qquad \text{(L-30)}$$

Under the conditions of equations (L-25), this expression reduces to

$$\frac{B^2}{\sigma^2} \approx \frac{EM}{N_0}\left[1 - 2\sqrt{1 + \frac{N_0}{8E}} \sqrt{2\alpha B_i T}\right] \qquad \text{(L-31)}$$

It can be seen that, as might be expected, as the pilot channel bandwidth is reduced, the system performance approaches that of the adaptive systems. As an example, consider a self-steering array on a bus that is receiving information from a lander. Suppose that 10^6 symbols are transmitted per

second. To insure good reception of the waveforms, it is assumed that $B_iT = 5$. The use of an AFC loop on the local oscillator may allow a pilot bandwidth of, say, 100 Hz. Then,

$$\alpha = \frac{100}{5 \times 10^6} = 0.2 \times 10^{-4}$$

and

$$2\alpha B_i T = 2 \times 10^{-4}$$

and

$$\frac{B^2}{\sigma^2} \approx \frac{EM}{N_0}\left[1 - 2\sqrt{2\left(1 + \frac{N_0}{8E}\right)}10^{-2}\right] \tag{L-32}$$

which, for signal-to-noise ratios greater than 5/8, is

$$\frac{B^2}{\sigma^2} \approx \frac{EM}{N_0}\left[1 - 0.028\right] = \frac{EM}{N_0}(0.972) \tag{L-33}$$

It is evident that the addition of a single frequency tracking loop to control the common local oscillator can permit the performance of the phase inversion systems to compare favorably with that of the adaptive systems in which phase-locked loops are required at each element in the array.

Signal-to-Noise Ratio of Reradiated Signal

In retrodirective operation of the type under consideration, the signal and noise properties of the signal transmitted by the retrodirective system will be affected by the signal and noise properties of the received pilot when the system is operated as a linear device. The received pilot signal in the nth channel may be written

$$V_{pn}(t) = v_n + n_{pn} + j_{pn} \tag{L-34}$$

where

$$s_{pn} = K \sqrt{g_{en}} \, \lambda_p \, C \cos \left[(\omega_p - \omega_o) t + \phi_{pn} - \zeta + \xi_n \right] \tag{L-35a}$$

$$n_{pn} = \oiint \sqrt{g_{en}} \left[X_p \cos \left([\omega_p - \omega_o] t + \psi_{pn} + \xi_n \right) + Y_p \sin \left([\omega_p - \omega_o] t + \psi_{pn} + \xi_n \right) \right] d\Omega$$

$$\equiv c_n \cos [\omega_p - \omega_o] t + d_n \sin [\omega_p - \omega_o] t \tag{L-35b}$$

where

$$\overline{c_m c_n} = \overline{d_n d_m} = k B_j D A_m G \sqrt{T_{aem} T_{aen}} \, \delta_{mn} \tag{L-36a}$$

$$\overline{c_m d_n} = 0 \qquad \text{all } m, n \tag{L-36b}$$

where δ_{mn} is the Kronecker delta.

$$v_{pn} = a_n''(t) \cos (\omega_p - \omega_o) t + b_n''(t) \sin (\omega_p - \omega_o) t \tag{L-37}$$

where

$$\overline{a_m'' a_n''} = \overline{b_m'' b_n''} = 2 B_p \left[T_e D A_m G + T_m A_m G + T_{amp} G \right] \delta_{mn} \tag{L-38a}$$

$$\overline{a_m'' b_n''} = 0 \qquad \text{all } m, n \tag{L-38b}$$

138

The signal is at the intermediate frequency $(\omega_p - \omega_o)$. This intermediate frequency is then upconverted to the desired microwave frequency which will be near the frequency of the incoming wave if the same array is used for both transmission and reception; otherwise a second, scaled array can be used and the transmission frequency selected on the basis of other considerations. It is assumed here that the same array is used for both receiving and transmitting functions. To obtain the phase inversion necessary to direct the retransmitted signal, the pilot i-f signal and the microwave signal are mixed in an up-converter and the difference frequency is selected. This difference frequency signal is of the form

$$
E_n = K'' \sum_n \sqrt{g_{en}(\theta, \varphi)} \; f_T(t) \left\{ \sqrt{g_{en}(\theta_i, \varphi_i)} \; K\lambda_p \; C \cos\left[\omega_T t + \Phi(t) - \Phi_{pn}(\theta_i, \varphi_i) - \zeta_n(\theta_i, \varphi_i) + \zeta_{Tn}(\theta, \varphi) + \Phi_{Tn}(\theta, \varphi)\right] \right.
$$
$$
\left. + (a_n'' + c_n) \cos\left[\omega_T t + \zeta_{Tn}(\theta, \varphi) + \Phi_T(\theta, \varphi)\right] + (b_n'' + d_n) \sin\left[\omega_T t + \zeta_{Tn}(\theta, \varphi) + \Phi_{Tn}(\theta, \varphi)\right] \right\}
\qquad (L-39)
$$

where $f_T(t)$ and $\Phi(t)$ are amplitude and phase modulations, respectively. The summation is taken over all elements, and for simplicity, it has been assumed that all elements are identically polarized. From this expression the signal and noise properties of the reradiated signal are readily obtained.

# APPENDIX M. SPECTRUM OF SIGNAL PLUS NOISE

The spectrum of the signal plus noise at the output of the second mixer results from the mixing of two noisy signals, each with a flat noise spectrum over its bandwidth. Consequently, the noise spectrum is no longer flat. In this appendix the spectrum of such a system is considered. Figure M-1 shows the spectrum of the incoming signals and noise before they are mixed. The signals lie in the center of their bands. The pilot and information carrier frequencies are assumed to be coherent; i. e. , one is derived from the other by frequency offset so that random fluctuations in frequency and phase will be removed when the signals are mixed and the difference frequency is taken. Therefore, such fluctuations are not included in the analysis. Two cases are illustrated. In the first, the pilot and information channel bandwidths are large to allow for doppler shifts (figure M-1a). In the second case, the doppler shifts are tracked out so that a narrowband pilot channel is used and the information bandwidth B_i determines the bandwidth of that channel (figure M-1b). The analysis is carried through with the assumption that the signals are in the centers of their respective bands.

The signal from the second mixer is proportional to the product of the information signal plus its noise and the pilot signal plus its noise, as illustrated in equation (M-1).

$$v(t) = a \left[s_i(t) + n_i(t) \right] \left[s_p(t) + n_p(t) \right] \tag{M-1}$$

where the subscript i refers to the information channel and p to the pilot channel. The power spectrum of the output is given by the Fourier transform of the autocorrelation function of v(t) (ref. 28) in which the autocorrelation function is given by

$$R_v(\tau) = \overline{v(t) \; v(t + \tau)} \tag{M-2}$$

PILOT SPECTRUM

INFORMATION SPECTRUM
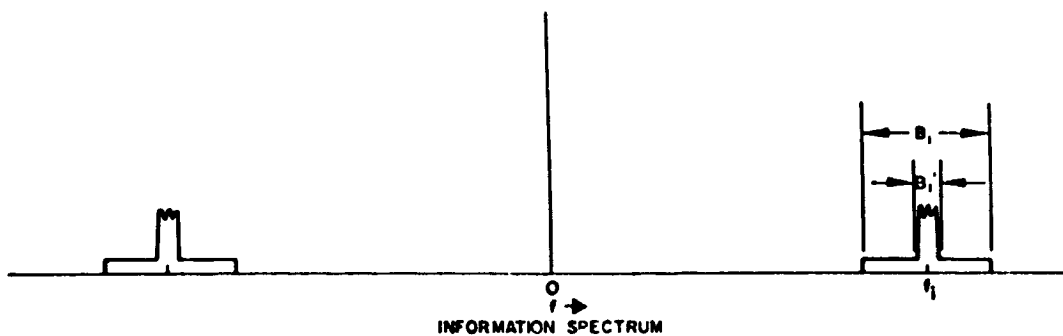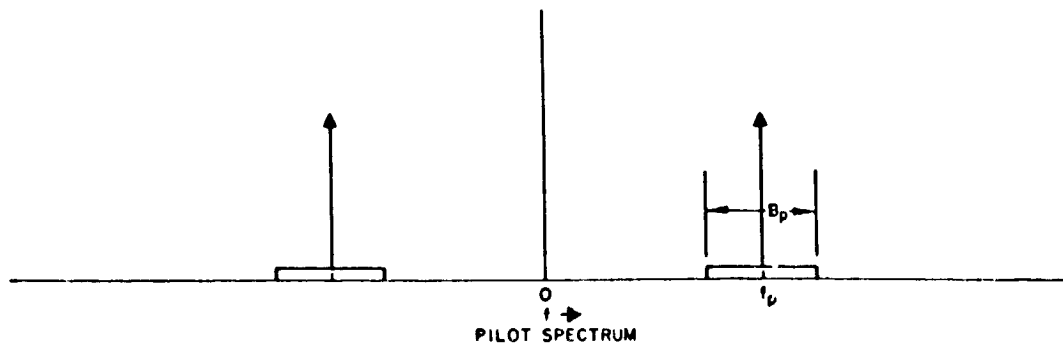
(a) WIDEBAND CHANNELS TO ACCOMMODATE
DOPPLER SHIFTS

PILOT SPECTRUM

INFORMATION SPECTRUM
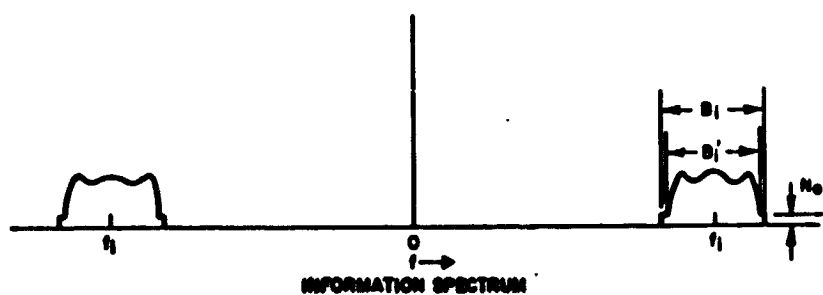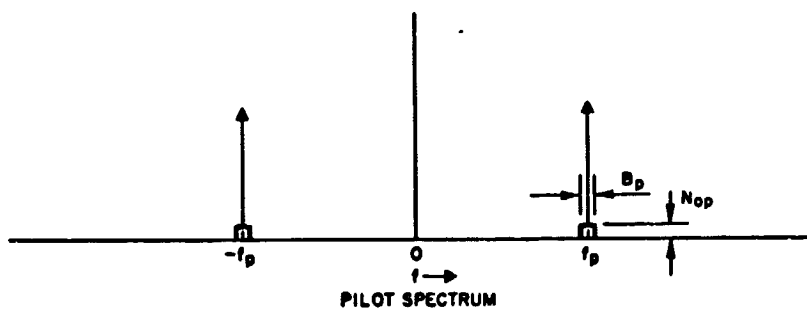
(b) NARROWBAND CHANNELS WITH
DOPPLER SHIFTS REMOVED

Figure M-1. Spectrum of signals before mixing.

The terms in equation (M-3) are evaluated below:

$$\int_{-\infty}^{\infty} S_{si}(f') S_{np}(f-f') df = N_{0p} \int_{f-\left(f_p+\frac{B_p}{2}\right)}^{f-\left(f_p-\frac{B_p}{2}\right)} S_{si}(f') df' + N_{0p} \int_{f+f_p-\frac{B_p}{2}}^{f+f_p+\frac{B_p}{2}} S_{si}(f') df'$$

(M-4)

The shape of this spectrum about the frequency $(f_i - f_p)$ depends on the relative bandwidths of S_{si} and the pilot channel noise. In the first case under consideration, the pilot noise bandwidth, B_p, is greater than the signal bandwidth B_i', and a representative form of the spectrum given in equation (M-4) is illustrated in figure M-2. In that figure P_{Si} is the total information signal power.

The noise-noise products also contribute to the total noise. This is given by

$$\int_{-\infty}^{\infty} S_{ni}(f') S_{np}(f-f') df'$$

(M-5)

The evaluation of this integral leads to the spectrum shown in figure M-3.
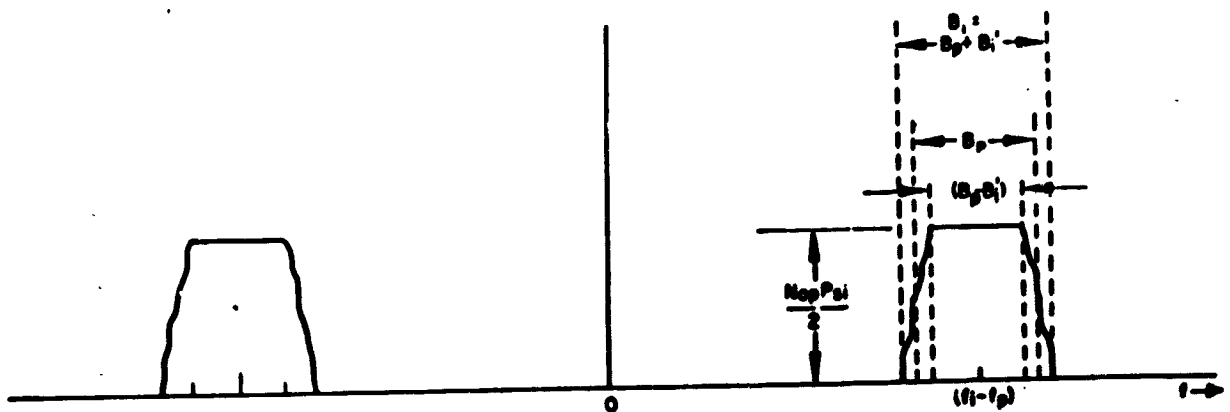

Figure M-2. Spectrum of product of signal and pilot noise.
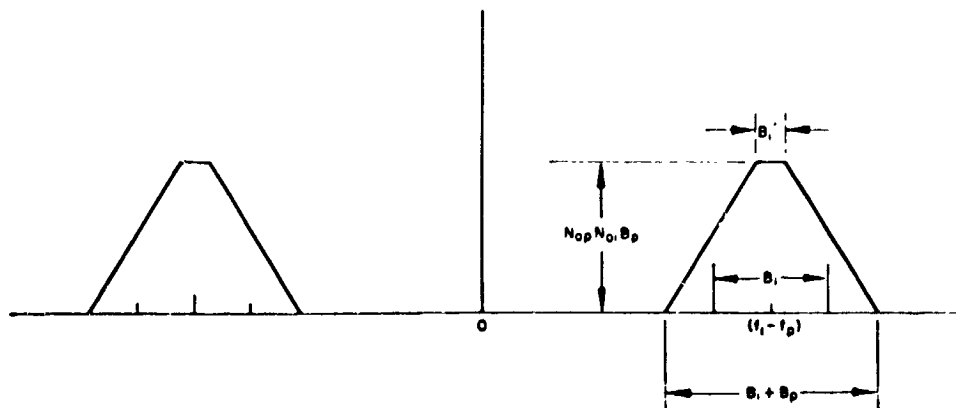
Figure M-3. Spectrum of product of pilot channel noise
and information channel noise.

The spectrum of the cross product of signal and pilot is just the signal
spectrum centered at the difference frequency (f_i - f_p). Its value is
($P_p/2$) S_i. The spectrum resulting from cross products of pilot signal and
information channel noise is rectangular with bandwidth B_i and centered
about the difference frequency (f_i - f_p). Its height is ($P_p/2$) N_{0i}. The total
spectral density is the sum of all these contributions and is illustrated in
figure M-4.

A similar analysis for the second case leads to a spectrum of the
product of signal and pilot noise illustrated in figure M-5. The term
P'_{si} (f - f_i + f_p) is that portion of the information signal power that lies in a
bandwidth B_p.centered at (f - f_i + f_p).

The spectrum of the noise-noise products is shown in figure M-6. The
spectrum of the pilot signal and information channel noise is of the same
form as in the first case, and the spectrum of the product of pilot signal and
information signal is again just that of the information signal translated to
the range about f_i - f_p. Its intensity is $\frac{P_p}{2}$ S_{si} (f - f_i + f_p). The total
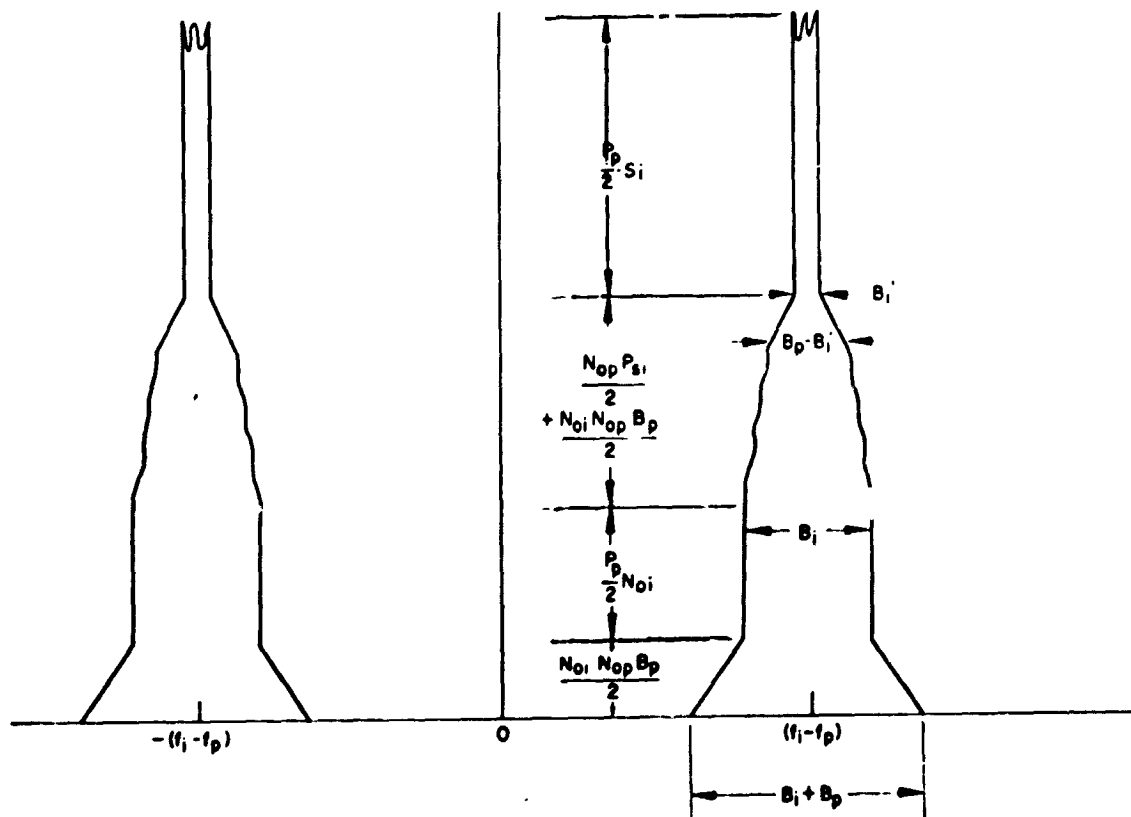spectrum is illustrated in figure M-7.

Figure M-4. Spectrum of signal and noise for case one.
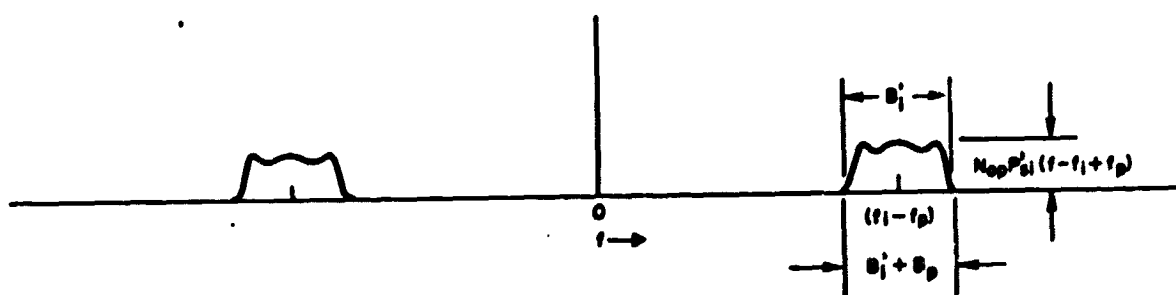

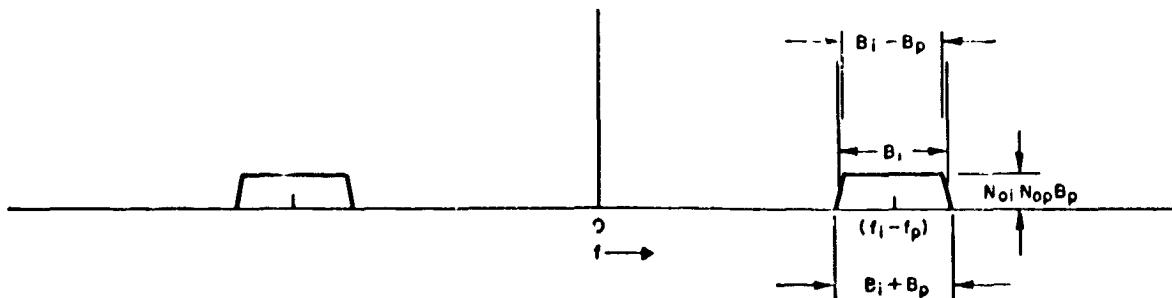Figure M-5. Spectrum of product of signal and pilot noise for case two.

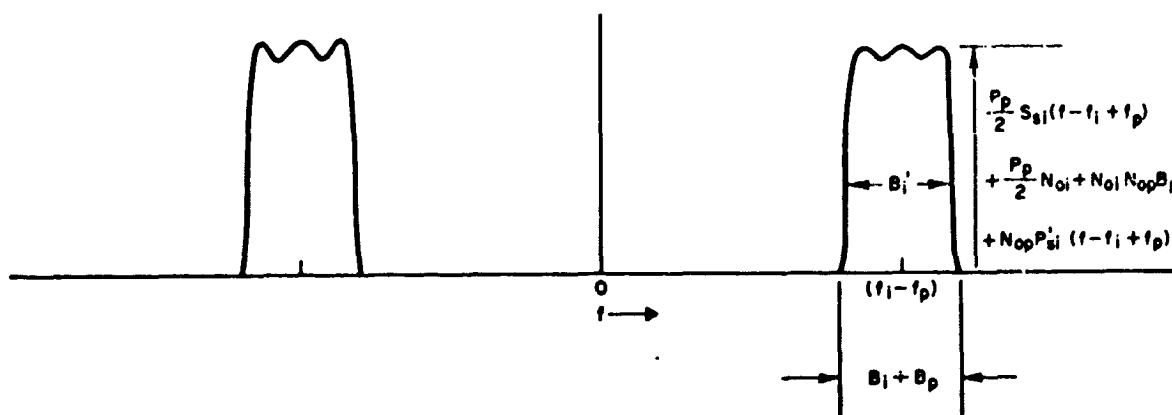Figure M-6. Spectrum of noise-noise products for case two.

Figure M-7. Spectrum of signal and noise for case two.

The noise-noise product terms are nongaussian while all others are gaussian. The ratio of gaussian terms to nongaussian terms is

$$R = \frac{P_p}{2N_{0p} B_p} + \frac{P_{si}}{2N_{0i} B_p} \qquad \text{(case one)} \quad \text{(M-6a)}$$

$$R = \frac{P_p}{2N_{0p} B_p} + \frac{P'_{si} (f - f_i + f_p)}{2N_{0i} B_p} \qquad \text{(case two)} \quad \text{(M-6b)}$$

For high pilot signal-to-noise ratios, R becomes large and the effect of the nongaussian terms becomes negligible.

146

APPENDIX N. CORRELATION OF EXTERNALLY GENERATED NOISE

In Appendix L the question arose of the correlation from element to element of externally generated noise. In this appendix it is shown that the correlations are ordinarily small.

In the analysis α_{inq} represents the correlation coefficient from element n to element q of noise in the information bandwidth and α_{pnq} represents the same coefficient for noise in the pilot bandwidth. Then α_{inq} may be written as

$$\alpha_{inq} = \frac{\overline{n_{i_n} n_{i_q}}}{\sqrt{\sigma_{in} \sigma_{iq}}} \tag{N-1}$$

When equations (L-4) and (L-5) are used for the noise terms, equation (N-1) becomes

$$\alpha_{inq} \equiv \frac{\oint\!\!\!\oint \sqrt{g_{e_n} g_{e_q}} \, \overline{\left[X_i^2 + Y_i^2\right]} \, e^{-j\left(\psi_n - \psi_q + \xi_n - \xi_q\right)} \, d\Omega}{\sqrt{\oint\!\!\!\oint g_{e_n}\left[X_i^2 + Y_i^2\right] d\Omega \ \oint\!\!\!\oint g_{e_q}\left[X_i^2 + Y_i^2\right] d\Omega}} \tag{N-2a}$$

$$\alpha_{pnq} \equiv \frac{\oint\!\!\!\oint \sqrt{g_{e_n} g_{e_q}} \, \overline{\left[X_p^2 + Y_p^2\right]} \, e^{j\left(\psi_{pn} - \psi_{pq} + \xi_n - \xi_q\right)} \, d\Omega}{\sqrt{\oint\!\!\!\oint g_{e_n}\left[X_p^2 + Y_p^2\right] d\Omega \ \oint\!\!\!\oint g_{e_q}\left[X_p^2 + Y_p^2\right] d\Omega}} \tag{N-2b}$$

To illustrate what form the α_{inq} might assume, three examples are considered. The first is that of a linear array of isotropic radiators as illustrated in figure 1-1. In this case the r_n are given by nd and $\theta_n = 0$. Then

$$\psi_n = -\frac{\omega_c}{v} \, nd \, \cos\theta, \quad \xi_n = 0 \qquad \text{(N-3a, b)}$$

$$\alpha_{inq} = \frac{\int_0^{2\pi} \int_0^{\pi} \overline{\left[X_i^2 + Y_i^2\right]} e^{-j\left[\frac{\omega_c}{v}(n-q) d \cos\theta\right]} \sin\theta \; d\theta d\phi}{\int_0^{2\pi} \int_0^{\pi} \overline{\left[X_i^2 + Y_i^2\right]} \sin\theta \; d\theta d\phi} \qquad \text{(N-3c)}$$
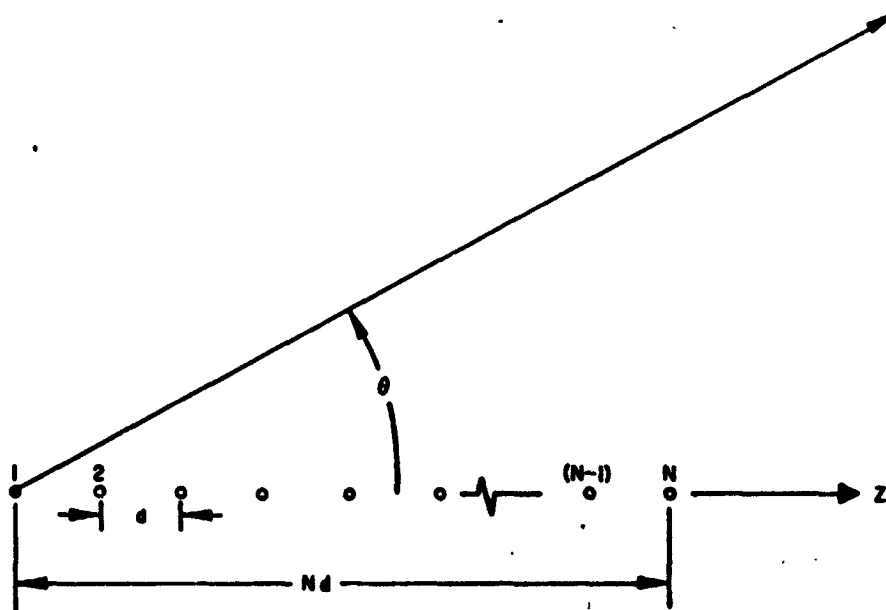

Figure N-1. Linear array of N elements.

If $X_i^2 + Y_i^2$ is uniform over all angles, this expression becomes

$$\alpha_{inq} = \frac{1}{2} \int_0^\pi e^{-j\frac{\omega_c}{v}(n-q)d\cos\theta} \sin\theta\, d\theta = \frac{1}{2} \int_{-1}^1 e^{-j\frac{\omega_c}{v}(n-q)dx}\, dx \tag{N-4a}$$

$$= \frac{1}{2}\; \frac{e^{-j\frac{\omega_c}{v}(n-q)d} - e^{j\frac{\omega_c}{v}(n-q)d}}{-j\frac{\omega_c}{v}(n-q)d} = \frac{\sin\frac{\omega_c}{v}(n-q)d}{\frac{\omega_c}{v}(n-q)d} \tag{N-4b}$$

In a similar manner,

$$\alpha_{pnq} = \frac{\sin\frac{\omega_p}{v}(n-q)d}{\frac{\omega_p}{v}(n-q)d} \tag{N-5}$$

For half wavelength spacing, the coefficients vanish.

The second example to be considered is a collinear array of dipoles. If mutual coupling is ignored, the effective gain function is

$$\sqrt{g_e} = \sqrt{\frac{3}{2}}\,\sin\theta \tag{N-6}$$

If, once again, the incident noise is uniform over all angles, there results

$$\alpha_{inq} = \frac{\displaystyle\int_0^\pi \sin^2\theta\, e^{-j\frac{\omega_c}{v}(n-q)d\cos\theta} \sin\theta\, d\theta}{\displaystyle\int_0^\pi \sin^3\theta\, d\theta} \tag{N-7a}$$

$$= \frac{\displaystyle\int_{-1}^1 (1-x^2)\cos\frac{\omega_c}{v}(n-q)dx\, dx}{\frac{4}{3}} \tag{N-7b}$$

$$\alpha_{inq} = 3\left\{ \frac{\sin\frac{\omega_c}{v}(n-q)d}{\left[\frac{\omega_c}{v}(n-q)d\right]^3} - \frac{\cos\frac{\omega_c}{v}(n-q)d}{\left[\frac{\omega_c}{v}(n-q)d\right]^2} \right\} \tag{N-7c}$$

In a similar manner there results

$$\alpha_{pnq} = 3\left\{\frac{\sin\frac{\omega_p}{v}(n-q)d}{\left[\frac{\omega_p}{v}(n-q)d\right]^3} - \frac{\cos\frac{\omega_p}{v}(n-q)d}{\left[\frac{\omega_p}{v}(n-q)d\right]^2}\right\}$$

(N-8)

For half wavelength spacing, the α_{pnq} become

$$\alpha_{pnq} = -\frac{3(-1)^{n-q}}{\pi^2(n-q)^2}$$

(N-9)

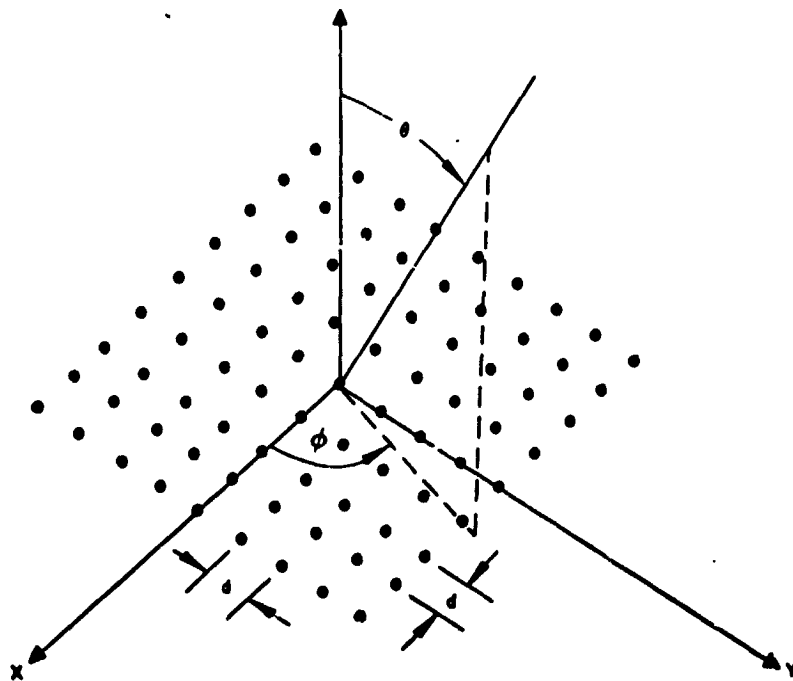For n-q > 1 this value becomes rapidly small.

Figure N-2. Rectangular array arrangement for computation of correlation coefficients.

The third example is that of a rectangular array of identical antenna elements assumed to be located as illustrated in figure N-2. The elements have an element gain function given by

$$g_e = \frac{4\pi}{\lambda^2} a_e \cos\theta \qquad 0 \le \theta \le \frac{\pi}{2}$$

$$= 0 \qquad\qquad \frac{\pi}{2} < \theta < \pi \qquad\qquad (\text{N-10})$$

The x and y coordinates of the elements are denoted by md and rd, respectively, d being the element separation along the axes. Substitution of equation (N-10) into equations (N-2) and use of the phase function appropriate to the geometrical arrangement of figure N-2 gives the following expression for a uniform noise background.

$$\alpha_{(n-m)(q-r)} = \frac{\displaystyle\int_0^{2\pi}\int_0^{\pi} \sin\theta\cos\theta\, d\theta\, d\varphi \exp\left[-j\frac{\omega d}{c}\sqrt{(n-m)^2+(q-r)^2}\sin\theta\cos\varphi\right]}{\displaystyle\int_0^{2\pi}\int_0^{\pi} \sin\theta\cos\theta\, d\theta\, d\varphi}$$

$$= 2\int_0^{\pi} J_0\left(\frac{\omega d}{c}\sqrt{(n-m)^2+(q-r)^2}\,\sin\theta\right)\sin\theta\cos\theta\, d\theta$$

$$= \frac{2 J_1\left(\frac{\omega d}{c}\sqrt{(n-m)^2+(q-r)^2}\right)}{\frac{\omega d}{c}\sqrt{(n-m)^2+(q-r)^2}} \qquad\qquad (\text{N-11})$$

APPENDIX O. DERIVATION OF EQUATIONS FOR VARIANCE OF NOISE TERMS IN A PHASE INVERSION SYSTEM

Equations (L-18a, b) give the variance of the noise terms in a system that uses phase inversion by mixing to obtain self-steering on reception. The variances of the terms that are made of signal-noise products are of the form

$$z = \int_0^T a_n(t)\, dt \tag{O-1}$$

The variance, σ_z^2, is given by

$$\sigma_z^2 = \left[\int_0^T a_n(t)\, dt\right]^2 = \overline{\int_0^T \int_0^T a_n(t_2)\, a_n(t_1)\, dt_2\, dt_1} \tag{O-2a}$$

$$\sigma_z^2 = \int_0^T \int_0^T \overline{a_n(t_2)\, a_n(t_1)}\, dt_2\, dt_1 = \int_0^T \int_0^T R_n(\tau)\, dt_2\, dt_1 \tag{O-2b}$$

where $R_n(\tau)$ is the autocorrelation function of the noise (stationary). The transformation

$$\left. \begin{array}{l} t_2 = t_1 + \tau \\[2mm] t = t_1 \end{array} \right\} \tag{O-3}$$

gives

$$\sigma_z^2 = \int_0^T \int_{t-T}^{t} R_n(\tau)\, d\tau\, dt = \int_{-T}^{T} R_n(\tau)\, g(-\tau)\, d\tau \tag{O-4}$$

where

$$g(\tau) = \tau + T \qquad\qquad -T < \tau < 0$$

$$g(\tau) = T - \tau \qquad\qquad 0 < \tau < T$$

(O-5)

The last form was derived by using the relation between the autocorrelation function and the spectral density, together with the convolution theorem for Fourier transforms.

For a rectangular passband from $-\Omega$ to Ω, the noise spectrum is

$$S(\omega) = N_0 \left[U(\omega + \Omega) - U(\omega - \Omega) \right]$$

(O-6)

where

$$N_0 = \frac{\pi}{\Omega} \sigma_n^2$$

(O-7)

Then

$$R(\tau) = \frac{1}{2\pi} \int_{-\infty}^{\infty} S(\omega) \exp(j\omega\tau) \, d\omega$$

(O-8a)

$$R(\tau) = \frac{N_0 \Omega}{\pi} \frac{\sin \Omega \tau}{\Omega \tau}$$

(O-8b)

With this expression for $R(\tau)$, the variance σ_z^2 becomes

$$\sigma_z^2 = \int_0^T \int_{t-T}^{t} R(\tau) \, d\tau \, dt = \frac{2 N_0}{\pi} T \, Si(\Omega T)$$

(O-9)

The calculation of the variance of the noise-noise product terms is considered next. The variance is given by

$$\sigma_1^2 = \overline{\left[\int_0^T a_n''(t) a_n'(t) \, dt \right]^2}$$

(O-10a)

$$= \int_0^T \int_0^T \overline{a_n''(t_1) a_n'(t_1) a_n''(t_2) a_n'(t_2)} \, dt_1 \, dt_2$$

(O-10b)

On making the substitutions

$$t_1 = t - \tau$$
$$t_2 = t$$

(O-11)

the expression (O-10b) may be reduced to

$$\sigma_1^2 = \int_{t=0}^{t-\tau} \int_{\tau=t-T}^{\tau=t} \overline{a_n''(t+\tau)a_n''(t)a_n'(t+\tau)a_n'(t)} \, d\tau \, dt$$

(O-12)

But

$$\overline{a_n''(t+\tau)a_n''(t)} = R_n''(\tau)$$

$$\overline{a_n'(t+\tau)a_n'(t)} = R_n'(\tau)$$

where $R_n''(\tau)$ and $R_n'(\tau)$ are, respectively, the autocorrelation functions of a_n'' and a_n'. Therefore, equation (O-12) may be rewritten as

$$\sigma_1^2 = \int_{t=0}^{t=T} \int_{\tau=t-T}^{\tau=t} R_n''(\tau)R_n'(\tau) \, d\tau \, dt$$

(O-13)

$R_n(\tau)$ may be computed from the spectral density, $S(\omega)$, by

$$R_n(\tau) = \frac{1}{2\pi} \int_{-\infty}^{\infty} S(\omega) \exp[j\omega\tau] \, d\omega$$

When $\mathcal{S}(\omega)$ is flat with density N_0 over a bandwidth Ω/π, $R_n(\tau)$ is given by

$$R_n(\tau) = \frac{N_0 \Omega}{\pi} \frac{\sin \Omega \tau}{\Omega \tau} \tag{O-14}$$

and

$$R_n''(\tau) R_n'(\tau) = \frac{N_0^2 \Omega_p \Omega_i}{\pi^2} \frac{\sin \Omega_p \tau}{\Omega_p \tau} \frac{\sin \Omega_i \tau}{\Omega_i' \tau} \tag{O-15}$$

where the subscript i refers to the information channel and the subscript p to the pilot channel. When this equation is substituted into equation (O 13) and the subsequent integrals are evaluated, the following expression results.

$$\sigma_1^2 = \frac{N_0^2}{\pi^2} \Big\{ \Omega_i(1+a)T \, Si[\Omega_i(1+a)T] - \Omega_i(1-a)T \, Si[\Omega_i(1-a)T]$$

$$- Cin[\Omega_i(1+a)T + Cin\Omega_i(1-a)T] \tag{O-16}$$

$$+ \cos[\Omega_i(1+\alpha)T] - \cos[\Omega_i(1-a)T] \Big\}$$

where

$$a \equiv \frac{\Omega_p}{\Omega_i} \equiv \frac{B_p}{B_i} \leq 1 \; ; \tag{O-17}$$

$$Cin(x) \equiv \int_0^x \frac{(1 - \cos t)}{t} \, dt \tag{O-18}$$

As $B_i T$ becomes much greater than one, the first two terms become predominant and σ_1^2 approaches the value

$$\sigma_1^2 = N_0^2 a B_i T \qquad \begin{cases} B_i T \gg 1 \\ a < 1 \end{cases} \tag{O-19}$$

Tne condition $B_iT \gg 1$ is necessary to approach the computed error probabilities since they were derived with this assumption implied. In a similar manner values can be obtained from equation (O-9):

$$\sigma_{zi}^2 = N_0 T \qquad B_i'T \gg 1 \qquad\qquad\text{(O-20)}$$

When $\alpha B_i T$ is much greater than one, as would be the case when the pilot channel bandwidth is nearly the same as the information channel bandwidth, equation (O-9) for the pilot channel also reduces to

$$\sigma_{zp}^2 = N_0 T \qquad\qquad\text{(O-21)}$$

On the other hand, when $\alpha B_i T$ is less than $1/\pi$, which would be the case when the pilot channel bandwidth is much less than the information channel bandwidth, equation (O-9) for the pilot channel becomes

$$\sigma_{zp}^2 = N_0 2\alpha B_i T^2 \qquad \alpha B_i T < \frac{1}{\pi} \qquad\qquad\text{(O-22)}$$

The various approximations (O-19) through (O-22) may be used to derive the expressions for the total noise variance as given in equation (L-18a, b).

REFERENCES

1. Villeneuve, A. T. ; Ksienski, A. A. ; and Young, G. O. : Study of Applications of Retrodirective and Self-Adaptive Electromagnetic Wave Phase Controls to a Mars Probe. First Quarterly, Report No. P66-82 (NAS 2-3297), Antenna Department, Aerospace Group, Hughes Aircraft Company, March 1966.

2. Villeneuve, A. T. ; Ksienski, A. A. ; and Young, G. O. : Study of Applications of Retrodirective and Self-Adaptive Electromagnetic Wave Phase Controls to a Mars Probe. Second Quarterly, Report No. P66-160 (NAS 2-3297), Antenna Department, Aerospace Group, Hughes Aircraft Company, May 1966.

3. Howard, J. E. ; Villeneuve, A. T. ; Young, G. O. ; and Ksienski, A. A. : Study of Applications of Retrodirective and Self-Adaptive Electromagnetic Wave Phase Controls to a Mars Probe. Third Quarterly, Report No. P66-230 (NAS 2-3297), Antenna Department, Aerospace Group, Hughes Aircraft Company, August 1966.

4. Villeneuve, A. T. ; Ksienski, A. A. ; Young, G. O. ; and Howard, J. E. : Study of Application of Retrodirective and Self-Adaptive Electromagnetic Wave Phase Controls to a Mars Probe. Fourth Quarterly, Report No. P67-61 (NAS 2-3297), Antenna Department, Aerospace Group, Hughes Aircraft Company, October 1966.

5. Gangi, A. F. : The Active Adaptive Antenna Array System. IEEE Trans. on AP, vol. AP-11, no. 4, July 1963, pp. 405-414.

6. Cutler, C. C. ; Kompfner, R. ; and Tillotson, L. C. : A Self-steering Array Repeater. Bell Syst. Tech. J. , vol. 42, no. 8, August 1963, pp. 2013-2032.

7. Belfi, C. A. ; et al. : A Satellite Data Transmission System. IEEE Trans. on AP, vol. AP-12, no. 2, March 1964, pp. 200-206.

8. Ghose, R. N. : Electronically Adaptive Antenna Systems. IEEE Trans. on AP, vol. AP-12, no. 2, March 1964, pp. 161-169.

9. Pon, C. Y. : Retrodirective Array Using the Heterodyne Technique. IEEE Trans. on AP, vol. AP-12, no. 2, March 1964, pp. 176-180.

10. Rutz-Phillipp, E. M. : Spherical Retrodirective Array. IEEE Trans. on AP, vol. AP-12, no. 2, March 1964, pp. 187-194.

11. Sichelstiel, B. A. ; Waters, W. M. ; and Wild, T. A. : Self-focusing Array Research Model. IEEE Trans. on AP, vol. AP-12, no. 2, March 1964, pp. 150-154.

12. Skolnik, M. I. ; and King, D. D. : Self-phasing Array Antennas. IEEE Trans. on AP, vol. AP-12, no. 2, March 1964, pp. 142-149.

13. Svoboda, D. E. : A Phase-locked Receiving Array for High-frequency Communications Use. IEEE Trans. on AP, vol. AP-12, March 1964, pp. 207-215.

14. Kummer, W. H. ; and Villeneuve, A. T. : Spacecraft Antenna Systems. Interim Engineering Report, Report No. P65-35 (NAS 5-3545), Antenna Department, Aerospace Group, Hughes Aircraft Company, Jan. 1965.

15. Kummer, W. H. ; and Birgenheier, R. A. : Spacecraft Antenna Systems. Final Engineering Report, Report No. P66-66 (NAS 5-3545), Antenna Department, Aerospace Group, Hughes Aircraft Compan , Feb. 1966.

16. Viterbi, A. J. : Principles of Coherent Communication. McGraw-Hill Book Co. , Inc. , 1966.

17. Gardner, F. M. : Phaselock Techniques. John Wiley and Sons, Inc. , 1966.

18. Arthurs, E. ; and Dym, H. : On the Optimum Detection of Digital Signals in the Presence of White Gaussian Noise -- A Geometric Interpretation and a Study of Three Basic Data Transmission Systems. IRE Trans. on CS, vol. CS-10, no 4, pp. 336-372, Dec. 1962

19. Viterbi, A. J. : Phase-coherent Communication over the Continuous Gaussian Channel. Chapter Seven of Digital Communications with Space Applications, S. W. Golomb, ed. Prentice-Hall, Inc. , 1964.

20. Charles, F. J. ; and Lindsey, W. C. : Some Analytical and Experimental Phase-locked Loop Results for Low Signal-to-noise Ratios. Proc. IEEE, vol. 54, no. 9, pp. 1152-1166, Sept. 1966.

21. Stiffler, J. J. : On the Allocation of Power in a Synchronous Binary Communication System. Proc. Natl. Tlmtrng. Conf. , section 5-1, pp. 1-11, 1964.

22. Van Trees, H. L. : Optimum Power Division in Coherent Communications Systems. IEEE Trans. on SET, vol. SET-10, no. 1, pp. 1-9, March 1964.

23. Price, R. ; and Green, Jr. , P. E. : A Communication Technique for Multipath Channels. Proc. IRE, vol. 46, no. 3, pp. 555-570, March 1958.

24. Costas, J. P. : Information Capacity of Fading Channels under Conditions of Intense Interference. Proc. IEEE, vol. 51, no. 3, pp. 451-461, March 1963.

25. Glenn, A. B. ; and Lieberman, G. : Performance of Digital Communications Systems in an Arbitrary Fading Rate and Jamming Environment. IEEE Trans. on CS, vol. CS-11, no. 1, pp. 57-68, March 1963.

26. Grobner, W. ; and Hofreiter, N. : Integraltafel. Vol. 2, Equation 86, p. 66. Springer-Verlag, 1949.

27. Fleck, J. T. ; and Trabka, E. A. : Error Probabilities of Multiple-state Differentially Coherent Phase Shift Keyed Systems in the Presence of White Gaussian Noise. Detect Memo No. 2A in Investigation of Digital Data Communications Systems, J. G. Lawton, ed. (Report No. UA-1420-S-1), Cornell Aeronautical Laboratory, Inc. , 1961.

28. Davenport, W. B. ; and Root, W. L. : An Introduction to the Theory of Random Signals and Noise, pp. 158-161 and 165-167. McGraw-Hill Book Co. , Inc. , 1958.